Multicomponent Fractional Quantum Hall Effects

Simon Charles Davenport

Wadham College

University of Oxford

A thesis submitted for the degree of

Doctor of Philosophy in Theoretical Physics

Trinity Term 2013

Multicomponent Fractional Quantum Hall Effects

Simon Charles Davenport

Wadham College
University of Oxford

Doctor of Philosophy in Theoretical Physics

Trinity Term 2013

Abstract

This thesis scrutinizes the condensed matter physics phenomenon known as the fractional quantum Hall effect (FQHE), in particular fractional quantum Hall effects occurring in multicomponent systems. Broadly speaking, the FQHE can be defined as a many-electron quantum phenomenon, driven by strong interactions, that occurs in two-dimensional electron gasses in the presence of a perpendicular external magnetic field (and it is also predicted to occur for any two-dimensional particles, such as confined cold atoms, in an external gauge field). Multicomponent systems are systems where the constituent particles (such as electrons or cold atoms) possess internal degrees of freedom, for instance a spin or valley index. These internal degrees of freedom are often overlooked when modeling the FQHE.

Taking into account the multicomponent degree of freedom yields an abundance of possibilities for the intellection of new types of so-called "topological phases of matter", which are ubiquitously associated with the FQHE. In this thesis several different cases are considered. The first topic discussed herein is a study of phase transitions that can take place between FQHE phases with different net values of their multicomponent degrees of freedom. Examples are phase transitions between phases of different uniform net spin polarization, tunable as a function of certain system parameters. Some significant technical refinements are made to a previous model and comparisons are made with a variety of different experiments. The results are relevant for multicomponent FQHEs occurring in GaAs,AlAs and SiGe semiconductor systems where the electronic structure is confined to two dimensions, as well as in two-dimensional materials such as graphene.

The second topic discussed herein is the introduction of the multiparticle multicomponent pseudopotential formalism. This methodology is oriented towards considerably expanding an existing framework for the construction of exactly solvable FQHE models by parameterizing multicomponent interactions. The final topic is the first example application of this new formalism to the construction of an exactly solvable FQHE model.

Acknowledgements

It is a great pleasure to thank the following people.

First and foremost, I thank my supervisor Steve Simon for his contagious enthusiasm and stimulating discussions throughout the course of my DPhil; Eddy Ardonne and Nicolas Regnault for their amicable collaboration on work related to this thesis; and my thesis examiners John Chalker and Kareljan Schoutens.

It is a privilage to have been associated with the Rudolf Peierls Centre for Theoretical Physics these past few years. I have greatly benefitted from interactions with many of the faculty, postdocs and students with whom I shared that time: John Chalker, Fabian Essler, John Cardy, Fiona Burnell, Rahul Roy, Eliot Kapit, Jesper Romers, Adam Nahum, Curt von Keyserlink, Neil Robinson, Fenner Harper, Gábor Halász, Darren Tan, Steffen Schaper, Jack Cohen, Lisa Möevius, and Irwin Zaid. I thank Michelle Bosher and Sarah Loving for administrative support. I also acknowledge the use of computer time on the "Hydra" cluster for computational calculations contributing to this thesis and I particularly thank Jonathan Patterson for his earnest technical support.

In the course of completing this work I have undoubtedly profited from numerous insightful discussions; I particularly thank Duncan Haldane, Bert Halperin, Mansour Shayegan, Loren Pfeiffer, Amir Yacoby, Kirill Shtengel, Joost Slingerland, Wei Pan, Csaba Töke, Andrea Cappelli, Bert Schellekens, Ruben Pauncz, Jacob Katriel, Jerome Dubail and Gunnar Möller.

I am grateful to the Institute Henri Poincaré in Paris and to NORDITA in Stokholm for hospitality during prolonged visits, where significant parts of this research were completed.

During my time in Oxford, I have enjoyed a happy association with Wadham College. I thank my college advisor C. V. Sukumar for his encouragement throughout my studies and Wadham for its financial support.

Finally, I especially thank my mother and brothers Matthew and Alexander for their patience and steadfast support.

The research presented in this thesis was made possible by the generous financial provision of the EPSRC under grant numbers EP/I032487/1 and EP/I031014/1.

Contents

List of Abbrevations

FQHE — fractional quantum Hall effect

IQHE — integer quantum Hall effect

2DEG — two-dimensional electron gas

MOSFET — metal–oxide–semiconductor field-effect transistor

MBE — molecular beam epitaxy

UHV/CVD — ultrahigh-vacuum chemical-vapour-deposition

SET — single electron transistor

LL — Landau level

LLL — lowest Landau level

2nd LL — second Landau level

CF — composite fermion

CFT — conformal field theory

NASS — non-Abelian spin-singlet

SSG — spin-singlet gaffnian

List of Figures

List of Tables

CHAPTER 1

Introduction

1.1 An Overview

This thesis concerns itself with the physics of the fractional quantum Hall effect (FQHE), a particularly striking and spectacular example of many-body quantum mechanical phenomena that exhibit themselves in the physical world. At the time of writing, it is now more than 30 years since the experimental discovery of the FQHE in 1982.[1] The study of the effect has, since then, spawned many entirely new physical concepts and ways of thinking that have been gainfully applied to numerous other problems in condensed matter physics. Examples include the inception of a new paradigm of so-called topological phases of matter and topological phase transitions between such phases, concepts that lie beyond the Landau paradigm of classifying phases by their local symmetries;[2,3] and the introduction of quasiparticle excitations that possess anyonic and even non-abelian exchange statistics, greatly expanding on the notion that quasiparticles can be either bosons or fermions.[3–5] Such ideas have since been applied to study physical problems not only in semiconducting materials where electrons can exhibit the FQHE, but also, for instance, to exotic classes of superconductors (known as p wave superconductors),[6] to (fractional) topological insulators,[7] to "flat band" models with strong interactions,[8–10] and to the highly controlled environment of cold atomic gasses.[11]

Even in the well-established field of the FQHE, new experimental results and trends of thinking often come to the fore that lead theorists to expand upon previous ideas. One topic that has received renewed attention is the multicomponent nature of the FQHE: for example the fact that electrons have a spin degree of freedom.[12–16] Such multicomponent degrees of freedom are often overlooked, and taking these into account yields an abundance of possibilities for developing previous theories,[6,17,18] and discovering novel experimental results.[19–22] Interest in multicomponent FQHEs has been driven, in part, by experimental studies of multicomponent condensed matter systems such as graphene, and in part, by the ongoing process of FQHE model building, that is, the process of constructing exactly solvable theoretical models that describe topological phases of mater, which it is hoped occur in physically realizable systems.[5,17] The research presented in this thesis touches on both of these driving factors: we

shall present contributions to the understanding of some fascinating aspects of experimentally observed properties of multicomponent FQHE systems, and contributions that extend some of the foundations for FQHE model building in the context of multicomponent systems. An ultimate goal of this model building is to construct phases that admit quasiparticles possessing non-abelian statistics, which might, in principle, be used in the application of so-called topological quantum computation.[3] Along the way, we learn about the fascinating manner in which quantum mechanics manifests itself in condensed matter physics.

The purpose of this introductory chapter will be to provide relevant and, we hope, insightful background material on the quantum Hall problem, and to decode some of the associated jargon. Major breakthroughs and significant improvements in the understanding of the effect are reflected in the many excellent books on the subject that have been written in the intervening years since its discovery.[23–28] Undoubtedly, it is impossible to cover in depth all of the developments of the past decades, and as such we have been highly selective in what we review here.

Broadly speaking, the FQHE can be defined as a many-electron quantum phenomenon, driven by strong interactions, that occurs in two-dimensional electron gasses in the presence of a perpendicular external magnetic field (and it is also predicted to occur for any two-dimensional particles, such as confined cold atoms, in an external gauge field). To start with, let us break down this statement and consider each piece in some detail: what do we mean by a two-dimensional electron gas? What is a Hall effect? How does it become quantized? What is fractional? The aim will be to define the quantum Hall problem itself, and in the process introduce the nomenclature and summarize the fundamental concepts that will be called on again later on. After this preliminary background, we shall turn to motivations for the research presented in the remainder of this thesis, on the multicomponent nature of the fractional quantum Hall effect.

1.2 Preliminary Background

1.2.1 The Two-Dimensional Electron Gas

Archetypal physical systems where an effective *two-dimensional electron gas* (2DEG) can be accomplished are *metal–oxide–semiconductor field-effect transistors* (MOSFETs) and *semiconductor heterostructures*; that is either heterojunctions, occurring at the planar interface of two semiconductor materials with different band gaps, or quantum wells, occurring where a planar

layer of one type of semiconductor is embedded into another semiconductor with a larger band gap. Typical constituent materials are Ga (gallium), Al (aluminum), Si (silicon) and Ge (germanium), and these are alloyed into semiconductor materials such as GaAs, or $Al_xGa_{1-x}As$, with an alloy proportion $0 \leq x \leq 1$ (typically $x \sim 0.3$). Typical experiments to study the fractional quantum Hall effect use the highest mobility semiconductor technology available, most notably Si MOSFETs and GaAs–AlGaAs modulation doped heterojunctions. Such structures are routinely engineered using the techniques of ultrahigh-vacuum chemical-vapor-deposition (UHV/CVD),[29] and molecular beam epitaxy (MBE),[30] respectively. With MBE, the desired semiconductor structure is deposited onto a substrate one layer at a time, providing the absolute control over the composition of the crystal structure necessary for engineering ultra-high mobility systems. [†] With UHV/CVD the semiconductor structure is chemically deposited onto a substrate, leading to somewhat lower quality samples compared with MBE. Nevertheless, sufficiently high mobility samples can be constructed for the observation of the FQHE (see, e.g., ref. [32]).

Certain classes of semiconductors, such as the GaAs and AlGaAs, have remarkably similar crystal structures and similar, but not quite identical band gaps. In a heterojunction containing both materials the first of these properties makes it possible to engineer an extremely sharp boundary between them (which greatly reduces the presence of structural defects, hence, leads to very high electron mobility). With appropriate tuning, the band gap centres of the two materials can be roughly lined up as shown in fig. 1.1a. In order to engineer a 2DEG, donor impurities such as Si are added to a layer in AlGaAs, separated from the junction by a spacer layer of undoped AlGaAs (see fig. 1.1b). These donor electrons are inclined to move to the GaAs conduction band, which results in an electric polarization across the spacer layer. Consequently the band structure is modified such that close to the interface the conduction band exhibits a potential barrier on the side of the larger band gap material and a corresponding potential well in the smaller band gap material, as shown schematically in fig. 1.1b. The affected regions are microscopic in scale (typically on the order of a few 10s of nm) and, consequently, motion of electrons in the well is strongly quantized in the direction normal to the interface (the quantum mechanical problem is approximately equivalent to that of free electrons occupying bound states in a triangular potential well).[33] Since the degree of freedom perpendicular to the plane of the heterojunction is effectively restricted, these conditions result in the formation of

[†] The minimum mobility, μ, for the effect to be observed is around $\mu \sim 10^5 \mathrm{cm}^2/\mathrm{Vs}$,[23] and indeed the record for the highest mobility GaAs semiconductor, $\mu = 37.8 \times 10^6 \mathrm{cm}^2/\mathrm{Vs}$, is associated with crystal growth techniques specifically developed to study the FQHE.[31] Electron mobility is a rough metric for electronic disorder.

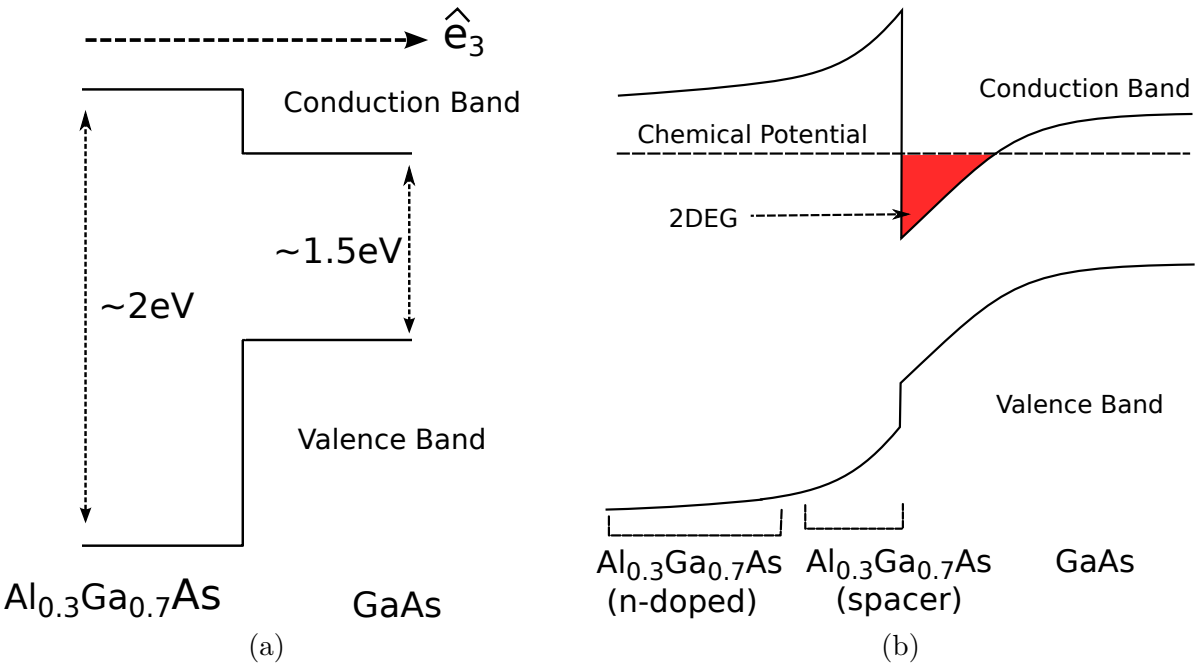

Figure 1.1: A schematic diagram of the band structure at the planar interface of two semiconductors with different band gaps (not to scale). $\hat{\mathbf{e}}_3$ denotes the unit vector out of the plane of the two-dimensional interface. If donor impurities such as Si are placed on the AlGaAs side then, rather than a sharp step in the band structure at the interface (left), the donor electrons rearrange themselves to form a potential barrier in the larger band gap material, and a corresponding potential well in the smaller band gap material (right). Electrons in the well occupy bound states due to the approximately triangular potential. The degree of freedom normal to the interface becomes quantized and a two-dimensional electron gas (2DEG) is formed in the well. The chemical potential can be set with a top gate voltage (see fig. 1.3).

a 2DEG close to the interface. The electron density in the well can be varied by changing the chemical potential, which is achieved by the addition of a metallic layer to the structure with a tunable potential (such a structure is often called a "top gate", see fig. 1.3). Similar features occur in quantum well heterostructures, where a layer of, e.g., GaAs is sandwiched between two layers of, e.g., AlGaAs. In that case the potential well is roughly square in shape (rather than roughly triangular).

Other substances that exhibit 2DEG behaviour are materials that are, by their very nature, two-dimensional conductors. The most famous example of such a material is graphene.[34] The case of graphene is somewhat distinct compared with semiconductor systems, principally because the band dispersion close to the K and K' points in the Brillouin Zone of graphene is linear, which can be pictured as a pair of structures known as "Dirac cones" (see fig. 1.2). The fact that the dispersion is linear leads to relativistic electron dynamics when the chemical potential is tuned close to the centre of these Dirac cones.

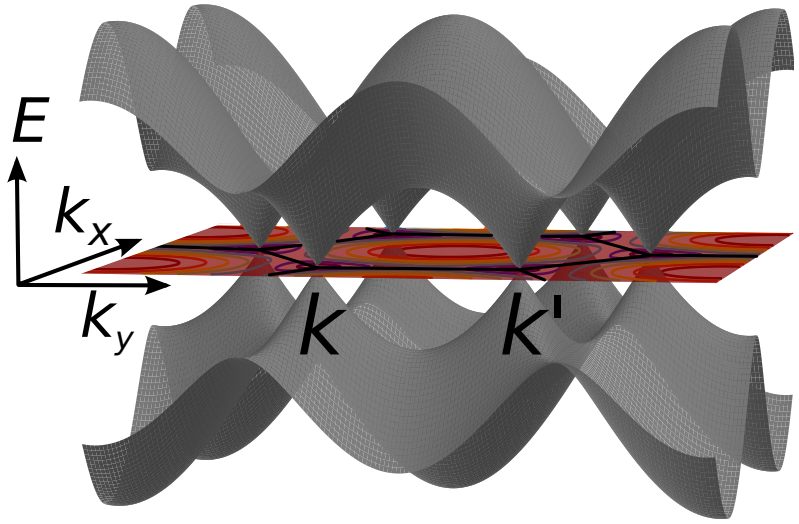

Figure 1.2: A sketch of the remarkable band structure of graphene: Dirac cones occur at the K and K' points in the Brillouin zone.

1.2.2 The Classical Hall Effect

The electronic transport properties associated with 2DEGs placed in magnetic fields are known as *Hall effects*. The transport properties of interest are the longitudinal (ρ_{xx}) and transverse (ρ_{xy}) resistivity measured in a 2DEG, such as that formed in a GaAs–AlGaAs heterojunction. A schematic of a typical experimental apparatus is shown in fig. 1.3. The key tunable quantity is the ratio of electron density to magnetic flux number density, which is known as the *filling factor*, denoted by ν.

$$\nu = \rho_e \Phi_0 / B = N / N_\Phi,$$

where ρ_e is the number density of electrons in the 2DEG, B is the magnetic flux density, N is the number of electrons in the 2DEG, N_Φ is the number of magnetic flux quanta, and $\Phi_0 = hc/e$ is a magnetic flux quantum.

The classical expectation for the observed ρ_{xx} and ρ_{xy} in an experiment such as that shown in fig. 1.3 was determined in 1879 by Edwin Hall, after whom the effect is named.[35] Classically, the mobile electrons constituting the current I, are deviated in their trajectory by the presence of the perpendicular magnetic field B, in such a way as to result in a charge imbalance in the transverse direction. This, in turn, gives rise to a so-called Hall voltage along the transverse direction (measured by V_y in fig. 1.3) that acts to rebalance the deviated path of the current. After attaining equilibrium, and assuming a uniformly flowing current along the longitudinal

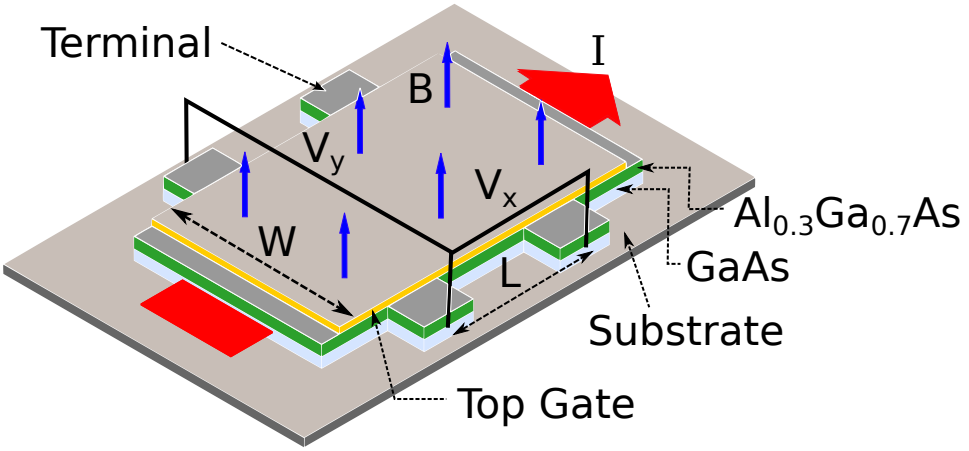

Figure 1.3: An apparatus with which to perform measurements of the electronic transport properties exhibited in Hall effects. A current is passed through the 2DEG region formed at the interface of GaAs and $Al_{0.3}Ga_{0.7}As$ (see fig. 1.1), and the region is exposed to a perpendicular magnetic field, B. The longitudinal (V_x) and transverse (V_y) voltages are measured as a function of the current I and magnetic field B and the longitudinal (ρ_{xx}) and transverse (ρ_{xy}) resistivity are deduced from these measurements. The electron density in the 2DEG is tuned via an applied top gate voltage. The apparatus is often known as a "Hall bar".

(x) direction, the transverse and longitudinal conductivity are given by [†]

$$\sigma_{xy} = -\frac{V_y}{I} = -\frac{\nu e^2}{h} \quad , \quad \sigma_{xx} = \frac{V_x}{I} \times \frac{L}{W},$$

where L and W are the length and width of the Hall bar (see fig. 1.3). In other words, the classical prediction for the Hall effect is that σ_{xy} will be proportional to the filling factor and that σ_{xx} will be fixed. [‡]

1.2.3 Experimental Observations of the Quantum Hall Effect

The most striking features of the integer quantum Hall effect (IQHE) and the FQHE can be observed in electronic transport measurements of the longitudinal and transverse resistivity in ultra-high mobility samples measured at very low temperatures (typically less than ~ 0.5 Kelvin is required to see the FQHE). Plots of the famous "skyline" of longitudinal resistivity peaks and the simultaneous plateaux in the transverse resistivity are shown in fig. 1.4.

In the low temperature, high mobility regime, the classical interpretation of the Hall effect evidently spectacularly breaks down. The key experimental observations are as follows:

[†]Note that the transverse and longitudinal *conductance* are defined by $I_x = -G_{xy}V_y$ and $I_x = G_{xx}V_x$ whilst the and transverse and longitudinal *conductivity* are defined by $j_x = -\sigma_{xy}E_y$ and $j_x = \sigma_{xx}E_x$, for transverse and longitudinal electric field $-E_y$ and E_x and longitudinal 2D current density j_x. The relations $\sigma_{xx} = G_{xx}L/W$ and $\sigma_{xy} = G_{xy}$ assume a uniform current density along the x direction.

[‡]The resistivity tensor is given by inverting the conductivity tensor. For simplicity we assume a homogeneous, isotropic substance, which means that $\sigma_{xy} = -\sigma_{yx}$ and $\sigma_{xx} = \sigma_{yy}$, and it follows that, $\rho_{xx} = \frac{\sigma_{xx}}{\sigma_{xx}^2+\sigma_{xy}^2}$, and $\rho_{xy} = -\frac{\sigma_{xy}}{\sigma_{xx}^2+\sigma_{xy}^2}$.

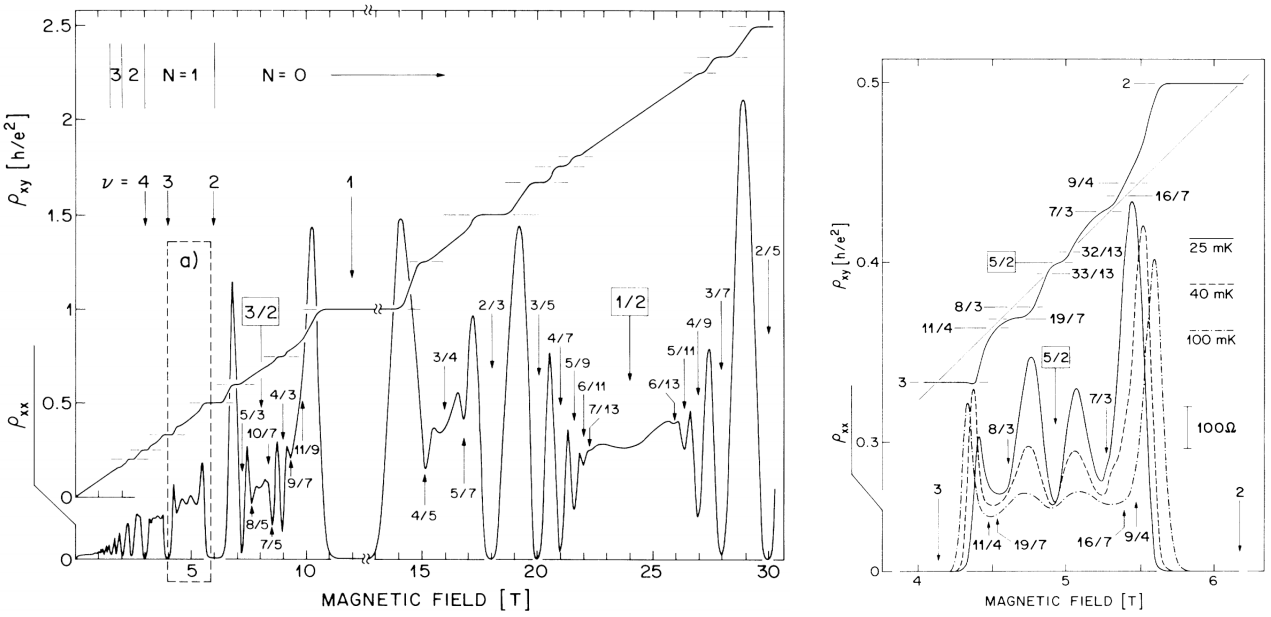

Figure 1.4: An overview of the observed fractions in electronic transport measurements of the IQHE and FQHE: the famous "skyline". Longitudinal (ρ_{xx}) and transverse (ρ_{xy}) resistivity measurements are shown on the same plot. The right panel zooms in on the area labeled a) on the left panel, showing in more detail the FQHE structure in the second Landau level. The filling factor ν is defined in the text. Reprinted figures with permission from ref. [37], R. Willett *et al.*, Phys. Rev. Lett. **59**, 1776 (1987). Copyright (1987) by the American Physical Society.

as the filling factor is tuned, for instance, by keeping the electron density fixed and varying the magnetic field strength, throughout a relatively wide region close to an integer value ($\nu = 1, 2, 3, \ldots$) or certain rational fractional value (e.g. $\nu = 1/3, 2/5 \ldots$ [†]), the longitudinal resistivity, ρ_{xx}, drops to zero and the transverse resistivity becomes fixed at a value given precisely by $\rho_{xy} = h/\left(\nu_{\text{exact}} e^2\right)$, where ν_{exact} is an exact integer or special rational fraction closest to the actual value of ν. Far away from these exact values, the resistivity follows the classically expected result. The key signatures associated with the FQHE are the exceptionally stable states that appear to form at these special rational fractional values of the filling factor ν, distinct from plateaux at integer values of ν, which are associated instead with the IQHE.

It is enlightening to note that the distinction between a longitudinal and transverse resistance is really a *topological* property. A four terminal resistance measurement gives ρ_{xy} if current and voltage contacts alternate along the boundary of the conductor, and ρ_{xx} otherwise (see fig. 1.3; the current contacts are the points where the current labelled I enters and leaves the system, the voltage contacts are at the terminals where the leads labelled with V_x and V_y are connected).[36]

[†]Note that the $\nu = 1/3$ plateau cannot be seen in fig. 1.4, but it was one of the first to be discovered experimentally.[1]

1.3 The Origin of the Integer Quantum Hall Effect

We can begin to understand many aspects of both the integer and fractional quantum Hall effects by studying a quantum mechanical treatment of the problem.

1.3.1 The Quantum Problem of Band Electrons in a Magnetic Field

Presently, we consider the very general quantum mechanical problem of electrons in a conducting solid exposed to an uniformly applied magnetic field.[38–40] Electrons in a conducting solid reside in a crystalline structure, which at first sight one might think would complicate the situation significantly compared to a free electron problem. However, in the absence of strong interactions and strong disorder, we can absorb all of the impact of the crystalline potential into a band structure defined by effective masses m_j^* along the jth cartesian direction with $j = 1, 2, 3$, and treat the electrons as if they were free particles. In the anisotropic case the effective masses m_1^*, m_2^* and m_3^* differ. For simplicity, we shall assume an isotropic, non relativistic band structure with effective masses $m_j^* = m^*$ for $j = 1, 2, 3$, and we shall ignore the physical edges of the system and the electron spin for this calculation.

Due to the Lorentz force, moving electrons will perform cyclotron orbits in an orientation normal to the direction of any applied field magnetic field. Let us denote the magnetic field by $\mathbf{B} = \nabla \times \mathbf{A}$, with a magnetic vector potential $\mathbf{A}$. The problem can be solved in a gauge-independent way, with any convenient gauge choice. Without loss of generality therefore, we chose $\mathbf{B} = (0, 0, B)$ and $\mathbf{A} = -\frac{1}{2}\mathbf{r} \times \mathbf{B}$ (the *symmetric gauge*) with $\mathbf{r} = (r_1, r_2, r_3)$ denoting the position of the electron in three dimensions. The Hamiltonian describing the quantum mechanical behaviour of each single electron can be expressed as,[40]

$$H_0 = \frac{1}{2m^*}\left\{\left(\hat{P}_1 - \frac{eBr_2}{2c}\right)\hat{\mathbf{e}}_1 + \left(\hat{P}_2 + \frac{eBr_1}{2c}\right)\hat{\mathbf{e}}_2 + \hat{P}_3\hat{\mathbf{e}}_3\right\}^2, \tag{1.1}$$

where r_j and $\hat{P}_j = -i\hbar\partial/\partial r_j$ are, respectively, the position and momentum operators along the jth cartesian direction ($j = 1, 2, 3$), $\hat{\mathbf{e}}_j$ are cartesian unit vectors, e is the fundamental electron charge, c is the speed of light in vacuo, and $\hbar$ is Planck's constant divided by 2π. Multiplying out the brackets, we arrive at

$$H_0 = \frac{\hat{P}_1^2}{2m^*} + \frac{\hat{P}_2^2}{2m^*} + \frac{\hat{P}_3^2}{2m^*} + \frac{eB}{2m^*c}\left(r_1\hat{P}_2 - r_2\hat{P}_1\right) + \frac{B^2e^2}{8m^*c^2}\left(r_1^2 + r_2^2\right).$$

The corresponding Schrödinger equation, $H_0\Psi(\mathbf{r}) = E\Psi(\mathbf{r})$, can be written in the form:

$$\hbar\omega_C \left\{ -\frac{l_0^2}{2}\left[\frac{\partial^2}{\partial r_1^2} + \frac{\partial^2}{\partial r_2^2}\right] + \frac{i}{2}\left[r_2\frac{\partial}{\partial r_1} - r_1\frac{\partial}{\partial r_2}\right] + \frac{1}{8l_0^2}\left(r_1^2 + r_2^2\right) + \right\} \Psi(\mathbf{r}) + \frac{\hbar^2}{2m^*}\frac{\partial^2}{\partial r_3^2}\Psi(\mathbf{r}) = E\Psi(\mathbf{r}), \tag{1.2}$$

where we have introduced the *cyclotron frequency* $\omega_C = eB/m^*c$, and the *magnetic length* $l_0 = \sqrt{\frac{\hbar c}{eB}}$. [†]

The Schrödinger equation can be recast in a more enlightening form with the following three steps. First we change the co-ordinate system: introducing the complex co-ordinates $z = (r_1 + ir_2)/l_0$ and $\bar{z} = (r_1 - ir_2)/l_0$, such that $l_0\partial/\partial r_1 = \partial/\partial z + \partial/\partial\bar{z}$ and $l_0\partial/\partial r_2 = i\partial/\partial z - i\partial/\partial\bar{z}$, eq. (1.2) is equivalent to

$$\hbar\omega_C \left\{ -\frac{1}{2}\left[4\frac{\partial^2}{\partial z\partial\bar{z}}\right] + \frac{1}{2}\left[z\frac{\partial}{\partial z} - \bar{z}\frac{\partial}{\partial\bar{z}}\right] + \frac{1}{8}\left(z\bar{z}\right) \right\} \Psi(\mathbf{r}) + \frac{\hbar^2}{2m^*}\frac{\partial^2}{\partial r_3^2}\Psi(\mathbf{r}) = E\Psi(\mathbf{r}).$$

Second, the part associated with motion parallel to the applied magnetic field (along the $\hat{\mathbf{e}}_3$ direction), can clearly be separated with $\Psi(\mathbf{r}) = \psi(z,\bar{z})\phi(r_3)$. With no additional constraints, the solutions for $\phi(r_3)$ are simply plane waves $\phi_{k_3}(r_3) \propto exp(ik_3r_3)$ with momentum k_3. Finally, we introduce the following set of raising and lowering operators: [‡]

$$\hat{a} = \frac{1}{\sqrt{2}}\left(\frac{z}{2} + 2\frac{\partial}{\partial\bar{z}}\right), \qquad \hat{a}^\dagger = \frac{1}{\sqrt{2}}\left(\frac{\bar{z}}{2} - 2\frac{\partial}{\partial z}\right), \tag{1.3}$$

which satisfy the commutation relation $\left[\hat{a},\hat{a}^\dagger\right] = 1$. Combining these steps, eq. (1.2) can be written in the following simplified form:

$$\left\{\hbar\omega_C\left(\hat{a}^\dagger\hat{a} + \frac{1}{2}\right) + \frac{\hbar^2}{2m^*}\frac{\partial^2}{\partial r_3^2}\right\}\psi(z,\bar{z})\phi_{k_3}(r_3) = E\psi(z,\bar{z})\phi_{k_3}(r_3). \tag{1.4}$$

The energy eigenvalues are effectively those of a quantum harmonic oscillator, labelled by a quantum number n with $n = 0, 1, \ldots$,

$$E(n,k_3) = \hbar\omega_C\left(n + \frac{1}{2}\right) + \frac{\hbar^2k_3^2}{2m^*}. \tag{1.5}$$

We note at this point that if we had instead considered relativistic electrons then the energy eigenvalues would be of the form $E(n, k_3 = 0) \sim \mathrm{sgn}(n)\sqrt{|n|}$ with n now any positive or negative integer, with sign $\mathrm{sgn}(n)$. This case applies to materials such as graphene, which we shall discuss later. [34]

Another good quantum number is the angular momentum, $\hbar m$, parallel to the applied magnetic field (along the $\hat{\mathbf{e}}_3$ direction), which corresponds to the operator $\hat{L}_3$ (we shall shortly

[†]Note that throughout this thesis we shall use g.c.s (or Gaussian) units and not SI units.

[‡]Note that $\left(\frac{\partial}{\partial z}\right)^\dagger = -\frac{\partial}{\partial\bar{z}}$, which follows from $\int_{\mathcal{D}} u^*(z,\bar{z})\left(\frac{\partial}{\partial z}\right)v(z,\bar{z})dzd\bar{z} = -\int_{\mathcal{D}} v(z,\bar{z})\left(\frac{\partial}{\partial\bar{z}}\right)^* u^*(z,\bar{z})dzd\bar{z}$ for square-integrable complex functions u and v such that the boundary term vanishes.

show that m takes the integer values $m = -n, -n+1, \ldots$). It will be insightful to try to express $\hat{L}_3$ in terms of raising and lowering operators such as $\hat{a}$ and $\hat{a}^\dagger$ written above. To that end we now introduce an alternative set of commuting operators, given by:

$$\hat{b} = \frac{1}{\sqrt{2}}\left(\frac{\bar{z}}{2} + 2\frac{\partial}{\partial z}\right), \qquad \hat{b}^\dagger = \frac{1}{\sqrt{2}}\left(\frac{z}{2} - 2\frac{\partial}{\partial \bar{z}}\right),$$

which satisfy the commutation relation $\left[\hat{b}, \hat{b}^\dagger\right] = 1$. $\hat{L}_3$ can then be expressed in terms of both sets of $\hat{a}$ and $\hat{b}$ operators as

$$\hat{L}_3 = -i\hbar\left(r_1\frac{\partial}{\partial r_2} - r_2\frac{\partial}{\partial r_1}\right) = \hbar\left(z\frac{\partial}{\partial z} - \bar{z}\frac{\partial}{\partial \bar{z}}\right) = \hbar(\hat{b}^\dagger\hat{b} - \hat{a}^\dagger\hat{a}).$$

The orbitals $\psi(z, \bar{z})$ that satisfy eq. (1.4) and form a basis of its Hilbert space will be labeled by the quantum numbers n and m that we introduced above. To define the Hilbert space, we start with the vacuum state,

$$\psi_{n=0,m=0}(z, \bar{z}) = \frac{1}{\sqrt{2\pi}}e^{-\frac{1}{4}|z|},$$

which is clearly annihilated by both the $\hat{a}$ and $\hat{b}$ operators, and, hence, $\hat{L}_3$ also. Acting on the vacuum with $\hat{b}^\dagger$ increases m by one unit while preserving n, whereas acting on the vacuum with $\hat{a}^\dagger$ increases n by one unit and also decreases m by one unit. Therefore m takes the integer values $m = -n, -n+1, \ldots$. The orbitals that compose the Hilbert space are, thus, generated by

$$\psi_{nm}(z, \bar{z}) = \frac{\left(\hat{b}^\dagger\right)^{m+n}}{\sqrt{(m+n)!}}\frac{\left(\hat{a}^\dagger\right)^n}{\sqrt{(n)!}}\psi_{0,0}(z, \bar{z}) = \frac{(-1)^n}{\sqrt{2\pi}}\sqrt{\frac{n!}{2^m(m+n)!}}z^m L_n^m\left(\frac{|z|^2}{2}\right)e^{-\frac{1}{4}|z|^2}, \quad (1.6)$$

where L_n^m are associated Laguerre polynomials.

In the special case where $n = 0$, the single particle orbitals are given by

$$\psi_{0m}(z, \bar{z}) = \frac{1}{\sqrt{2\pi 2^m m!}}z^m e^{-\frac{1}{4}|z|^2}, \quad (1.7)$$

with $m = 0, 1, \ldots$. The special property of these $n = 0$ orbitals is that, excluding the Gaussian factor, they are *analytic functions* of z (by virtue of the fact that they are holomorphic complex functions). More generally, a solution to the Schrödinger equation is any linear combination of the above orbitals, thus taking the form (in the $n = 0$ case):

$$\psi = f(z)\, e^{-\frac{1}{4}|z|^2}.$$

where $f(z)$ is any analytic function of z.

We conclude this discussion with the following observations. Looking at eq. (1.5), it is

apparent that the energy of the electron's motion in the plane perpendicular to the applied field becomes completely quantized into a set of bands separated in energy by an amount $\hbar\omega_C$ (for fixed k_3). These bands, labelled by the quantum number n, are known as *Landau levels* (LLs). The case $n = 0$ is known as the lowest Landau level (LLL), $n = 1$ will be called the second Landau level (2nd LL), and so on. Finally, the motion parallel to the applied field $\mathbf{B}$ is unaffected. In fact, these conclusions remain true no matter the shape of the band structure; the only difference compared to the isotropic case calculated here will be that the shape of the orbitals $\psi_{nm}(z, \bar{z})$ will be altered accordingly.[41]

We also comment here that if the particle has an additional degree of freedom, such as spin, which we discuss below, we will need to specify the state of this spin as well. For example, we might write the following wave function:

$$\psi = f(z)\, e^{-\frac{1}{4}|z|^2} \, |\uparrow\rangle .$$

For an electron with spin $\mathbf{S}$, there would be an addition Zeeman term in the Hamiltonian, $g\mu_B \mathbf{B} \cdot \mathbf{S}$, where g is the g-factor of the host material and μ_B is the Bohr magneton. Taking the electron spin-1/2 degree of freedom into account, each LL is further split into a spin-up and spin-down copy, separated in energy by a Zeeman energy per electron $E_Z = g\mu_B B$. Each pair of spin-up/spin-down LLs is then separated from the next pair by the cyclotron energy.

1.3.2 Why Two Dimensions is Important

Having seen in sec. 1.2.1 under what circumstances conduction electrons can be considered to inhabit a two-dimensional system, we now pose the question, what happens if a magnetic field is applied normal to the two-dimensional interface in a heterojunction, for instance?

In that case the $\phi(r_3)$ wave functions representing the electron motion parallel to the magnetic field (and perpendicular to the plane of the 2DEG in our heterojunction) are roughly those of a triangular potential well defined by a confining potential $V(r_3) = \infty$ for $r_3 < 0$ and $V(r_3) = \mathcal{E} r_3$ otherwise. The solutions to the Schrödinger equation for $\phi(r_3)$ in this example are Airy functions $\phi_q(r_3) \propto \mathrm{Ai}\left[\left(\frac{2m^*}{\hbar^2\mathcal{E}^2}\right)^{1/3}\{\mathcal{E} r_3 - E(q)\}\right]$, distinguished by quantum number q with $q = 0, 1, \ldots$. The corresponding eigenvalues are $E(q) = -\left(\frac{\hbar^2\mathcal{E}^2}{2m^*}\right)^{1/3} \mathrm{Ai}[0]_q$, where $\mathrm{Ai}[0]_q$ is the qth zero of the Airy function. [†]

The case of particular relevance to the quantum Hall regime occurs when the degree of freedom parallel to the magnetic field does not play a significant role. If we assume that

[†]Note that we chose a convention to label the Airy functions zeros starting from $q = 0$, i.e., $\mathrm{Ai}[0]_0 = -2.33811\ldots$, $\mathrm{Ai}[0]_1 = -4.08795\ldots$ etc.

the confining potential is steep enough such that the corresponding $E(q)$ eigenvalues are well separated, that is, $\hbar\omega_C \ll -\left(\frac{\hbar^2\mathcal{E}^2}{2m^*}\right)^{1/3}\mathrm{Ai}[0]_1 + \left(\frac{\hbar^2\mathcal{E}^2}{2m^*}\right)^{1/3}\mathrm{Ai}[0]_0$, then the system will lie in the lowest ($q = 0$) subband of the confining potential well. The only remaining degrees of freedom then are the Landau levels. Within the Hilbert space of the remaining n and m degrees of freedom, those states with the same n quantum number are then degenerate, but distinguishable by their m quantum number. Due to Pauli exclusion, electrons must singly occupy eigenstates $\psi_{nm}(z, \bar{z})$, such that no two electrons have the same quantum numbers n and m. It can be shown that the degeneracy per unit area is given by the number of magnetic flux quanta N_Φ per unit area, $N_\Phi = B/\Phi_0$, where $\Phi_0 = hc/e$.

The key feature of this particular two-dimensional band structure is that the energy spectrum is completely discrete: once a LL has been filled, then there will be a large energy gap (i.e. $\hbar\omega_c$ or $g\mu_B B$) to the next available LL. This feature was not present in the three-dimensional case because the k_3 momentum was (effectively) a continuous parameter, whereas now that degree of freedom has been restricted.

The existence of these energy gaps in the two dimensional LL band structure is essential to explain the integer plateaux observed in transport experiments (corresponding to the IQHE). Due to the degeneracy, B/Φ_0, of quantum Hall orbitals in a given LL, an integer filling factor corresponds to a completely filled spinless LL: $\nu = 1$ corresponds to a filled spin-down LLL, $\nu = 2$ corresponds to a completely filled LLL (both spin-up and spin-down), and so on. When the electron density is such that a LL is completely filled then, just as in ordinary band insulators, there is an energy gap to reach the next unoccupied electron state, leading to insulating behaviour, i.e. a minimum in the longitudinal conductivity and, hence, resistivity. The fact that these minima are broadened (in the sense that the resistivity minima occur over quite a wide region around each precise integer value of ν) can be understood by taking into account disorder (for more details, see, e.g., refs. [23, 26, 27]). The relatively small cyclotron energy gap also explains why these phenomena are only seen at low temperatures: the quantum mechanical regime is accessed when the thermal energy is less than the LL energy scale, i.e. when $\hbar\omega_C \gg k_B T$, where k_B is Boltzmann's constant.

One way to understand the quantized transverse resistivity is to take into account the physical boundary, or edge of the system in the plane perpendicular to the applied magnetic field, and to distinguish it from the bulk of the system contained within that boundary.[4,36] The quantized resistance plateaux can be understood as the condition that there are a certain number of extended, conducting edge modes that can be accessed: precisely one for each filled

LL (for more details, see, e.g., refs. [23, 26, 27]). Alternatively, the quantized Hall conductivity can be thought of as a "topological invariant" of the LL band structure.[42]

1.4 The Origin of the Fractional Quantum Hall Effect

1.4.1 Experimental Considerations

The FQHE case encompasses all the additional quantum Hall plateaux that are not explained by the integer effect, i.e. those plateaux occurring at special rational fractional filling factors. The fact that the density becomes pinned to particular values of ν implies that there should be a corresponding cusp in an energy vs. density curve at that fraction. That, in turn, implies a discontinuity, Δ, in the chemical potential.[15] According to the single particle picture, which so well explained the integer quantum Hall effect, there should be no energy gap for a fractionally filled LL—the cyclotron energy gap only applies to filled LLs. It must be the case, therefore, that this new energy gap emerges from many-particle interactions between electrons within the LLs. One concludes that the FQHE is an interaction-driven phenomenon that prominently demonstrates a complex substructure to the Landau levels, determined by the energy scale Δ, which is much less than the cyclotron energy scale separating the Landau levels.

Recall that the somewhat delicate transport properties associated with the quantum Hall effect are observed only at very low temperatures and are almost always only clearly visible in the purest (highest mobility) semiconductor samples. The low temperature regime can be understood as the condition that the temperature scale must be less than the energy gap, Δ, presumed to be associated with the effect. The condition for high mobility can be understood as the condition that the fluctuation in the disorder potential is not too large compared to Δ.[23] The fact that the fractional quantum Hall energy scale is much smaller than the cyclotron energy scale confirms the finding that to observe the fractional case the temperature and mobility constraints are much more stringent than for the integer case.

A crucial piece of observational evidence, in addition to the resistivity plateaux, is the direct measurement of such energy gaps, Δ.[43] The evidence can be found most readily in measurements of transport activation energy, which is determined by measuring the longitudinal resistivity, ρ_{xx}, as a function of temperature at a particular fixed filling factor, e.g., $\nu = 2/3$. The temperature dependence is fitted to an Arrhenius equation, $\rho_{xx} \propto \exp(-\Delta/2k_BT)$, and the energy gap Δ is extracted from data fitting. The fact that there is a finite energy gap for excitations above the ground state underlines a prominent property of the FQHE: that it

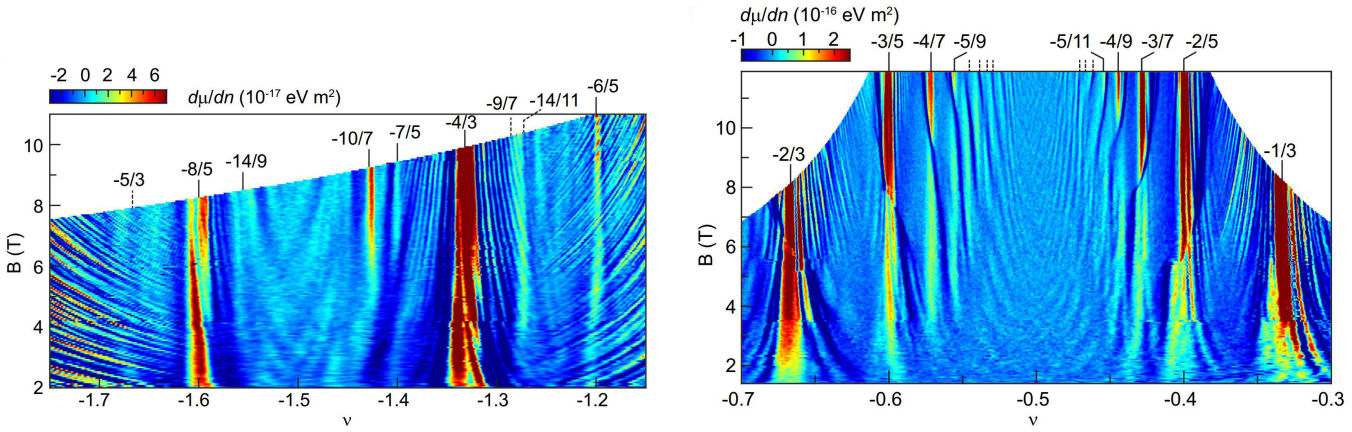

Figure 1.5: Local compressibility measurements performed in suspended graphene samples under high magnetic field. The red colour indicates incompressibility, and the blue color indicates compressibility. Local surface measurements of the electrostatic capacitance are made using a single-electron transistor (SET) placed above the graphene layer. The response of the capacitance measurement to electrostatic potential modulations from below the layer provides a local probe of the compressibility. Note that the band dispersion in graphene is relativistic, and that these data correspond to filling factors between the $n = 0$ and $n = -1$ Landau levels, which is denoted by filling factors $-2 < \nu < 0$ (including two spin species). Reprinted figures with permission from ref. [22], B. E. Feldman *et al.*, Phys. Rev. Lett. **111**, 076802 (2013). Copyright (2013) by the American Physical Society.

can be thought of as an *incompressible quantum fluid*. It is incompressible in the sense that changing the area by δA at constant filling factor requires an energy $\delta E = \nu|\delta A|\Delta/2\pi l_0^2$.

More direct and particularly striking evidence for the incompressible nature of the FQHE can be seen in measurements of the local compressibility in suspended graphene, shown in fig. 1.5. Suspended graphene is a naturally two-dimensional material, but, unlike semiconductor heterostructures, it has an exposed two-dimensional surface, and therefore the 2DEG be directly probed with, for instance, a single-electron transistor (SET). The local compressibility can be deduced by modulating an electrical potential beneath the graphene layer and measuring the corresponding local capacitance signal with the SET above the layer. The compressibility data convincingly demonstrate that for filling factors corresponding to certain rational fractions, the electronic structure is indeed highly incompressible. The results also demonstrate that for filling factors away from those particular rational fractions, the electronic structure remains compressible (i.e., away from the special rational fractional filling factors, the energy gap Δ closes).

1.4.2 The FQHE Hamiltonian

The FQHE can be described by a model Hamiltonian of the form

$$H_{\text{FQHE}} = \sum_j (H_0)_j + \sum_{j<k} V(|\mathbf{r}_j - \mathbf{r}_k|) + g\mu_B \sum_j \mathbf{S}_j \cdot \mathbf{B}, \tag{1.8}$$

where H_0 is the Hamiltonian for the noninteracting single-particle problem given in eq. (1.1), V is a two-body electrostatic interaction between particles at positions $\mathbf{r}_j$ and $\mathbf{r}_k$, and indices $j, k = 0, \ldots, N$ label the electrons, with N being the number of electrons in the system. The last term takes into account the combined Zeeman energy of the electrons due to their spin $\mathbf{S}_j$.

The simplest form for the interaction potential would be to assume that the electrons are point charges and that they interact via a (three-dimensional) Coulomb interaction,

$$V(|\mathbf{r}_j - \mathbf{r}_k|) = \frac{e^2}{\epsilon\,|\mathbf{r}_j - \mathbf{r}_k|},$$

where ϵ is the relative permittivity of the material. More realistically, the electron wave functions have some finite extent out of the plane of the 2DEG. The electrostatic interaction between electrons will then depend on the shape of the wave functions normal to the 2DEG plane (for instance, the Airy function wave functions corresponding to a triangular potential well). Such corrections to the potential are known as *finite-thickness corrections*.[33,44,45] For simplicity, finite thickness corrections are often neglected, as a first approximation.

For simplicity too, we also often neglect inter-Landau level effects, as a first approximation, and project the Hamiltonian onto a single LL (which can be justified by the large energy gap between LLs). Inter-Landau interactions can subsequently be added perturbatively. Such corrections are referred to as *Landau level mixing*.[46–51]

Let us now discuss how one can go about trying to solve the Hamiltonian eq. (1.8) ignoring the complication of Landau level mixing. A particularly interesting case will be the lowest Landau level (which corresponds to the quantum number $n = 0$), because in that case the many body wave functions are analytic polynomials in the electron co-ordinates z_j (excluding the Gaussian exponential factors). Also, given a solution in the LLL, corresponding solutions in higher LLs can be simply obtained using the LL raising operator defined in eq. (1.3). Projected to the LLL, the Hamiltonian is composed only of the interaction terms:

$$H_{\text{LLL}} = \sum_{j<k} V(|\mathbf{r}_j - \mathbf{r}_k|) + g\mu_B \sum_j \mathbf{S}_j \cdot \mathbf{B}. \tag{1.9}$$

Determining the solutions to this Hamiltonian, eq. (1.9), is particularly difficult because the of the interaction-driven nature of the FQHE, but this is one reason why studying the

problem has yielded such a wealth of interesting physics. The main stumbling block is that it is not possible consider the interactions as small perturbations to a non-interacting single-particle problem—the Hamiltonian contains only one scale of strong interactions. Instead we must solve the interacting problem from scratch.

The first step in the solution will be to construct the Fock space in which to describe the eigenfunctions of the Hamiltonian, eq. (1.8) in general [and eq. (1.9) in particular]. This Fock space is constructed from the Hilbert space of the single particle Hamiltonian, eq. (1.1) and is, therefore, expressed as set of occupation numbers for the single-particle orbitals defined in eq. (1.6), labelled by the quantum numbers m and n. If we project onto a the $n = 0$ LL then the states in the Fock space can be written as $\psi = |N_{m=0}, N_{m=1}, \ldots\rangle$, where $\sum_m N_m = N$ and N_m counts the number of electrons in the mth orbital, with $m = 0, 1, \ldots, N_\Phi$ and $N_m \in \{0, 1\}$ for fermions. The LLL Fock space is therefore spanned by *monomials* in the coordinates $z_1, \ldots, z_N$ (excluding the Gaussian factor). Ignore the spin degree of freedom for now, the general solutions to eq. (1.9) can then be expressed as

$$\psi(z_1, \ldots, z_N) = f(z_1, \ldots, z_N)\, e^{-\frac{1}{4}\sum_{j=1}^{N}|z_j|^2},$$

where $f(z_1, \ldots, z_N)$ is general linear combination of monomials, i.e. an analytic polynomial in the complex electron co-ordinates. Also, since this is a many-body wave function describing (spinless) fermions, $f(z_1, \ldots, z_N)$ must be a fully antisymmetric function.

In order for the Hamiltonian in eq. (1.9) to correctly reproduce experimental observations of the FQHE, the solutions must satisfy the following fundamental condition: there must be a cusp in the density vs. energy profile at precisely the filling factors corresponding to rational fractions, e.g. $\nu = 1/3$, that have been observed. There must be a corresponding energy gap, Δ, in the thermodynamic limit for neutral excitations above each ground state. This energy gap is to be understood as the gap for quasiparticle excitations occurring at exactly the filling factor at the density cusp, e.g., at $\nu = 1/3$. (Strictly speaking, since Δ is an activation energy, it is given by the sum of the excitation energies to create a quasielectron-quasihole pair in the thermodynamic limit.)

There are variety of approaches used to study its solutions in a number of special cases; in particular, it can be exactly solved numerically for very small system sizes, and also there are several approaches to approximate certain sets of solutions both numerically and analytically. In the following sections we shall provide a brief overview of some selected methodology.

1.5 Exact Solution for Finite-Sized Systems

1.5.1 Introduction to Pseudopotentials

In analyzing fractional quantum Hall physics an important tool is the Haldane pseudopotential.[52] The language of pseudopotentials not only provides a convenient parametrization of the problem but also makes it easy to write down certain model Hamiltonians that are solvable, thus providing a key piece of our understanding of the FQHE. The formalism is particularly useful in applications to exact numerical methods. We shall discuss the connection to exactly solvable cases later on, but for now we shall simply describe how the pseudopotentials are defined and how they can be used to parameterize the problem.

In the simple case where the interaction is two-body and there is a single species of spin-polarized electrons, the pseudopotential, V_L, is defined as the energy cost for two electrons to have a given relative angular momentum L. These pseudopotentials give a complete (and minimal) description of any rotationally and translationally invariant two-body interaction within a single LL.

Very generally, a wave function for two particles can be decomposed into relative and centre-of-mass components. For two-body wave functions within the LLL, we can write a complete basis:

$$\psi_{L,l}(z,\bar{z}) \equiv |L,l\rangle = |L\rangle \otimes |l\rangle$$

where l is the centre-of-mass angular momentum and L is the relative angular momentum (i.e., the relative angular momentum about the common centre-of-mass of the N particles). Explicitly we mean the centre-of-mass wave function is given by

$$|l\rangle = \frac{1}{\sqrt{2\pi l! 2^l}} (z_1+z_2)^l \, e^{-\frac{1}{8}|z_1+z_2|^2}$$

and the relative wave function is

$$|L\rangle = \frac{1}{\sqrt{2\pi L! 2^L}} (z_1-z_2)^L e^{-\frac{1}{8}|z_1-z_2|^2}, \tag{1.10}$$

It is important that these wave functions form a complete set. Physically we deal with particles that are either fermions or bosons and so in fact the space of two particle eigenstates exists only for odd L for fermions (or even L for bosons) in order to obey the correct symmetry.

To decompose a two-body interaction, such as that written in eq. (1.9) [ignoring the Zeeman term for now] into a basis of pseudopotentials, we define

$$V_L = \langle L| \, V(|\mathbf{r_1} - \mathbf{r_2}|) \, |L\rangle \, . \tag{1.11}$$

Since the interaction is translationally invariant, it is independent of the centre of mass degree of freedom of the two particles. [†] We can then rewrite the Hamiltonian given as

$$H = \sum_{j<k} V(|\mathbf{r}_j - \mathbf{r}_k|) \equiv \sum_{L,l} \sum_{i<j} |L, l\rangle \, V_L \, \langle l, L| \, , \tag{1.12}$$

where it is implied that in each term of the sum, the two-particle ket $|L, l\rangle$ involves particles i and j. Again, since the interaction is translationally invariant, interaction between particles i and j never changes their common centre of mass, so we may work with only the relative wave functions. Further, the interaction eq. (1.11) and, hence, the Hamiltonian eq. (1.12) is diagonal in L on account of the fact that the interaction potential is rotationally invariant and, therefore, conserves relative angular momentum. The intuition behind this rewriting of the Hamiltonian is that any two particles with relative angular momentum L incur an energy cost V_L. Pseudopotentials in higher LLs are defined in terms of the LLL pseudopotentials using the LL raising operator given in eq. (1.3).

1.5.2 Numerical Exact Diagonilzation

For small systems of electrons, eq. (1.9) can be solved exactly. In other words, it is possible, with sufficient computation resources, to determine the exact set of orbital occupation numbers and, hence, monomials, providing the exact ground state and quasiparticle excitation spectrum of eq. (1.9) for a given number of electrons N and for a given number of flux quanta N_Φ.

The first exact diagonalization study was undertaken by in ref. [53]. Following ref. [11], a Hamiltonian, such as that written in eq. (1.9), can be written in second-quantized form in terms of the fermion or boson creation and annihilation operators $\hat{c}_m$ and $\hat{c}_m^\dagger$, labelled by the angular momentum quantum number m (and, in general, the LL quantum number n, but let us only consider $n = 0$ here, and let us consider the spinless case).

$$H = \frac{1}{2} \sum_{\alpha,\beta,\gamma,\delta} V_{\alpha,\beta,\gamma,\delta} \hat{c}_\alpha^\dagger \hat{c}_\beta^\dagger \hat{c}_\gamma \hat{c}_\delta,$$

[†] We can define translationally invariant to mean that the wave function, excluding the Gaussian factor, is invariant under $z_i \to z_i + a$, applied for all $i = 1, \ldots, N$, with the same arbitrary complex number a.

where $\alpha, \beta, \gamma, \delta$ label the orbitals m and

$$V_{\alpha,\beta,\gamma,\delta} \equiv \langle \alpha\beta|H|\delta\gamma\rangle = \int d^2z \int d^2z' \psi_\alpha(z,\bar{z})^* \psi_\beta(z',\bar{z'})^* V(z-z') \psi_\gamma(z,\bar{z}) \psi_\delta(z',\bar{z'}), \quad (1.13)$$

where $\psi_m(z,\bar{z})$ are the single-particle LLL orbitals defined in eq. (1.7), and $V(z-z')$ represents a generic two-body interaction, such as Coulomb. Assuming a rotationally invariant interaction and inserting the definition of the pseudopotentials into eq. (1.13) results in a particularly simple expression for the matrix elements:

$$V_{\alpha,\beta,\gamma,\delta} = \sum_{L,l} V_L \langle \alpha\beta|L,l\rangle \langle l,L|\delta\gamma\rangle .$$

In this expression the integrals $\langle \alpha\beta|L,l\rangle$ and $\langle l,L|\delta\gamma\rangle$ will be the same regardless of the interaction $V(z-z')$. This interaction is entirely encoded in the values of the pseudopotentials V_L: it could be the Coulomb interaction, a modification of that to take into account e.g. finite thickness corrections, or any other two body interaction altogether, depending on the model in question.

To determine the exact energy spectrum for a given number of particles N and a given number of flux N_Φ one writes a matrix with elements

$$M_{ij} = \langle \psi_i|H|\psi_j\rangle ,$$

where the wave functions $\psi_i = |N_{m=0}, N_{m=1}, \ldots\rangle$ for $m = 0, \ldots, N_\Phi$ are a complete set of all the possible basis states in the Fock space for that given N and N_Φ. The size of the Fock space is given by $\binom{N_\Phi+1}{N}$ for fermions and $\binom{N+N_\Phi}{N}$ for bosons, so we see that the size of the matrix to be diagonalized grows exponentially with the system size. If we also take into account a spin-1/2 degree of freedom, then the Fock space grows larger still. Despite this limitation, the resulting matrices are very sparse, and there are a number of intrinsic symmetries that can be exploited in order to divide up the task into block diagonalizations.[11,54] Practically speaking, one is limited to at the very most $N \sim 20$ particles using even the very latest supercomputing systems.[54]

Using the convenient parameterization in terms of two-body pseudopotentials it is possible to determine the exact energy eigenvalues and exact eigenstates (polynomials) of any two-body interaction for small finite sized systems, in particular for the Coulomb interaction. Such results form one of the cornerstones of any argument proposing any solution to the quantum Hall Hamiltonian. A typical study of a FQHE model compares the ground-state energy and eigenvector overlaps between the exact numerical solution and a proposed trial solution for

accessible finite-sized systems. Let us now turn to methods used to determine appropriate trial solutions.

1.6 Single Component Trial Wave Functions

1.6.1 The Hartree–Fock Approach

The Hartree–Fock method has been extensively used to study the FQHE problem and was one of the first methods applied to it (see e.g. refs. [23, 24, 26]). The method amounts to the assumption that the many-body wave functions describing a system of electrons can be written as a single Slater determinant, and that the electron distribution can be determined iteratively, approximating the many-body interaction as a self-consistent mean field.[55,56]

In the FQHE context, the prediction of Hartree–Fock theory in the LLL is for Wigner crystal or charge density wave behaviour.[57] Physically, the Wigner crystal result can be understood simply as the electrons minimizing their mutual interaction energy by sitting as far apart as possible and with uniform density, in a crystal-like arrangement. Although this picture is physically very simple, it does not provide an explanation for the quantization of the Hall conductivity. In addition, comparisons of the Hartree–Fock predictions for the ground-state energy are found to be roughly 10% above the exact results for finite sized systems with a Coulomb interaction and for a range of LLL filling factors.[53] Although the Hartree–Fock approach does not provide an accurate explanation for the FQHE in the LLL, for higher LLs on the other hand, the predictions are expected to become much more accurate.[58]

1.6.2 The Variational Approach

The technique of variational wave functions has been very successfully applied to the study of the FQHE. In this specialized context, one typically postulates certain special analytical trial wave functions, although there is no true variational parameter in principle: the approach is variational only in the sense that a different trial wave function might give a better or worse bound on the energy eigenvalues of the exact solutions. Concurrently, the model wave function should be able to reproduce all the experimental observations, so just because it provides a better bound on the energy does not necessarily mean that the wave function is correct.[27]

For a given trial wave function, one can use the technique of variational quantum Monte Carlo to calculate, for instance, the associated density distribution or pair distribution functions. That information can then be used to calculate the associated energetic properties, such

as the Coulomb energy.[59–63] Some technical aspects of how the variational quantum Monte Carlo algorithm is applied to the study of FQHE trial wave functions are given in appendix A.

Shortly we shall discuss some of the most well studied trial wave functions that have been proposed for the FQHE. In almost all cases where the calculation is possible, properties such as the Coulomb energy have been found to be in extremely close agreement with the exact numerical solution for for finite-sized systems (to within fractions of 1%).

1.6.3 The Laughlin Wave Function

Laughlin's wave function is a trial ground-state wave function that was originally introduced to explain the $\nu = 1/3$ effect.[64] The insight of Laughlin was to propose the following wave function as a possible approximate solution to eq. (1.9):

$$\psi_{\text{Laughlin}} = \prod_{i<j}(z_i - z_j)^m \exp\left(-\frac{1}{4}\sum_i |z_i|^2\right).$$

This wave function is a (translationally invariant) analytic polynomial that resides in the Fock space of the LLL. Notably, it is also the unique exact highest density zero energy eigenstate of a special model interaction of a derivative of delta function form $\sum_{i<j} \nabla^{2(m-2)}\delta^{(2)}(z_i - z_j)$ for integers $m > 2$ (where $\nabla^2 \equiv 4\partial_z\partial_{\bar{z}}$).[65]

The filling factor of this wave function can be deduced as follows: consider calculating the electron density distribution, given by $\rho(z_1) = \int |\psi(z_1, \ldots, z_N)|^2 d^2z_2 \ldots d^2z_N$. To roughly see the solution to this integral, consider substituting in the Laughlin wave function and expanding out the brackets. In the integrand, one would find terms such as $|z_1|^{2m(N-1)} \exp\left(-\frac{1}{2}|z_1|^2\right)$, but no larger power of $|z_1|$. The maximum value of this one parameter function occurs at $|z_1| = \sqrt{m(N-1)}$ and, due to the Gaussian factor, the value of the wave function drops sharply as a function of $|z_1|$ immediately after its maximum. [†] Terms with lower powers of $|z_1|$ have maxima occurring at smaller values of $|z_1|$; indeed one can picture adding up all of the possible terms and finding that the electron density distribution lies on a uniform disc of radius $l_0\sqrt{2m(N-1)}$. [‡] The area of the disc is given by $2\pi m(N-1)l_0^2$. Since the disc is exposed to a magnetic flux density B the number of flux quanta is given by

$$N_\Phi = \frac{2\pi B l_0^2 m(N-1)}{\Phi_0} = m(N-1).$$

[†] To make the correspondence between the highest degree of z in the wave function and the number of flux enclosed more concrete one can work in the sphere geometry (see appendix B for the definition of the sphere geometry).

[‡] Once can perform the density integral, e.g. by a numerical Monte Carlo method, to confirm this.

In the thermodynamic limit, the filling factor is given by $\nu = N/N_\Phi = 1/m$ e.g. $\nu = 1/3$ for $m = 3$.

A key feature of Laughlin's theory is that the addition of magnetic fluxes such that the filling factor becomes slightly less than $\nu = 1/3$, is described by a quasiparticle wave function of the following form, e.g., for one quasihole at position z_0 one would write the wave function:

$$\psi = \prod_i (z_i - z_0) \prod_{i<j} (z_i - z_j)^m \exp\left(-\frac{1}{4}\sum_i |z_i|^2\right). \tag{1.14}$$

Intriguingly, the quasihole thus described has fractional charge e/m, and obeys fractional, or *anyonic*, exchange statistics, meaning that the exchange of two such quasiholes is associated with a phase $\exp(2\pi i\nu)$.[4,66] Contrast that with the case of boson wave functions, which pick up a factor of 1 when two bosons are exchanged, or fermions, which correspond to a factor of -1. One can also write quasielectron wave functions for the case where flux is removed: one way that these can be written is by replacing the z_i with the operator $2\partial/\partial z_i$ in the first factor written in eq. (1.14), where it is to be understood that such devatives do not act on the Gaussian exponential factor.[64]

Laughlin argued that the combination of one quasihole and one quasi electron excitation leads to an excited state occurring at the same filling factor as the ground state (i.e. exactly $\nu = 1/m$), and further that there is a finite energy gap for both types of excitation in the thermodynamic limit. Thus, such a combined excitation would give rise to the energy gap, Δ, in the thermodynamic limit. Drawing the energy vs. density profile of the Laughlin state, one finds, therefore, that there is a cusp occurring precisely for the $\nu = 1/3$ ground-state wave function. We see that Laughlin's model describes "an incompressible fluid with fractionally charged excitations".[64]

Laughlin's model evidently reproduces the experimentally observed features required and so provides a convincing explanation for stable ground states of the residual electrostatic interaction occurring at filling factors $\nu = 1/m$. We note that the special interaction for which Laughlin's wave function is the exact ground state is hardly reminiscent of the physical Coulomb interaction, but nevertheless the wave function itself turns out to be very close to the exact solution to the Coulomb Hamiltonian: it agrees with the exact ground-state energy and excitation energy to within a fraction of 1% for small finite-sized systems where comparisons can be made.[27]

A slight modification to Laughlin's theory, first proposed in refs. [67, 68], is to perform a *particle-hole conjugation* operation. This is in the sense of the standard band electrons

and band holes. In other words, a particle-hole conjugation operation restricted to a single LL, including both electron spin species, applied to a wave function describing filling factor ν results in an identical wave function for band holes occurring at filling factor $\nu_{\text{P–H}} = 2 - \nu$. In the Laughlin case, this describes filling factors $2 - 1/m$. [†]

Generalizations of the Laughlin wave function that can describe filling factors with numerators other than 1 (see fig. 1.4) were proposed in refs. [4, 52, 67]. The "hierarchy" construction proposes that the quasiparticles associated with a Laughlin state of electrons, themselves condense into a Laughlin state of quasiparticles. This procedure can be iterated as many times as required, and the resulting filling factors that can be described in this model are written as continued fractions with odd denominators, leading to trial wave functions for filling factors 2/5, 2/7, etc.

1.6.4 The Composite Fermion Model

An alternative method to generate trial wave functions that describe the same set of fractions as the hierarchy construction is given by the composite fermion (CF) model. Extensive reviews of the composite fermion model and its applications to the description of the FQHE can be found in refs. [27] and [28]. To summarize the main concepts, briefly: the key notion of CF theory is that the problem of strongly interacting two-dimensional electrons in a magnetic field can be roughly approximated by non-interacting fermions in an effective magnetic field. The direction of the effective magnetic field can be either parallel or antiparallel to the physical magnetic field. These non-interacting composite fermions (CFs) can be pictured as electrons bound to a certain number, $2p$, of magnetic flux quanta, which acts to reduce the effective magnetic field. In the effective magnetic field, there exist effective LLs. These are analogous to the LLs that occur for noninteracting electrons in the presence of a magnetic field. The FQHE of electrons is then interpreted as an integer quantum Hall effect of CFs with $2p$ fluxes attached and occupying a certain number n of the effective LLs.

The major successes of the CF model are a set of trial wave functions, constructed with the above picture in mind, that provide an extremely accurate description of the stable plateaux associated with the FQHE. [‡] Quantities, such as the energy gaps, calculated with CF trial wave functions are typically in excellent agreement with experiment. The principal filling

[†] We might also consider particle-hole conjugation within a LL of a single spin species only, and in that case $\nu_{\text{P–H}} = 1 - \nu$.

[‡] We note that the hierarchy construction leads to wave functions with the same topological characteristics as the CF wave functions, for instance the same quasiparticle statistics, however the CF wave functions are much more quantitatively accurate compared to experiments and to exact numerical results. [69]

factors encompassed by the CF model are given by

$$\nu_{\mathrm{CF}} = n/(2pn \pm 1)$$

for positive integer values of p and n (cf. fig. 1.4). The sign in the denominator corresponds to the direction of the effective magnetic field. The Laughlin wave function is built into the model, being the case of a + sign in the denominator and setting $n = 1$ and $p = 1$. Particle-hole conjugate CF states occur at filling factors $2 - \nu$. We shall discuss the forms of the CF trial wave functions in more detail during the course of presenting chapter 2 and so we shall omit further description at this stage.

One drawback of the CF model is that the trial wave functions it postulates represent an uncontrolled approximation to the exact solution to the Coulomb Hamiltonian, eq. (1.9), albeit they are extremely close to being exact for the LLL. Evidence of the exactness of the trial wave functions comes from comparison with numerical calculations of the exact solutions of the Coulomb Hamiltonian. Collected numerical evidence assessing the accuracy of CF trial wave functions is collected here in appendix D (see also ref. [27]). It is worth noting also that the FQHE in higher LLs (i.e., fractions with $\nu > 2$) is not thought to be so well described by the CF model.[27,70] Also, it is not yet known if the CF wave functions correspond to a particular exactly solvable model Hamiltonians (such as a derivative of delta function type), except for special cases such as the Laughlin wave function.[27]

1.6.5 Conformal Field Theory and the Moore–Read Wave Function

A clear omission from the set of filling factors encompassed by either the hierarchy model or the CF model is the even denominator FQHE observed, for instance, at $\nu = 5/2$, as can be seen in fig. 1.4. Although there has been some progress to understand the observation in terms of CF theory,[71,72] the 5/2 case can be much more satisfyingly understood using the approach of conformal field theory.

To describe in detail the connection between certain (rational) conformal field theories and the FQHE here would be somewhat tangential—and is not completely necessary for understanding the research topics presented in this thesis—nevertheless the connection will be referred to in chapter 4 and is relevant also to chapter 3. To put the research presented in this thesis into context, it is highly insightful to briefly summarize the approach.

Conformal field theory (CFT) itself is a quantum field theory of systems with symmetry under conformal transformations, that is, angle-preserving co-ordinate mappings.[73] Often, but

not exclusively, it is studied in two dimensional systems where the infinite dimensional group of conformal transformations is described by analytic functions (since any analytic function describes a conformal mapping). There are many factors that motivate the approach to describe aspects of the FQHE using the machinery of conformal field theory. Chief amongst these factors is that it provides a remarkable theory to describe the even-denominator effect at $\nu = 5/2$. Conformal field theory is a powerful mathematical framework with which to construct trial FQHE wave functions that are analytic polynomials satisfying certain vanishing rules, and with which to make predictions about the properties of the quasiparticles associated with these theories. The CFT approach is also closely related to other field theoretical approaches to describe the FQHE, which we shall not review here (see, e.g., refs. [74–77]).

An important breakthrough in the understanding of the $\nu = 5/2$ FQHE was the inception, in ref. [5], of trial wave functions constructed using a CFT argument. The ground-state Moore–Read or Pfaffian wave function can be written in the form

$$\psi_{\text{Moore–Read}} = \prod_{i<j} (z_i - z_j)^m \mathbf{Pf}\left[\frac{1}{(z_i - z_j)}\right] \exp\left(-\frac{1}{4}\sum_i |z_i|^2\right),$$

where m is a positive integer and $\mathbf{Pf}[M_{ij}]$ denotes the Pfaffian of a matrix M_{ij} whose elements in this case are given by $M_{ij} = 1/(z_i - z_j)$ if $i \neq j$ and 0 otherwise. [†] This wave function can also be understood as the exact highest density zero energy eigenstate of a three-body contact interaction (added to a two-body interaction $\sum_{i<j} \nabla^{2(m-2)}\delta^{(2)}(z_i - z_j)$ if $m > 2$).[78]

With $m = 2$, the Moore–Read wave function describes filling factor $\nu = 1/2$ (where no FQHE plateaux occurs). The 2nd LL version of this wave function [obtained by applying a LL raising operator, defined in eq. (1.3)] describes $\nu = 5/2$. [‡]

Quasiparticle excitations above this ground state possesses an energy gap and, crucially, exhibit *non-Abelian statistics*. What that means is that the exchange statistics associated with these quasiparticles are encoded in a non-commuting matrix. Contrast this with bosonic statistics, which is simply a factor of 1 when two particles are exchanged, or fermionic statistics, which corresponds to a factor of -1 [Laughlin or composite fermion quasiparticles pick up a phase angle of $\exp(2\pi i\nu)$ when two quasiparticles are exchanged].[4,27,66,82]

The concept of non-Abelian statistics has led to proposals for manipulation of quantum information, which would be encoded in non-Abelian exchanges, or braids, of such quasiparticles.

[†] Up to a sign, the Pfaffian is given by the square root of the determinant of the matrix M.

[‡] An alternative wave function to describe $\nu = 5/2$, known as the anti-Pfaffian, can be constructed from a (spinless) particle-hole conjugate of the Moore–Read wave function.[79,80] The particle-hole conjugation operation within a single LL will not, in principle, result in a different energy. However, when multiple LLs are taken into account, the particle-hole symmetry can be broken by terms that mix different LLs.[49–51,81]

These proposals are associated with the term "topological quantum computation".[3]

Finally, we note here that CFT is often associated with the study of two-dimensional critical phenomena. We stress that the FQHE plateaux are not critical phenomena, although transitions between different plateaux certainly are (see, e.g., ref. [83]). The connection with CFT is purely at the mathematical level of constructing analytic functions obeying certain symmetries and having certain vanishing properties.

1.7 The Multicomponent Nature of the FQHE

So far in our review of the FQHE we have almost completely ignored the spin of the electrons. In fact, there are many cases where we may want to consider a more complex model where electrons are endowed with additional degrees of freedom, such as a spin or valley index, and the FQH wave functions may not be fully polarized. In these situations we say that the wave function is *multicomponent*, meaning that it involves an important contribution from electrons having different values of these additional internal degrees of freedom. The multicomponent nature of the FQHE is the focus of the research presented in this thesis.

1.7.1 Examples of Multicomponent Systems

The simplest example of a multicomponent quantum Hall system is one with spin. In conventional GaAs systems, due to the small g-factor, even in fairly high fields, spin unpolarized or spin partially polarized quantum Hall states may occur.[12–14] The favorability of spin non-polarized states is generally determined by the ratio of the Zeeman energy per electron, $E_Z = g\mu_B B$ the energy associated with flipping a spin in magnetic field strength B, to the Coulomb energy per electron, the energy associated with the spatial configuration of electrons in the quantum Hall system. For many quantum Hall states (particularly composite fermion states), the Coulomb energy can be lower if spins are not fully polarized.[27] As a result, if the Zeeman energy is not too large, the most energetically favorable ground states may not be fully spin polarized. Furthermore, there are experimental methods to engineer an even smaller g-factor, making multicomponent models even more relevant.[84]

Valley degrees of freedom are another way which quantum Hall systems may be multicomponent. For example, in both AlAs quantum wells,[85] and graphene,[22,86–88] the band structure is such that each electron has a spin and valley degree of freedom. Analogous to the electron spin, in these cases, the valley index may take one of two possible values, so we think of the

valley as a "pseudospin" or "isospin". Silicon MOSFETs may be even more complicated: depending on the crystal orientation with respect the 2DEG layer, the electrons will have a valley index which takes one of two, four, or even six values.[89–92] Another important case where electrons have an additional degree of freedom is in quantum Hall bilayers, where the layer index plays the role of a pseudospin.[93–95] Two further applications are to systems where multiple Landau levels can be occupied where the internal degree of freedom would be the Landau level index, and systems such as wide quantum wells where multiple subbands play a role.[96] All of these multicomponent quantum Hall systems have been the subjects of intense theoretical and experimental study.

A number of promising techniques have been proposed that aim to mimic the physics of band electrons in a magnetic field with systems of finely tuned ultra cold atomic gasses. One method is to artificially place a gas of cold bosons in a rotating frame of reference, since doing so is mathematically identical to a system of charged particles in a magnetic field.[11] Another technique is to carefully engineer an artificial gauge field, which can be thought of as a tuned momentum shift applied in a spatially dependent manner.[97] At the time of writing, technical limitations prevent experiments from reaching the quantum Hall regime with such techniques, although it is anticipated that experimental realizations will eventually be possible. Bosons in cold atomic gas realizations of the quantum Hall regime, as compared to electrons, must have integer spin. One could easily imagine a quantum Hall effect of spin-1 bosons which would have three internal states rather than the two of an electron. Other possibilities for multi-component Bose systems exploit multiple hyperfine states of an atom, or multiple subbands that occur for bosons in a magnetic field on an optical lattice.[98,99]

1.7.2 Multicomponent Trial Wave Functions

The earliest theoretical model of a multicomponent quantum Hall wave function was proposed in ref. [15]. Halperin's wave function to describe a two-component system with $N/2$ spin-up electrons and $N/2$ spin-down electrons is written as

$$\psi_{\text{Halperin}} = \prod_{i<j}^{N/2}(z_i^{\uparrow} - z_j^{\uparrow})^{m_{\uparrow\uparrow}} \prod_{i<j}^{N/2}(z_i^{\downarrow} - z_j^{\downarrow})^{m_{\downarrow\downarrow}} \prod_{i,j}^{N/2}(z_i^{\uparrow} - z_j^{\downarrow})^{m_{\uparrow\downarrow}} \exp\left(-\frac{1}{4}\sum_{\sigma=\uparrow,\downarrow}\sum_{i=1}^{N/2}|z_i^{\sigma}|^2\right),$$

where $m_{\uparrow\uparrow}$, $m_{\downarrow\downarrow}$, and $m_{\uparrow\downarrow}$ are positive integers. This wave function is clearly a generalization of the Laughlin wave function to the multicomponent case, where now the Fock space is labelled by a spin degree of freedom $\uparrow$ or $\downarrow$ in addition to the degree, m, of the z variables.

Multicomponent wave functions are also very neatly encompassed by the CF model, where the effective LLs can be labelled by the multicomponent degree of freedom and the CFs can occupy a certain number of such multicomponent effective LLs: for instance a spin-singlet state can be written by having one effective LL occupied with spin-up CFs and one effective LL occupied with spin-down CFs. We shall discuss these multicomponent CF wave functions in considerable detail in chapter 2.

The Moore–Read wave function too has been generalized to a spin-singlet form, known as the non-abelian spin-singlet (NASS) state.[17] There is a whole host of other multicomponent wave functions that have been proposed.[6,18,100–104] In addition to these various ground-state trial wave functions, there has been considerable interest in multicomponent excitations, such as reversed-spin excitations,[59,105,106] and spin textures known as Skyrmions,[107–113] and also in valley nematic phases that are anticipated in quantum Hall systems.[114,115]

In chapter 2, we discuss the topic of phase transitions that occur between different multicomponent states as a function of certain system parameters. These transitions have been observed in a wide variety of different systems exhibiting the FQHE. In particular we use the two-component CF model to investigate the properties of transitions between quantum Hall ground states that occur at the same filling factor but have different uniform net degrees of spin or valley polarization. Motivation for this chapter comes from experimental work: there is an astonishingly rich selection of experimental measurements where such phase transitions are observed. In prior theoretical work studying these phase transitions, the CF model has proven highly successful. We shall discuss the prior experimental and theoretical work in detail in the chapter. Our work makes some important refinements and some significant extensions to the earlier theoretical work, including drawing several new conclusions that have been relevant to subsequent experimental work.

1.8 Fractional Quantum Hall Model Building

Let us now elaborate on the connection between pseudopotentials and exactly solvable model interactions in the case where interactions are of the conventional two-body form. Consider a model interaction potential $\nabla^2\delta^{(2)}(z)$, which is equivalent to the value of the V_1 pseudopotential being positive, but $V_L = 0$ for $L > 1$. In this case, we are imposing an energy cost for any two particles to have relative angular momentum of $L = 1$: the exact highest density zero energy state for N electrons (the highest density state for N electrons where no two electrons have

relative angular momentum of 1) is precisely the $\nu = 1/3$ Laughlin wave function.[52,65] † Because of this exact solvability for arbitrary N, much can be established in detail about this type of model Hamiltonian. While the model Hamiltonian may not be too similar to any particular physical Hamiltonian (such as the Coulomb Hamiltonian), nonetheless, the ground state may be very close to the physical one. More importantly, the ground state of the model gives an easily studied representative of an entire phase of matter.

The connection between exactly solvable model interactions written in terms of a small set of non-zero pseudopotentials and more physical interactions such as the Coulomb interaction can in principle be made more precise using arguments based on exact numerical studies. A fundamental argument that is often used in the validation of FQHE trial wave functions is the adiabatic connection between the contrived interaction that has, for instance, the Laughlin wave function as its exact ground state, and a physical interaction, such as the Coulomb interaction:[81,116] *If the spectrum of the contrived Hamiltonian and the physical Hamiltonian can be adiabatically connected without closing the thermodynamic energy gap between the ground state and the first excited state, then the properties of the phase of the contrived Hamiltonian (such as fractional charges and statistics) also occur in the physical system.* Practically, this argument could be implemented by interpolating the pseudopotentials between those of a contrived interaction (such as $V_1 > 0$ only) and those of a Coulomb interaction (which has all odd L V_L fixed for spinless fermions) and determining whether or not the energy gap closes. This task is non-trivial because it is often difficult to extrapolate to the thermodynamic limit using such small finite sized systems. Also, it is not possible to apply this approach to CF model wave functions, where exactly solvable Hamiltonians corresponding to the wave functions have not been constructed.[27]

Due to a large extent to interest in more exotic non-Abelian FQH states,[3] interest has turned from two body interactions (such as Coulomb) to N-body interactions with $N > 2$. While, in principle, such N-body interactions occur as a result of integrating out higher LLs,[117] and could, in principle, be engineered to exist in certain cold-atom systems,[118] the main interest in multi-body interactions is, again, due to the fact that certain interesting many-body wave functions are the exact highest density zero energy state of certain N-body interactions. The Moore–Read Pfaffian wave function is the exact highest density zero energy ground state of a model three-body interaction,[78] and, more generally, the Z_k Read–Rezayi wave function is

†More generally, for $\nabla^{4k-2}\delta^{(2)}(z)$ type interactions with positive integer $k = 1, \ldots$, the equivalent two-body pseudopotential representation contains non-zero contributions from all V_L pseudopotentials for $L = 2k-1, 2k-3, \ldots, 1$ (for spinless fermions). Nevertheless, a Laughlin wave function that is a zero energy eigenstate of, say $\nabla^6\delta^{(2)}(z)$, is also a zero energy eigenstate of $V_{L=3}$.[52,65] Similar arguments hold for other cases.

the highest density zero energy ground state of a $(k+1)$-body interaction.[119] Other interesting examples include the gaffnian[120] and Haffnian[121] wave functions, which, like the Pfaffian, are (highest density zero energy) ground states of special three-body interactions.

As with the simple case of two-body interactions, when studying FQH Hamiltonians with N-body interactions, it is quite useful to work with a generalization of Haldane's pseudopotential formalism to encompass multi particle interactions first proposed in ref. [122]. While this formalism is similar to that discussed by Haldane in that it decomposes the interaction into angular momentum components, it is somewhat more complicated because specifying the total relative angular momentum of N particles does not completely specify the relative wave function of the N particles as it does in the case of two particles. This complication is explained in detail in ref. [122]. Accounting for this complication, the multiparticle pseudopotentials can simply describe all of the special model Hamiltonians pointed out above (Moore–Read, Read–Rezayi etc.). In fact, in each of the above discussed cases, the Hamiltonian can always be described as simply forbidding any N particles from having relative angular less than some L.

All of the FQH states mentioned in this section so far describe spin-polarized or spinless system, i.e., the only degree of freedom for each electron is its orbital position. The added richness of multicomponent systems has made them a prime place to search for new FQH physics. In the search for novel non-Abelian FQH systems, several multicomponent candidates have been proposed,[6,17,18,101–104] including the so-called non-abelian spin-singlet (NASS) states[17] and the spin-charge separated states[102] for the two component case, as well as generalizations of these constructions to higher numbers of components.[103,104] Analogous to the situation with single component wave functions, many of these novel multicomponent wave functions are exact ground states of special N-body interactions. Here, however, interactions may be more complicated, depending on the spin-state as well as the position of the particles. While the concept of two-body Haldane pseudopotentials was generalized to the multicomponent case in refs. [106, 123–126], the multiparticle pseudopotential formalism introduced in ref. [122] did not consider multicomponent interactions. As such, it seems natural to try to generalize the pseudopotential formalism to the case of multicomponent N-body interactions. This goal will be the focus of chapter 3.

As in the single component case, the motivation for developing the pseudopotential formalism for multicomponent many-body-interactions is severalfold. On the one hand, pseudopotentials provide a complete parametrization of the problem for such systems. The usefulness of this is evidenced by recent works which have introduced pseudopotentials for multicomponent

many-body interactions for important special cases.[117,127] More importantly, the pseudopotential structure hints at what sorts of simple Hamiltonians may be written such that interesting quantum Hall states might be found as the highest density zero energy state of a particular set of pseudopotential coefficients.

In chapter 4, we present some of the details of a novel exactly solvable model, the first example of a model constructed in the framework of the generalized pseudopotentials presented in the preceding chapter. This spin-singlet trial wave function describes a thermodynamicly gapless compressible quantum fluid occurring at $\nu = 4/9$ for fermions, or $\nu = 4/5$ for bosons.

CHAPTER 2

Spin and Valley Transitions

In this chapter,[†] we study phase transitions between fractional quantum Hall (FQH) states of different uniform net degrees of spin or valley polarization, occurring for principle filling factors $\nu = 2/3$, $3/5$, and $4/7$ and their particle-hole conjugates at $\nu = 4/3$, $7/5$, and $10/7$. We describe how many aspects of these 'spin transitions' or 'valley transitions' can be understood in the context of a composite fermion (CF) model with spin-1/2 or two-valley degree of freedom, previously used to study spin transitions at filling factors $\nu = 2/5$, $3/7$ and $4/9$. At each of these fractions, there are several possible CF model wave functions that can be written down, with different spin polarizations depending on how many spin-up or spin-down CF Landau levels (LLs) are occupied. For the $\nu = 2/3$, $3/5$, and $4/7$ cases, we calculate the ground-state energy of the possible composite fermion wave functions and we predict transitions between ground states of different net spin polarization as the ratio of Zeeman energy to Coulomb energy is varied (or, equivalently, transitions between ground states of different net valley polarization as the ratio of valley splitting energy to Coulomb energy is varied).

Several experiments have observed such transitions and have made measurements of the critical Zeeman energy or critical valley splitting energy at which transitions occur, and we make direct comparison of CF theory predictions with these measurements. For more detailed comparison between theory and experiment, we include finite-thickness effects in our calculations for $\nu = 2/3$, $3/5$, and $4/7$ and we also implement finite thickness corrections for the $\nu = 2/5$, $3/7$ and $4/9$ cases where the effect was not previously taken into account. We find that the finite thickness correction in some cases partly accounts for the particle-hole asymmetry observed in spin transition measurements. For the lowest Landau level (LLL) case we find reasonable qualitative agreement between the experiments and CF theory. Finally, we consider CF states at filling factors $\nu = 2+2/3$, $2+3/5$, $2+4/7$, $2+2/5$, $2+3/7$, $2+4/9$ in the second Landau level (2nd LL), the 2nd LL being the next LL above the LLL. CF theory predicts a spin transition for $\nu = 2+2/3$ but not for any other fraction in the 2nd LL. This is consistent with experimental evidence of a spin transition at $\nu = 2+2/3$, but inconsistent with experimental evidence of a spin transition at $\nu = 2+2/5$.

[†]The material presented in this chapter is based, in part, on the publication S. C. Davenport and S. H. Simon, Phys. Rev. **B 85**, 245303 (see ref. [128]).

The structure of this chapter is as follows: first, in sec. 2.1 we shall briefly review selected experimental studies of spin and valley transitions; in sec. 2.2 we shall summarize the qualitative predictions of CF theory and then we shall write down the explicit forms of the CF wave functions that we are interested in. In sec. 2.3 we shall present the results for the Coulomb energy of the various ground-state trial wave functions in the LLL and 2nd LL, the critical Zeeman energy predicted by CF theory for the LLL and 2nd LL and the results of the finite thickness correction. We shall also compare our results to the experimentally measured values of the critical Zeeman energy in the LLL and in the 2nd LL. Finally, we shall make some remarks on our findings in sec. 2.4.

2.1 Observations of Spin and Valley Transitions

The degree of spin polarization of quantum Hall fluid has been explicitly measured as a function of the ratio of Zeeman to Coulomb energy for a variety of filling factors and in a number of different experiments in GaAs systems.[12–14,20,21,129–131] In this chapter we will principally focus on refs. [14] and [12] for the LLL case and refs. [21] and [20] for the 2nd LL case, where detailed comparison to our theoretical work is possible.

In ref. [14] a non-trivial net spin polarization is observed in GaAs heterojunctions at the following filling factors in the LLL: $\nu = 2/3$, $3/5$, $4/7$, $2/5$, $3/7$ and $4/9$. In these experiments the aim is to keep the filling factor fixed while varying the ratio of the Zeeman to the Coulomb energy. This is achieved by varying both the applied field strength and the density of electrons in the sample, keeping their ratio (hence ν) fixed. For each filling factor, plotting the net spin polarization as the field strength is varied, the experiments report a set of plateau with constant spin polarization, punctuated by a series of relatively sharp transitions (see fig. 2.1). Similar conclusions can be inferred from data presented in ref. [12] at filling factors $\nu = 4/3$, $7/5$, $10/7$, $8/5$, $11/7$ and $14/9$, also from GaAs heterojunctions. For high field and high electron density, the spin is polarized, but as the field strength and electron density are reduced, there are transitions to FQH states of successively smaller net spin polarization until, finally, some lowest value of net spin polarization is reached, with the particular lowest value depending on the filling factor. These transitions are observed to occur at some critical values of the applied field, B^{crit}, and there is, therefore, a corresponding critical Zeeman energy per electron, $E_Z^{\text{crit}} = g\mu_B B^{\text{crit}}$ (note that the g factor is material dependent, but the Bohr magneton is a constant). In refs. [21] and [20] similar spin transitions have been reported in GaAs systems at filling factors $8/3$ $(2 + 2/3)$ and $12/5$ $(2 + 2/5)$ respectively. In ref. [13] the Zeeman energy

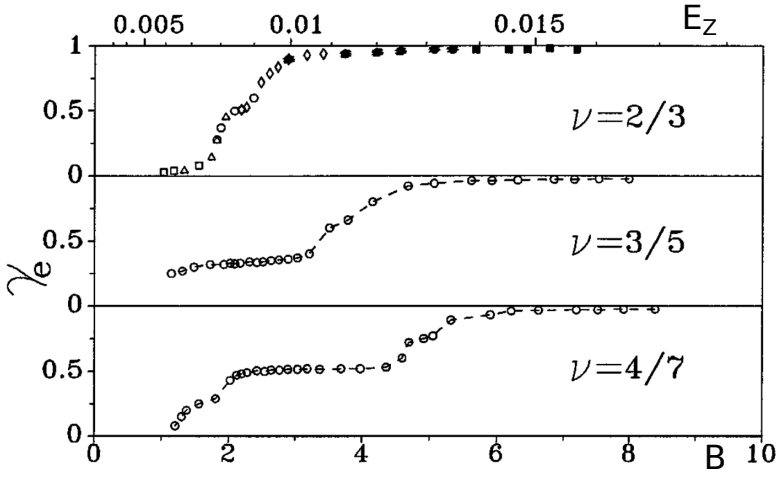

Figure 2.1: Measurements of the degree of spin polarization, $\gamma_e = \frac{N_\uparrow - N_\downarrow}{N_\uparrow + N_\downarrow}$, vs. magnetic flux density B and Zeeman energy per particle E_Z (in units of the Coulomb energy), for selected filling factors. Spin transitions are indicated at the relatively sharp changes in γ_e punctuating regions of roughly constant γ_e, as a function of B. Reprinted figure with permission from ref. [14], I. V. Kukushkin *et al.*, Phys. Rev. Lett. **82**, 3665 (1999). Copyright (1999) by the American Physical Society.

is tuned by exploiting the hydrostatic pressure dependence of the g-factor in GaAs,[132] rather than by changing the magnetic field; in this experiment, features associated with spin transions are measured at filling factors 2/5, 4/7 and 4/9.

The fractional quantum Hall effect present in systems such as AlAs, Si or graphene, possesses a valley degree of freedom, in addition to a spin degree of freedom. This valley degree of freedom corresponds to the presence of multiple conduction band minima (up to six for Si[89–92] and up to three for AlAs,[19,85] depending on the crystal plane and the design of the heterostructure or quantum well) or Dirac cones (two for graphene[86–88]). Under certain conditions, for instance AlAs placed under axial strain, the multiple conduction band minima (valleys) can be non-degenerate and the splitting energy, E_V, between the valleys can be tuned by varying an external parameter, in this case the applied strain. In such situations the ratio of the valley splitting energy to Coulomb energy plays an analogous role to the ratio of Zeeman to Coulomb energy in the spin case.

In refs. [19] and [133] analogous valley transitions between the two lowest lying conduction band minima are reported in AlAs systems placed under axial strain, at the following filling factors in the LLL: ν = 4/3, 7/5, 10/7, 13/9, 8/5, 11/7 and 14/9. In ref. [134] a valley transition was also measured in AlAs at filling factor 2/3. These measurements are achieved by varying the axial strain (hence valley splitting energy) and keeping the ratio of magnetic field to electron density (hence ν) fixed (since the magnetic field is fixed, spin transitions are

not expected to occur, and we assume that the spin is always fully polarized). For each filling factor, as the strain is varied, the experiments report a valley polarized state for high values of strain, with a single transition to a partially valley polarized state below a critical value of the valley splitting energy E_V^{crit}.

Concerning Si systems, ref. [92] reports that valley transitions occur between the two lowest lying band minima (valleys) as a function of the relative anisotropy of the valleys, tuned via the applied magnetic field. Valley transitions are indicated at the following filling factors in the LLL: $\nu = 8/5$, $14/9$, $20/13$, $22/15$, $16/11$, $10/7$, $4/3$, $6/5$, and $14/11$. Due to the more complicated nature of these transitions, we shall not make any direct comparisons of our results with these experiments.

Finally, in ref. [22] a limited series of phase transitions, reminiscent of either spin or valley transitions have been identified in FQH measurements in suspended graphene systems at LLL filling factors $-2/3$, $-3/5$, $-4/7$, $-5/9$, $-2/5$, $-3/7$, $-4/9$ and $-5/11$ (see also fig. 1.5). Concurrent theoretical work argues that these are expected to be signatures of spin transitions and not of valley transitions.[135]

2.2 Theory of Composite Fermions with a Spin or Valley Degree of Freedom

2.2.1 Qualitative predictions of CF theory

From a theoretical perspective, an insightful phenomenological understanding of the fractional quantum Hall effect (FQHE) has been acquired via the concept of the composite fermion (CF).[27] (See also chapter 1 for a brief summary). The principal set of filling factors encompassed by CF theory are given by

$$\nu = n/(2pn \pm 1) \tag{2.1}$$

where the sign here indicates the direction of the effective field relative to the real magnetic field, p is an integer such that $2p$ is number of 'attached fluxes', and there n is a positive integer denoting the number of filled effective LLs. Taking into account the two spin species, particle-hole conjugate versions of these states occur at filling factors $2 - \nu$.

In CF theory, trial quantum Hall states with a spin or valley degree of freedom can be constructed by simply associating that degree of freedom with the CFs themselves.[16,27] CFs of each spin or valley species can independently occupy a non-negative integer number $n_\uparrow$ and $n_\downarrow$ of

effective LLs; the filling factor remains as in eq. (2.1), but now with $n = n_\uparrow + n_\downarrow$. Consequently a whole series of CF wave functions is possible at each filling factor (a visualization of such a series of states can be found in refs. [27] and [16] and a modified version is presented here in fig. 2.2).

The experiments of refs. [14, 22] examined the $p = 1$ series for $n = 2, 3, 4$ with both positive and negative effective magnetic fields: $\nu = 2/5, 3/7$ and $4/9$ in the positive effective magnetic field case and $\nu = 2/3, 3/5$ and $4/7$ for the negative effective field case. refs. [12, 133] examined the particle-hole conjugates of these states at filling factors $2 - \nu$. For each filling factor the set of possible spin-dependent states is deduced by considering all possible non-negative integer values of $n_\uparrow$ and $n_\downarrow$ satisfying $n = n_\uparrow + n_\downarrow$. For a system of $N_\uparrow$ spin-up electrons and $N_\downarrow$ spin-down electrons, we shall define the "degree of spin polarization" by $\gamma_e = \frac{N_\uparrow - N_\downarrow}{N_\uparrow + N_\downarrow}$ and in the thermodynamic limit, where each effective LL contains the same number of electrons, it follows that

$$\gamma_e = \frac{n_\uparrow - n_\downarrow}{n_\uparrow + n_\downarrow}. \tag{2.2}$$

A description of the possible CF theory ground-states is summarized in fig. 2.2. (These definitions would equally well apply to a two-valley system by relabeling the spin up and down by a valley index.) Let us consider the interpretation in the spin case: if the Zeeman energy is sufficiently large, then it is expected that the spin will be fully polarized, and so in high magnetic fields the system is pictured by the rightmost diagrams in fig. 2.2. We then reduce the applied field, keeping the filling factor fixed by lowering the electron density at the same rate. When the critical field B^{crit} is reached, then it is energetically favorable for a transition to one of the states with lower net spin polarization, pictured in the diagrams successively to the left in fig. 2.2. This is energetically favorable as long as the difference in Coulomb energy between the two ground-state configurations compensates for the increase in Zeeman energy due to the spin depolarization.

At this juncture we reiterate the point introduced in chapter 1 that, ideally, the exact eigenstates associated with a quantum Hall system would be calculated by diagonalizing the Coulomb interaction within a given LL. As this calculation is intractable, except for very small systems, we rely instead on evidence that, for small finite-sized systems, CF trial wave functions provide strict upper bounds on, and very good approximations to, the ground-state energy, and have very high overlaps with the exact ground-state wave functions. Such is the case for both spinless and spinful quantum Hall systems (detailed evidence is collected here in appendix D;

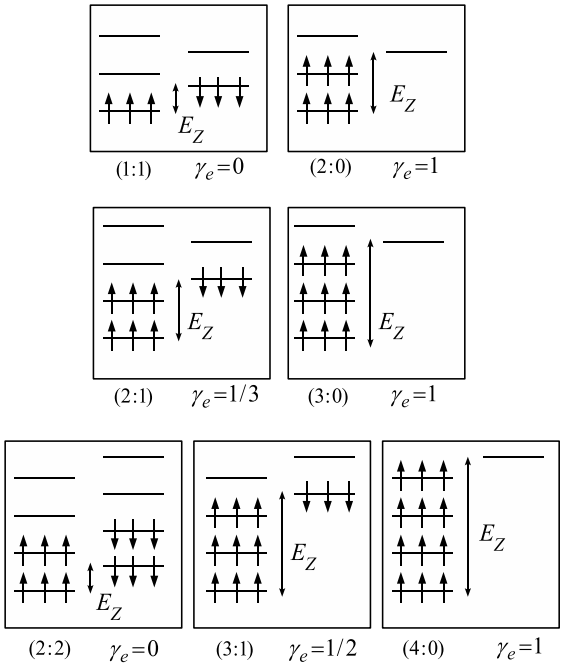

Figure 2.2: A Summary of the qualitative predictions of CF theory (modified from a similar figure in ref. [16]). The figure shows the filling of effective LLs with spin-up and spin-down composite fermions. Different cases are labelled by their quantum numbers $n_\uparrow$ and $n_\downarrow$, the number of filled spin-up and spin-down LLs, e.g., (1:1) denotes $n_\uparrow = 1$ and $n_\downarrow = 1$. The degree of spin polarization γ_e is calculated using eq. (2.2).

see also ref. [27] and references therein). Therefore, we expect CF trial wave functions to provide an accurate description of the physics of spin transitions for finite-sized systems and also in the thermodynamic limit.

Comparing these qualitative predictions to the experimental results presented in ref. [14], we find that the predictions for the number of transitions and for the degrees of spin polarizations are broadly correct as a first approximation (assuming, for the time being, that all possible transitions are energetically favorable and so always occur). In practice, the transitions are somewhat broadened and it is apparent that there are some small second-order plateaux occurring between the main transitions (see fig. 2.1). These effects are not well understood (see, e.g., ref. [27]) and so presently we shall only focus on the leading-order effects. Further, we shall assume that the experiment is an observation of ground-state quantum Hall behavior.

2.2.2 Quantitative predictions of CF theory

Transitions between quantum Hall ground-states with different spin/valley polarizations occur when the difference in Coulomb energy per electron between the two ground-state configurations compensates for the increase in Zeeman energy or valley splitting energy per electron due to

the spin/valley depolarization. The differences in the Coulomb energies per electron of various ground states at the same filling factor thus can be related to the critical Zeeman energy (or critical valley splitting energy) per electron for transitions between the various polarizations of the quantum Hall fluid.

By calculating the Coulomb energy per electron for composite fermion trial wave functions, Park and Jain were able to obtain theoretical predictions of the critical Zeeman energies per electron for filling factors $\nu = 2/5, 3/7$ and $4/9$ (the positive effective field case).[16] Their results for the predicted values of the critical Zeeman energy per electron for these three filling factors, for the most part, agree well with the values measured in both refs. [12] and [14]. For a technical reason, which we shall shortly allude to, these authors did not perform the same calculation and comparison for filling factors $\nu = 2/3, 3/5$ and $4/7$ (the negative effective field case).

CFs have been the subject of a great deal of theoretical analysis and there are well-developed techniques which have been established for calculating the associated Coulomb energy with trial ground-state wave functions using the Metropolis Monte Carlo procedure (see, e.g., refs. [16, 62, 63]). Nevertheless, for sufficiently large numbers of particles, the numerical evaluation of the trial wave functions with negative effective field turns out to be highly non-trivial—and much more complex than the positive effective field case—and, as such, prior to this work the associated Coulomb energies had not yet been accurately calculated in the thermodynamic limit for all the relevant cases (the spin polarized negative effective field case was first studied in ref. [63], but only for systems up to size $N = 16$–28, which is not sufficiently large to obtain accurate results for our calculation of the critical Zeeman energy). For the series of states of interest here, it proved necessary to design a new algorithm to perform the required calculations. The details of the algorithm are discussed in appendix C.

In this chapter we will present the results of our calculations of the Coulomb energy for the negative effective field case, we shall evaluate the critical Zeeman energies (or equivalently critical valley splitting energies) for transitions between different spin/valley states and then we shall compare our results to the relevant experimental measurements. As a first approximation, we calculate the interaction energy associated with the CF trial wave functions using a simple Coulomb interaction potential. Such an interaction would apply to a perfectly 2D geometry; however, a laboratory quantum Hall system cannot be considered perfectly 2D and more realistic model interactions must take into account the finite extent of the system in the direction perpendicular to the 2D plane. To study the effect of such a modification to the theory, we implement an interaction which takes into account finite-thickness effects for the

appropriate material (see, e.g., ref. [45]). Finally, we calculate the Coulomb energy appropriate for the 2nd LL analogies of the LLL CF trial wave functions discussed previously (i.e., filling factors $\nu = \nu_{\text{LLL}} + 2$). As neither the finite-thickness correction nor the 2nd LL potential was considered in the positive effective field study in ref. [16], we present our results for both positive and negative effective field filling factors.

2.2.3 LLL Composite Fermion Wave Functions in the Sphere Geometry

In order to study the bulk properties of a quantum Hall ground state we must choose a geometry that eliminates boundary effects. We have chosen to use the spherical geometry for this purpose, i.e., we shall study various finite-sized FQH states existing on the surface of a sphere.[52] To effect a magnetic field perpendicular to the surface of a sphere we must place a magnetic monopole at its centre such that the electrons see N_Φ flux quanta. As we increase the system size the total flux increases, but to fix the flux density at the surface of the sphere, the radius of the sphere must also increase. On extrapolation to the thermodynamic limit, therefore, a flat geometry is recovered and the edge effects are eliminated.

We shall now describe how CF states can be expressed as co-ordinate wave functions in the sphere geometry, in terms of the spinor co-ordinates u_i and v_i. (See appendix B for a more detailed discussion of the sphere geometry.)

Spin polarized CFs

The CF wave function describing interacting electrons in magnetic field B can be succinctly expressed as

$$\psi_{p,n} = \hat{P}_{\text{LLL}} \left[\Phi_0^{2p} \Phi_n \right], \tag{2.3}$$

where

$$\Phi_0 = \prod_{i<j} (u_i v_j - u_j v_i)$$

and where $\hat{P}_{\text{LLL}}$ denotes projection onto the lowest Landau level (LLL). Φ_n is a Slater determinant of non-interacting single-fermion wave functions with an effective magnetic flux which we denote by $2Q$ (i.e., the noninteracting fermions see $2Q$ flux quanta). The quantity Q is known as the effective monopole strength: it can take positive or negative integer or half-integer values.[27] The corresponding effective magnetic field thus can be aligned either parallel

or antiparallel to the real magnetic field. The intuition is that Φ_n represents an integer quantum Hall wave function for composite fermions in an effective magnetic field and with effective filling $n = \lim_{N\to\infty} N/(2Q)$, i.e., the number of occupied effective LLs is an integer n. For a finite sized system, $N/(2Q)$ may be slightly shifted from its thermodynamic value. CF wave functions are often simply denoted as ${}^{2p}\mathrm{CF}_n$ or ${}^{2p}\mathrm{CF}_{-n}$ where the sign corresponds to the sign of the effective field and n is now a positive integer.[27] We shall adopt this nomenclature for the remainder of our discussion. The CF states occur at filling factors given in eq. (2.1). We shall always consider non-interacting CFs.

Practically, the CF states are constructed as follows: for a system of N spin polarized electrons in the spherical geometry filling n CF LLs, the effective monopole strength is given by

$$Q = \pm\frac{N - n^2}{2n}, \tag{2.4}$$

with the sign depending on the sign of the effective magnetic field, B_{eff}. The magnetic flux experienced by the electrons due to the magnetic field B is then given by $N_\Phi = 2p(N-1)+2Q$ [from eq. (2.3)]. In the sphere geometry, the single-particle CF eigenfunctions are the set of what are called *monopole harmonics*.[27] These monopole harmonics are eigenfunctions of the effective LL with eigenvalue $n' = 0, \ldots, n-1$, of the orbital angular momentum with eigenvalue $l = |Q|, |Q|+1, \ldots, |Q|+n'$, and of the z component of orbital angular momentum with eigenvalue $m = -l, -l+1, \ldots, l$. It is simple to check that given eq. (2.4) the total number of single particle states is $\sum_{i=0}^{n-1}(2(|Q|+i)+1) = N$. For $Q < 0$, the monopole harmonics are of the following form[27,63]:

$$\begin{aligned} Y^{Q<0}_{n',m}(u_i, v_i) = (-1)^{n'} M_{Q,n',m} (u_i^*)^{-Q+m} (v_i^*)^{-Q-m} \\ \times \sum_{s=0}^{n'} (-1)^s \binom{n'}{s} \binom{2|Q|+n'}{|Q|+m+s} (u_i^* u_i)^s (v_i^* v_i)^{n'-s}, \end{aligned}$$

where i indicates the particle number and will run from 1 to the total number of particles N. Here $M_{Q,n',m}$ is an unimportant normalization factor. We can then write the Slater determinant as

$$\Phi_n = \det\left[Y^Q_{n',m}(u_i, v_i)\right] = \begin{vmatrix} Y^Q_{0,-|Q|}(u_1,v_1) & \cdots & Y^Q_{0,-|Q|}(u_N,v_N) \\ \vdots & & \vdots \\ Y^Q_{0,|Q|}(u_1,v_1) & \cdots & Y^Q_{0,|Q|}(u_N,v_N) \\ Y^Q_{1,-|Q|-1}(u_1,v_1) & \cdots & Y^Q_{1,-|Q|-1}(u_N,v_N) \\ \vdots & & \vdots \\ Y^Q_{n-1,|Q|+n-1}(u_1,v_1) & \cdots & Y^Q_{n-1,|Q|+n-1}(u_N,v_N) \end{vmatrix}.$$

In order to implement the LLL projection required by eq. (2.3), we follow the method introduced by Jain and Kamilla,[62] and then extended for the case of a negative effective field by Möller and Simon.[63] From a computational perspective, for large system sizes, the LLL projection of the Slater determinant is completely impractical (see ref. [27] for details of the LLL projection). The issue can be circumvented by moving the Jastrow factor inside the determinant and then applying $\hat{P}_{\mathrm{LLL}}$ to each of the resulting matrix elements first, before calculating the determinant:

$$\psi_{p,n} \approx \det\left[\hat{P}_{\mathrm{LLL}}\left(Y^{Q}_{n',m}(u_i,v_i)J_i^p\right)\right], \tag{2.5}$$

where

$$J_i = \prod_{j\neq i}(u_i v_j - u_j v_i)\,.$$

Although the result of this procedure is not mathematically identical to eq. (2.3), the resulting trial wave function would nevertheless describe fermions in the LLL, and the two prescriptions have been found to be extremely similar in cases where they can be compared to exact diagonalization of the Coulomb interaction.[27] An expression for

$$\hat{Y}^{Q}_{n',m}(u_i,v_i)J_i^p \equiv \hat{P}_{\mathrm{LLL}}\left(Y^{Q}_{n',m}(u_i,v_i)J_i^p\right)$$

in negative effective field was derived in ref. [63] and is given by

$$\hat{Y}^{Q}_{n',m}(u_i,v_i) \propto \sum_{s=0}^{n'}(-1)^s\binom{n'}{s}\binom{2\,|Q|+n'}{|Q|+m+s}u_i^s v_i^{n'-s}\left(\frac{\partial}{\partial u_i}\right)^{|Q|+m+s}\left(\frac{\partial}{\partial v_i}\right)^{|Q|-m+n'-s}.$$

Using this result, eq. (2.5) for the CF wave function can then be rewritten as

$${}^{2p}\mathrm{CF}_{-n} \equiv \psi_{p,n} \approx \det\left[\hat{Y}^{Q}_{n',m}(u_i,v_i)J_i^p\right], \tag{2.6}$$

In appendix C we discuss an efficient technique for numerically evaluating such wave functions.

CFs with spin

If the CFs have a spin degree of freedom, then we must associate a spin degree of freedom with the single-particle monopole harmonic wave functions (the valley case is constructed identically, so we shall revert to the spin language for the present discussion). Let us say we have N CFs with one of two possible spin polarizations, that is, $N_\uparrow$ spin-up CFs and $N_\downarrow$ spin-down CFs. These CFs can then independently occupy a number $n_\uparrow$ and $n_\downarrow$ of spin-up or spin-down effective LLs. The value of p is independent of the spin degree of freedom, since it is not involved in the

single particle monopole harmonic functions. The spin CF wave functions are of the general form:

$$\psi_{p,(n_\uparrow,n_\downarrow)} = \hat{P}_{\rm LLL}\left[\Phi_0^{2p}\Phi_{n_\uparrow}\Phi_{n_\downarrow}\right], \tag{2.7}$$

where the Slater determinants $\Phi_{n_\uparrow}$ and $\Phi_{n_\downarrow}$ are formed from monopole harmonics with the following structures:

$$Y^Q_{n'_\uparrow,m_\uparrow}(u_i,v_i)\otimes|\uparrow\rangle \quad , \quad Y^Q_{n'_\downarrow,m_\downarrow}(u_i,v_i)\otimes|\downarrow\rangle\,.$$

The effective monopole strength is now given by:

$$Q = \pm\frac{N_\uparrow - n_\uparrow^2}{2n_\uparrow} = \pm\frac{N_\downarrow - n_\downarrow^2}{2n_\downarrow}. \tag{2.8}$$

The possible eigenvalues of the monopole harmonics are now $n'_\uparrow = 0,\ldots,n_\uparrow$, $l_\uparrow = |Q|,\ldots,|Q|+n'_\uparrow$ and $m_\uparrow = -l_\uparrow,\ldots,l_\uparrow$, and similarly for the spin-down versions. Once we construct a Slater determinant of such states we can factor out the antisymmetric spin part of the wave function, and we only need to specify the spatial part.[27]

In accordance with the notation of ref. [27], we denote the series of spin un-polarized CF wave functions by ${}^{2p}\mathrm{CF}_{(n_\uparrow,n_\downarrow)}$ or by ${}^{2p}\mathrm{CF}_{(-n_\uparrow,-n_\downarrow)}$ if the effective field is antiparallel to the magnetic field, with $n_\uparrow$ and $n_\downarrow$ being positive integers (it is not possible to have positive $B_{\rm eff}$ for one spin species and negative $B_{\rm eff}$ for the other). The filling factor of the spin-dependent CF states is again given by eq. (2.1) but now with $n = n_\uparrow + n_\downarrow$.

The final step is to project the wave functions onto the LLL; the final form of the spatial part of the spin-dependent CF wave function is, thus,

$${}^{2p}\mathrm{CF}_{(-n_\uparrow,-n_\downarrow)} \equiv \psi_{p,(n_\uparrow,n_\downarrow)} \approx \det\left[\hat{Y}^Q_{n'_\uparrow,m_\uparrow}(u_i,v_i)J_i^p\right]\det\left[\hat{Y}^Q_{n'_\downarrow,m_\downarrow}(u_i,v_i)J_i^p\right], \tag{2.9}$$

where the i index runs from 1 to $N_\uparrow$ in the first determinant and from $N_\uparrow+1$ to $N_\downarrow$ in the second.[†] Note that the J_i function is exactly as in eq. (2.6) (i.e., it is a product over all spin-up and spin-down particles) and so in eq. (2.9) each matrix element in each determinant depends on the co-ordinates of all of the particles.

[†]Note that the wave function of the form $\psi(u_i,v_i)$ given in eq. (2.9) is not quite complete: in fact wave functions $\Phi(u_i,v_i)$ describing N fermions must be fully antisymmetric under any exchange of particle labels, but $\psi(u_i,v_i)$ in eq. (2.9) is only antisymmetric under exchange of labels 1 to $N_\uparrow$ and in labels $N_\uparrow+1$ to $N_\downarrow$. The correct expression for the full wave function would be obtained by including a spin part to the wave function, $X = |\uparrow\uparrow\ldots\downarrow\downarrow\rangle$, and then fully antisymmetrizing by applying the antisymmetrizing operator $\hat{\mathbf{A}}$, i.e., we must construct $\Phi(u_i,v_i) = \hat{\mathbf{A}}\psi(u_i,v_i)X$. In practice, when calculating matrix elements of the form $\int\Phi^\dagger\hat{\mathbf{O}}\Phi d\Omega_1\ldots d\Omega_N$, as long as the operator $\hat{\mathbf{O}}$ does not depend on the spin state the matrix element reduces to a value proportional to $\int\psi^\dagger\hat{\mathbf{O}}\psi$ because the spin wave functions are orthonormal. Thus the version of the wave function given in eq. (2.9) is sufficient.

In order to describe a system with a two-valley degree of freedom rather than a spin-1/2 degree of freedom, the CF theory wave functions are identical, only we replace the spin up/down label by a valley index.

2.3 Results of Monte Carlo Calculations

In this section we shall present the results of our calculations of the Coulomb energy per electron associated with the principal spin CF trial ground-state wave functions in negative effective field: ${}^2\mathrm{CF}_{-4}$, ${}^2\mathrm{CF}_{(-3,-1)}$, ${}^2\mathrm{CF}_{(-2,-2)}$, ${}^2\mathrm{CF}_{-3}$, ${}^2\mathrm{CF}_{(-2,-1)}$, ${}^2\mathrm{CF}_{-2}$, and ${}^2\mathrm{CF}_{(-1,-1)}$. For comparison we shall also present some results of our calculations for the positive effective field cases : ${}^2\mathrm{CF}_{4}$, ${}^2\mathrm{CF}_{(3,1)}$, ${}^2\mathrm{CF}_{(2,2)}$, ${}^2\mathrm{CF}_{3}$, ${}^2\mathrm{CF}_{(2,1)}$, ${}^2\mathrm{CF}_{2}$, and ${}^2\mathrm{CF}_{(1,1)}$, which were previously studied in ref. [16]. Using these results we shall deduce some quantitative predictions of CF theory for the critical Zeeman energy per electron at which transitions between different spin states occur.

2.3.1 Coulomb Energy

Our first calculation is the Coulomb energy per electron, E_C, of the CF trial ground-state wave functions. In general, the Coulomb energy associated with a state described by a wave function ψ is calculated using

$$\langle\psi|V|\psi\rangle = \int d\mathbf{r}_1 \ldots d\mathbf{r}_N \, |\psi|^2 \, V\left(\mathbf{r}_1, \ldots, \mathbf{r}_N\right), \tag{2.10}$$

where V is the Coulomb potential (in units of $e^2/\epsilon l_0$):

$$V = \sum_{i<j}^{N} \frac{1}{R_{ij}} + V_{\mathrm{BG}}.$$

Here R_{ij} is the distance between pairs of particles in the sphere geometry. We use the chord distance convention, $R_{ij}^{\mathrm{Chord}} = 2R_S \left|u_i v_j - v_j u_i\right|$, where R_S is the radius of the sphere. V_{BG} is the potential due to a uniformly changed positive background (this is required so the overall system is electrically neutral), and it is given by the self-energy of a uniformly charged sphere of charge $+Ne$ plus the electrostatic energy between the electrons and the uniformly charged sphere. Using the chord distance measure, $V_{\mathrm{BG}} = -\frac{N^2}{2R_S}$ (see ref. [60]).

One can numerically evaluate integrals of the form given in eq. (2.10) using a Metropolis Monte Carlo procedure (see appendix A for a brief description of how we implemented the Metropolis algorithm). The detailed results of our calculation of the Coulomb energy per electron of the seven negative effective field CF wave functions are presented in ref. [128]; plots

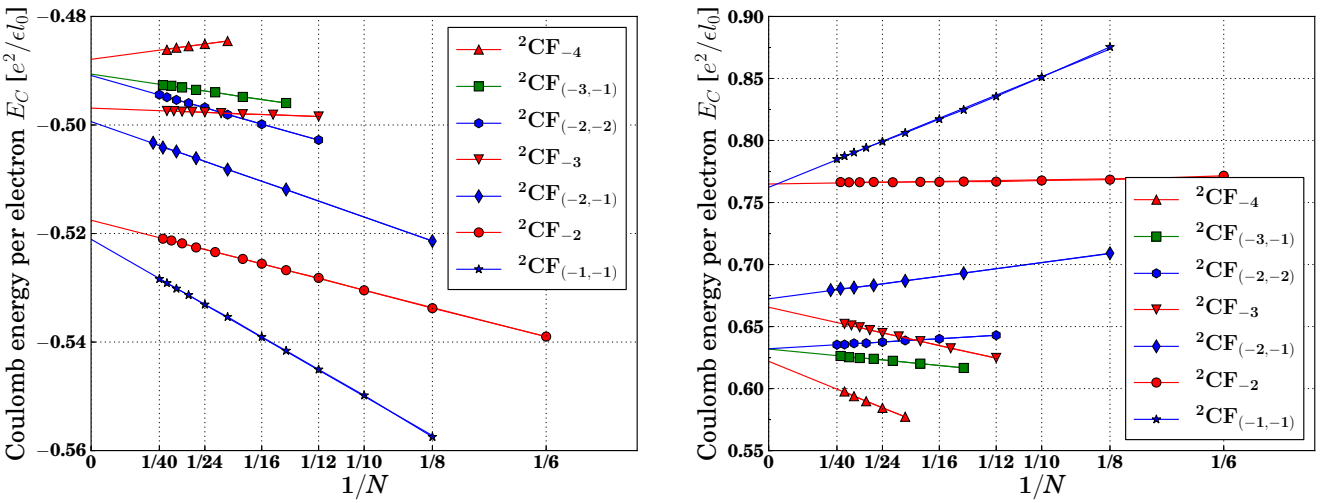

(a) LLL (b) 2nd LL

Figure 2.3: Extrapolations to the thermodynamic limit for the Coulomb energies per electron of various negative effective field CF wave functions in the LLL (left panel) and the 2nd LL (right panel). Linear extrapolations in $1/N$ are indicated by the solid lines, but quadratic extrapolations were also considered. Error bars are smaller than the data markers and so are not plotted. According to CF theory, spin transitions are energetically favorable in the LLL case, but not typically in the 2nd LL case [with the exception of $^2\mathrm{CF}_{-2} \to {}^2\mathrm{CF}_{(-1,-1)}$].

of the extrapolations to the thermodynamic limit are presented here in fig. 2.3 for the negative effective field case. In table D.1 of appendix D we also include some comparisons with exact diagonalization results for small systems.

2.3.2 2nd Landau Level Coulomb Interaction

An interesting consideration is to model equivalent CF wave functions in the 2nd LL, that is, the analogous CF states occurring at filling factor $\nu = \nu_{\mathrm{LLL}} + 2$. These results are relevant to experimental studies of spin transitions at $\nu = 8/3$ and at $\nu = 12/5$.[20,21] We note that there is some theoretical evidence that ground-state wave functions in the 2nd LL may *not* necessarily be of the CF type (see ref. [70]), however our calculation nevertheless provides a useful starting point to try to understand experimental observations.

One approach would be to construct explicit wave functions at this new filling factor, however, the CF wave functions in anything other than the LLL are difficult to evaluate. A more efficient alternative is possible, however: the problem of electrons interacting via the Coulomb interaction in a higher Landau level is mathematically equivalent to the problem of electrons in the LLL interacting via an effective potential $V^{\mathrm{eff}}(r)$. An appropriate form for the effective potential is derived in ref. [136], although, strictly speaking, this result was derived only for the disc geometry (the wave functions we use for our calculations are written in the

sphere geometry). However, since we will take the thermodynamic limit at the end of the calculation, we can still use the same potential in the sphere geometry since the disc and the sphere geometries are the same in the thermodynamic limit. The effective potential is given by

$$V^{\text{eff}}(r) = \frac{1}{r} + \sum_{i=0}^{6} c_i r^i e^{-r}, \tag{2.11}$$

with r in units of the magnetic length.

The values of the coefficients c_i appearing here are deduced by equating the two-body Haldane pseudopotential coefficients, V_m^{eff}, of the effective potential in the LLL, namely

$$V_m^{\text{eff}} = \frac{1}{2^{2m+1}m!} \int_0^\infty r dr V^{\text{eff}}(r) r^{2m} e^{-r^2/4},$$

to the pseudopotential coefficients of the Coulomb interaction in the 2nd LL, namely

$$V_m^1 = \int_0^\infty q dq \tilde{V}(q) \left(L_1 \left(\frac{q^2}{2} \right) \right)^2 L_m \left(q^2 \right) e^{-q^2},$$

where

$$\tilde{V}(q) = \int_0^\infty r dr V(r) J_0(qr).$$

In these expressions, L_m are Laguerre polynomials and J_0 are Bessel functions. It is sufficient to work with only the first seven coefficients and we have checked that the addition of more coefficients does not change the result significantly. In order to determine the coefficients c_0 to c_6 in eq. (2.11) we must equate V_m^{eff} to V_m^1 for $m = 1, 3, 5, \ldots, 13$ (since the pseudopotentials for $m = 0, 2, 4, \ldots$ etc. do not enter the Hamiltonian in the case of spinless fermions). Appropriate values of c_i are given in ref. [128].[†]

The effective Coulomb energies due to the modified interaction potential for the 2nd LL are given alongside the LLL values in ref. [128]; plots of the extrapolations to the thermodynamic limit are presented in fig. 2.3.

2.3.3 Comparison with Experiments

At this point we are now ready to calculate the predicted values for the critical Zeeman energy per electron E_Z^{crit} for spin transitions (or equivalently the critical valley splitting energy E_V^{crit}

[†]The differences between the disc geometry case and the sphere geometry case are the values of the coefficients c_i in eq. (2.11): in the disc geometry version of the potential the coefficients are derived using the disc geometry versions of the Haldane pseudopotentials, whereas in the sphere geometry the coefficients are derived using the sphere geometry versions of the pseudopotentials (see, for example, ref. [137]). In the disc geometry the values of the coefficients are independent of the flux; however, this is no longer true in the sphere geometry and a different set of coefficients (and therefore a different effective potential) must be calculated for each value of the flux. We have checked that in the thermodynamic limit the values of the sphere geometry coefficients tend toward the same fixed values given in ref. [128], and thus it is sufficient to only consider the simpler disc geometry version of the potential.

for valley transitions) and to make some comparisons with the experimental studies. To study each transition, e.g., at filling $\nu = \frac{4}{7}$, $\gamma_e = 1 \rightarrow \frac{1}{2}$ [for which the CF theory prediction comes from the transition ${}^2\mathrm{CF}_{-4} \rightarrow {}^2\mathrm{CF}_{(-3,-1)}$], we need to compare the two energies: first, there is the difference in Coulomb energy per electron, ΔE_C, between the two participant ground-state trial wave functions; second, for the spin case, there is the difference in Zeeman energy per electron, ΔE_Z, which is due to the difference in the net spin polarization of the two participant ground-state trial wave functions. The condition for a transition is that $\Delta E_C = \Delta E_Z$ at the point of transition.

The difference in Coulomb energy per electron, ΔE_C, is calculated directly from our results for the Coulomb energy per electron associated with each trial ground-state wave function—these differences are listed in table 2.1. The difference in Zeeman energy per electron as we go through a transition is equal to the energy E_Z^{crit} to flip a single spin in a magnetic field B^{crit} multiplied by the proportion of spins which need to be flipped as we go through that transition. In the thermodynamic limit, where the effective CF LLs are equally occupied, the proportion of flipped spins is simply $1/n$, where n is the total number of filled effective LLs of the CF wave functions partaking in the transition. Thus, at the transition we have $\Delta E_C = \Delta E_Z = E_Z^{\mathrm{crit}}/n$ and this leads to the relation

$$E_Z^{\mathrm{crit}} = n\Delta E_C. \tag{2.12}$$

(For the valley case the equivalent relation for the critical valley splitting energy is simply $E_V^{\mathrm{crit}} = n\Delta E_C$.) Using eq. (2.12) we have calculated predicted values for the critical Zeeman energy and critical valley splitting energy, and for the negative effective field case these predictions are listed in table 2.1.

For the LLL case, values of E_Z^{crit} can also be deduced from the experimental results presented in refs. [12, 14, 22] as we shall explain below. Values of E_V^{crit} for AlAs systems under axial strain are given in ref. [133]. We crudely estimate error bars of ± 0.001, in units of Coulomb energy, on all experimental measurements. For the negative effective field case, we list experimentally measured values of E_Z^{crit} and E_V^{crit} alongside the theoretical predictions in table 2.1. In fig. 2.4 we have plotted the predicted and measured values of E_Z^{crit} and E_V^{crit} given in table 2.1 as a function of the parameter n for negative and positive effective field cases.

In ref. [14] values of E_Z^{crit} are derived from the measurements of the degree of spin polarization γ_e as a function of magnetic field strength at fixed filling factor (see fig. 2.1). Accompanying each transition is a broadened step in the degree of spin polarization. We take the critical field

Fraction	$\frac{4}{7}$ (or $\frac{10}{7}$, $-\frac{4}{7}$)	$\frac{4}{7}$ (or $\frac{10}{7}$, $-\frac{4}{7}$)	$\frac{3}{5}$ (or $\frac{7}{5}$, $-\frac{3}{5}$)	$\frac{2}{3}$ (or $\frac{4}{3}$, $-\frac{2}{3}$)
Transition	$\gamma_e = 1 \rightarrow \frac{1}{2}$	$\gamma_e = \frac{1}{2} \rightarrow 0$	$\gamma_e = 1 \rightarrow \frac{1}{3}$	$\gamma_e = 1 \rightarrow 0$
CF Theory	${}^2\mathrm{CF}_{-4} \rightarrow {}^2\mathrm{CF}_{(-3,-1)}$	${}^2\mathrm{CF}_{(-3,-1)} \rightarrow {}^2\mathrm{CF}_{(-2,-2)}$	${}^2\mathrm{CF}_{-3} \rightarrow {}^2\mathrm{CF}_{(-2,-1)}$	${}^2\mathrm{CF}_{-2} \rightarrow {}^2\mathrm{CF}_{(-1,-1)}$
ΔE_C	0.0027(2)	0.0003(1)	0.0025(1)	0.00364(6)
No. CF LLs (n)	4	4	3	2
$E_Z^{\mathrm{crit}} = n\Delta E_C$	0.0108(7)	0.0010(5)	0.0075(3)	0.0073(1)
Experiment				
E_Z^{crit} (ref. [14])	0.013(1)	0.007(1)	0.012(1)	0.0088(10)
E_Z^{crit} (ref. [12])	0.018(1)	0.010(1)	0.017(1)	0.015(1)
E_Z^{crit} (ref. [22])	0.012(1)	N/A	0.010(1)	0.0086(10)
E_V^{crit} (ref. [133])	0.019(1)	N/A	0.017(1)	0.013(1)

Table 2.1: For each filling factor in the negative effective field case, the table shows the possible spin-transitions labelled by their degree of spin polarization γ_e [defined in eq. (2.2)]. We list the difference in Coulomb energy per electron, ΔE_C, between the two possible ground-state CF configurations, and the corresponding prediction for the critical Zeeman energy per electron, E_Z^{crit}, calculated using eq. (2.12) (or, equivalently, the critical valley splitting energy per electron, E_V^{crit}). To obtain ΔE_C we use a linear extrapolation scheme, weighted by the statistical errors on each finite-sized system data point. The relevant experimental values for E_Z^{crit} are taken from Kukushkin *et al.* (GaAs systems in ref. [14]), from Du *et al.* (GaAs systems in ref. [12]) and from Feldman *et al.* (suspended graphene systems in ref. [22]). The relevant experimental values for E_V^{crit} are taken from Padmanabhan *et al.* (AlAs systems in ref. [133]). We explain in the text how the experimental data and error bars are determined. All values are given in units of the Coulomb energy, $e^2/\epsilon l_0$.

B^{crit} to occur at the centre of the step, and we take the experimental error to be roughly the half-width of the broadening (which corresponds approximately to an error of $\pm$ 0.001 in the Zeeman energy, in units of Coulomb energy).

For ref. [12] we infer E_Z^{crit} at filling factors $\nu = 2/3, 3/5,\ 4/7,\ 2/5, 3/7$ and 4/9 from the critical fields for spin transitions observed in particle-hole conjugate states occurring at filling factors $\nu = 4/3,\ 7/5,\ 10/7,\ 8/5,\ 11/7$ and 14/9. Particle-hole conjugation does not, in principle, affect the Coulomb or Zeeman energy associated with the trial CF wave functions and so the predictions for the critical Zeeman energy are identical in principle, to the extent that Landau level mixing can be neglected. The aim of the experiments described in ref. [12] is to vary the ratio of Zeeman to Coulomb energy keeping the filling factor fixed. In order to achieve this the electron density is kept constant and the applied field B^{tot} is tilted by an angle θ from the vertical and increased in magnitude simultaneously, thus fixing the component of the field perpendicular to the plane, $B_\perp = B^{\mathrm{tot}} \cos\theta$.[†] The signature for transitions between states

[†]In principle, tilting the magnetic field can alter the effective interaction between the electrons by modifying the form of the wave function in the direction perpendicular to the electron layer. We have not accounted for this effect (see e.g., ref. [138]). However, we note that the magnetic length due to the in-plane field is never much less than the heterojunction width so this effect is not expected to be substantial (see table 2.2).

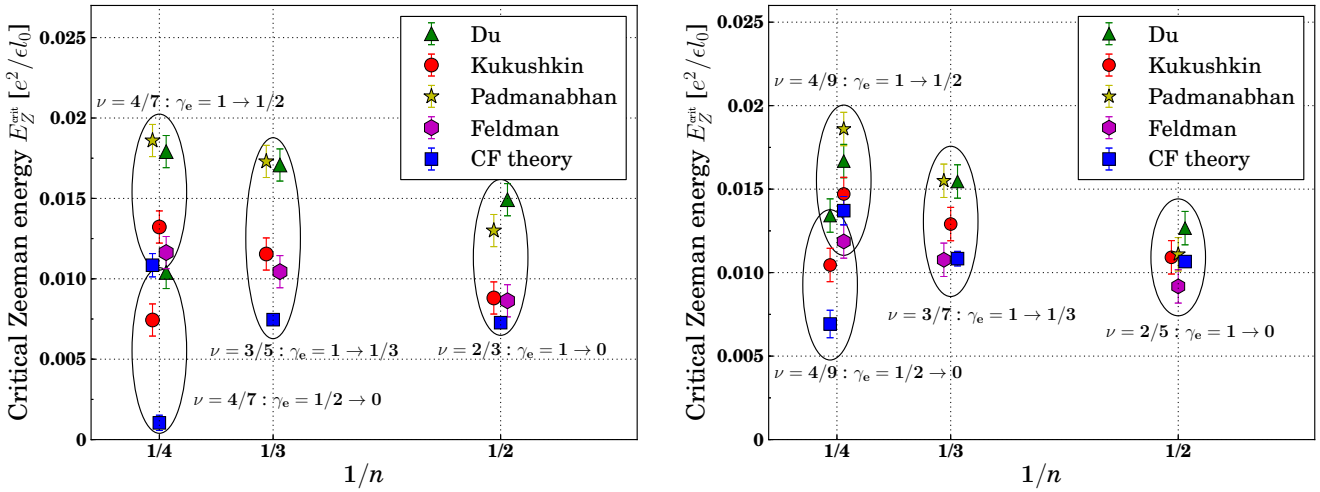

(a) Negative effective field

(b) Positive effective field

Figure 2.4: Predicted and measured values of the critical Zeeman energy per electron plotted against the reciprocal number of filled effective LLs, $1/n$, for the negative effective field case [left panel] and, for comparison, for the positive effective field case [right panel] (see also ref. [16], we present our own results here). Transitions are labelled by their degree of spin polarization γ_e [defined in eq. (2.2)] and data points corresponding to the same transition are circled. Data for the negative effective field figure are given in table 2.1. We found that a linear extrapolation scheme provided the most accurate results (the smallest standard deviation for the thermodynamic value of the Coulomb energy) for the negative effective field case, whereas a quadratic extrapolation scheme provided the most accurate results for the positive effective field case. (Note that each set of points in the plots occur at an integer value of n and we have added in left/right shifts for clarity of presentation only.)

of different spin polarization is a peak in the ratio of the longitudinal resistivity at a given filling factor to the longitudinal resistivity at filling $\nu = 3/2$. We take the critical field B^{crit} to occur at the centre of the peaks and we take the experimental error to be the half-width of the peaks (which corresponds approximately to an error of ± 0.001 in the Zeeman energy, in units of Coulomb energy). Using these values for B^{crit} we calculate the experimentally measured value of the critical Zeeman energy via $E_Z^{\text{crit}} = g\mu_B B^{\text{crit}}$, and then convert to units of $e^2/\epsilon l_0$ for comparison with our theoretically derived values in table 2.1 (for this calculation we take the g-factor of GaAs to be $g = -0.44$ and the relative permittivity to be $\epsilon = 12.6$).

In ref. [13] spin transitions are measured as a function of applied hydrostatic pressure at filling factors 2/5, 4/7, and 4/9. We calculate experimental estimates of the critical Zeeman energy from the values of hydrostatic pressure and magnetic field strength where the spin-transitions are reported. The g-factor dependence on the hydrostatic pressure can be read off from refs. [139] or [140], depending on whether the system is a heterojunction or quantum well (both were used in ref. [13]). We also take into account that the dielectric constant in GaAs has a moderate pressure dependence (see ref. [141]). For $\nu = 2/5$ we obtain $E_Z^{\text{crit}} = 0.00391$,

for $\nu = 4/7$ we obtain $E_Z^{\rm crit} = 0.00364$ and for $\nu = 4/9$ we obtain $E_Z^{\rm crit} = 0.00390$ (all in units of $e^2/\epsilon l_0$). These values appear to be significantly lower than both the CF theory predictions and other experimental measurements conducted in GaAs systems (c.f. fig. 2.4). The reason for this discrepancy is unclear.

In ref. [22] spin transition signatures were recognized in local compressibility measurements of the conduction electrons in suspended graphene samples at filling factors $-2/3$, $-3/5$, $-4/7$, $-5/9$, $-2/5$, $-3/7$, $-4/9$ and $-5/11$ (which are equivalent to $2/3$, $3/5$ etc. in conventional systems). The characteristic of a quantum Hall plateau in such measurements is a region of incompressibility at a fixed value of the filling factor. Compressibility measurements are plotted as a function of filling factor and magnetic field strength (with the electron density tuned accordingly to keep the ratio of magnetic field to number density fixed for a given filling factor). Spin transitions are identified as stripes of negative compressibility crossing the incompressible regions (see fig. 1.5). The critical magnetic field for the spin transition is simply the magnetic field at the point where the negative compressibility stripes occur. To obtain an estimate for $E_Z^{\rm crit}$, as a first approximation, we make the assumption that the g-factor of suspended graphene is 2, and the relative permitivity is taken from theoretical estimates in ref. [142] to be $\epsilon_r \sim 1.8$.[†] We estimate error bars of ± 0.001, in units of Coulomb energy.

Concerning the 2nd LL case, we have calculated the thermodynamic extrapolations for both positive and negative effective field (the negative effective field extrapolations are presented in fig. 2.3 but the positive effective field results are not shown). The CF theory predictions are somewhat striking: as can be seen from fig. 2.3 for the negative effective field case, the values of ΔE_C are now *negative*, with the single exception of the $\nu = 2 + 2/3$. For the positive effective field case we find that ΔE_C is always negative. In other words, with the possible exception of $\nu = 2 + 2/3$, according to the CF theory description of the 2nd LL it is *never* energetically favorable to have a non–polarized ground state. For the $\nu = 2 + 2/3$ our most accurate prediction for the critical Zeeman energy is $E_Z^{\rm crit} = 0.0028(8)$. In ref. [21] a spin transition is indicated at $\nu = 2 + 2/3$ with a value of $E_Z^{\rm crit} \sim 0.005$. Notably, in ref. [20] a spin transition is indicated at $\nu = 2 + 2/5$ which is not predicted by CF theory.

2.3.4 Finite Thickness Correction

In the experimental investigations of the FQHE discussed in refs. [14] and [12], the 2D geometry is realized in a GaAs–$Al_xGa_{1-x}As$ heterojunction setup. Due to the finite width of the potential

[†]The authors of ref. [22] anticipate from experimental evidence that the assumption of $g = 2$ is accurate, and it is expected that $\epsilon_r > 1$ due to a combination of screening from the substrate and from graphene itself.

well in heterojunctions, the geometry cannot be considered perfectly 2D and realistic wave functions must have some finite extent in the direction perpendicular to the 2D plane. The impact of the finite thickness correction can be calculated simply by modifying the interaction potential with which we evaluate the ground-state energy. Appropriate modified potentials are discussed, for example, in ref. [45]. Here we implement the following potential, known as the Fang–Howard potential, which is applicable to GaAs–$Al_xGa_{1-x}As$ heterojunctions. Note that this result was derived only for the disc geometry, however in the thermodynamic limit, the result will be correct for the sphere geometry also.

$$V_{\mathrm{FH}}(r,d) = V'_{\mathrm{BG}} + \int_0^\infty dk V_{\mathrm{FH}}(k,d) J_0(kr) k, \tag{2.13}$$

with

$$V_{\mathrm{FH}}(k,d) = \frac{e^2 l_0}{\epsilon} \frac{9}{8k} \frac{24 + 9kd + (kd)^2}{(3+kd)^3}.$$

The potential is a function of a thickness parameter d/l_0, which characterizes the extent of the wave function in the dimension perpendicular to the plane; $d = 0$ corresponds to a perfect 2D geometry. Note that the value of the background contribution to the potential, V'_{BG}, will depend on this new potential and will not be the same as for the Coulomb potential case. Using this modified interaction potential we have calculated the ground-state energy in the thermodynamic limit for a number of different values of d. Graphs showing the thermodynamic extrapolation of the ground-state energy as a function of the thickness parameter are presented in fig. 2.5.

The value of d for a particular GaAs–$Al_xGa_{1-x}As$ heterojunction can be estimated using known data about the system (see ref. [33]):

$$d = 3\left(\frac{33\pi m_z e^2 \rho_e}{2\epsilon\hbar^2}\right)^{-\frac{1}{3}}, \tag{2.14}$$

where m_z is the electron effective mass in the GaAs in the direction perpendicular to the plane of the heterojunction, which is $0.067m_e$;[143] and ρ_e is the areal density of electrons in the inversion layer. The value must then be expressed in units of the magnetic length l_0. Eq. 2.14 applies to systems where there is no magnetic field and where the density of charge carries in depletion region due to dopants is much less than the density of electrons in the inversion layer. However, the presence of a magnetic field is not expected to have a significant impact on the result,[33] and in the experimental studies we discuss here, the heterojunctions are not strongly doped, so eq. (2.14) is expected to apply. We will now describe how we estimate a value of d

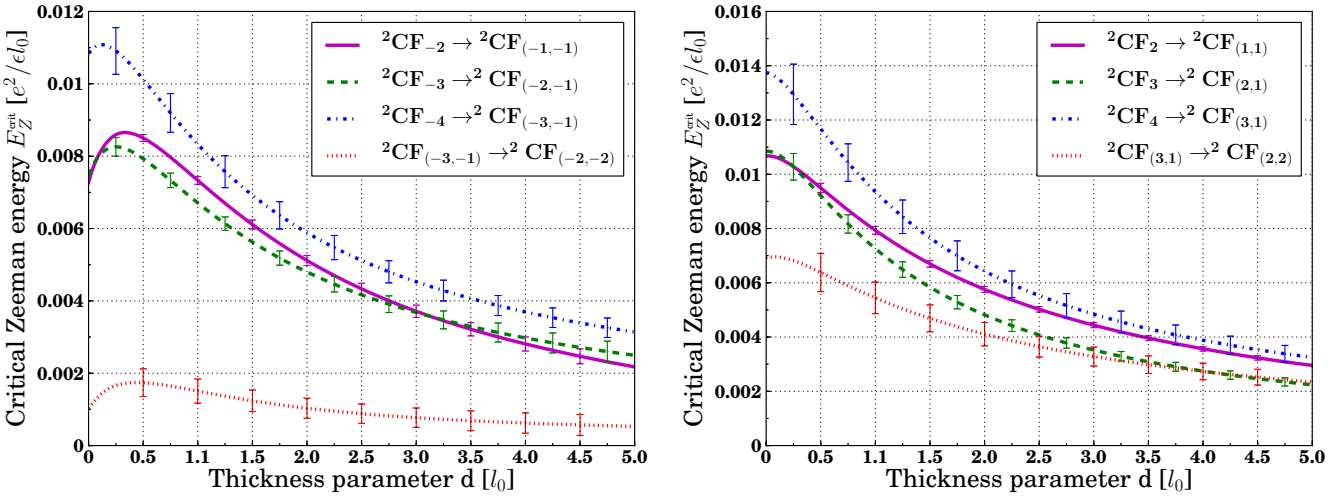

(a) Negative effective field

(b) Positive effective field

Figure 2.5: Theoretical predictions for the critical Zeeman energy per electron due to a finite-thickness potential $V_{\rm FH}(r,d)$ given in eq. (2.13), plotted as a continuous function of the thickness parameter d for selected CF states. The negative effective field case is shown in the left panel and the positive effective case is shown in the right panel. To obtain these curves, we calculate the energy due to $V_{\rm FH}(r,d)$ for finite sized systems with multiple values of the finite thickness parameter d between 0 and 5 and then perform an extrapolation to the thermodynamic limit weighted by statistical errors on each data point in each case. We found that a linear extrapolation scheme provided the most accurate results (the smallest standard deviation for the thermodynamic value of the Coulomb energy) for the negative effective field case, whereas a quadratic extrapolation scheme provided the most accurate thermodynamic results for the positive effective field case. The critical Zeeman energy is calculated using eq. (2.12). The resulting thermodynamic values are interpolated to obtain the plotted curve. Representative error bars for a selected data points are drawn at intervals on the plot. Note that the data have been smoothed between $d = 0.2$ and 0.3 in order to remove a numerical artifact. The energy is given in units of $e^2/\epsilon l_0$ and the thickness parameter is given in units of l_0.

appropriate for the parameters of each spin transition observed in both the Kukushkin *et al.* and Du *et al.* experiments.

In the experiments of Kukushkin *et al.* (ref. [14]) the system is set up such that the ratio of ρ_e to $B^{\rm crit}$ is fixed by the filling factor, i.e., $\rho_e = \nu B^{\rm crit}/\phi_0$ (here ϕ_0 is the flux quantum $\phi_0 = hc/e$), and, thus, in eq. (2.14) the value of d is a function of $B^{\rm crit}$. An additional dependence of d on $B^{\rm crit}$ enters through the magnetic length. Theoretical predictions for $B^{\rm crit}$ can be derived from the values of the critical Zeeman energy given in table 2.1 or, if we consider a system with non-zero d, from the results presented in fig. 2.5. Clearly, then, the theoretical prediction for $B^{\rm crit}$ itself depends on the chosen value of d, estimated from eq. (2.14). For each spin transition observed in the Kukushkin *et al.* experiments we determine a theoretical prediction for the value of d by requiring that the above conditions are self-consistently satisfied. We have tabulated these self-consistent estimates in table 2.2.

In the experiments of Du *et al.* (ref. [12]) there are two slight modifications to our estimation

Fraction	Transition	CF prediction	Kukushkin *et al.*		Du *et al.*	
			d	E_z^{crit}	d	E_z^{crit}
$\frac{4}{7}$	$\gamma_e = 1 \rightarrow \frac{1}{2}$	${}^2\text{CF}_{-4} \rightarrow {}^2\text{CF}_{(-3,-1)}$	1.41	0.0072(7)	0.595	0.0098(7)
$\frac{4}{7}$	$\gamma_e = \frac{1}{2} \rightarrow 0$	${}^2\text{CF}_{(-3,-1)} \rightarrow {}^2\text{CF}_{(-2,-2)}$	0.852	0.0016(5)	1.17	0.0014(5)
$\frac{3}{5}$	$\gamma_e = 1 \rightarrow \frac{1}{3}$	${}^2\text{CF}_{-3} \rightarrow {}^2\text{CF}_{(-2,-1)}$	1.31	0.0060(3)	0.636	0.0076(3)
$\frac{2}{3}$	$\gamma_e = 1 \rightarrow 0$	${}^2\text{CF}_{-2} \rightarrow {}^2\text{CF}_{(-1,-1)}$	1.30	0.0066(1)	0.776	0.0079(1)
$\frac{4}{9}$	$\gamma_e = 1 \rightarrow \frac{1}{2}$	${}^2\text{CF}_4 \rightarrow {}^2\text{CF}_{(3,1)}$	1.45	0.0078(8)	0.646	0.0109(8)
$\frac{4}{9}$	$\gamma_e = \frac{1}{2} \rightarrow 0$	${}^2\text{CF}_{(3,1)} \rightarrow {}^2\text{CF}_{(2,2)}$	1.25	0.00050(8)	0.861	0.0057(8)
$\frac{3}{7}$	$\gamma_e = 1 \rightarrow \frac{1}{3}$	${}^2\text{CF}_3 \rightarrow {}^2\text{CF}_{(2,1)}$	1.32	0.0063(4)	0.717	0.0083(4)
$\frac{2}{5}$	$\gamma_e = 1 \rightarrow 0$	${}^2\text{CF}_2 \rightarrow {}^2\text{CF}_{(1,1)}$	1.33	0.0071(2)	1.01	0.0079(2)

Table 2.2: The table presents estimates for the finite thickness parameter d in units of l_0 for different spin or valley transitions at various filling factors. Transitions are labelled by their degree of spin polarization γ_e [defined in eq. (2.2)]. The estimates are calculated using eq. (2.14) and experimental data taken from Kukushkin *et al.* (ref. [14]) or from Du *et al.* (ref. [12]), as described in the text. The table also presents modified theoretical predictions for the critical Zeeman energy per electron in units of $e^2/\epsilon l_0$ calculated by using the estimates for d with the modified potential given in eq. (2.13).

of d. First, in these tilted field experiments the value of ρ_e is fixed at 1.13 $\times 10^{11}$ cm^{-2}. Second, the effective magnetic length due to the in-plane field B^{tot} places an additional limit on the extent of the wave function perpendicular to the plane (since we assume that the wave function's extent out of the plane is never wider than its in-plane magnetic length). The in-plane field can be determined by the requirement that the filling factor is fixed and the number density of electrons is known, i.e., we require that $B_\perp = \rho_e \phi_0 / \nu$; the value of the total field is derived from the prediction of the critical Zeeman energy; the in-plane field $B_\parallel$ is given by $B_\parallel = \sqrt{(B^{\text{tot}})^2 - (B_\perp)^2}$. In fact, since our predictions for the critical Zeeman energy are relatively small compared to the values observed in Du's experiment, we find that our predicted values for B^{crit} are smaller than the values $B_\perp$ consistent with the experimental electron density and filling factor. It is, therefore, not possible in this case to construct a self-consistent value for $B_\parallel$ for any of the spin transitions observed in Du *et al.*. We can, however, use the experimentally observed values of the critical field to make an estimate of the value of d in units of l_0 for each transition using eq. (2.14). For each spin transition observed in the Du *et al.* experiments we determine a theoretical prediction for the value of d either from the experimentally observed values of the critical magnetic field, or from the magnetic length due to the in-plane field (whichever is smallest). In practice we find that the magnetic length due to the in-plane field is typically smaller than the values of d given by eq. (2.14).

In table 2.2 we present our estimates of d appropriate for each experimental setup described

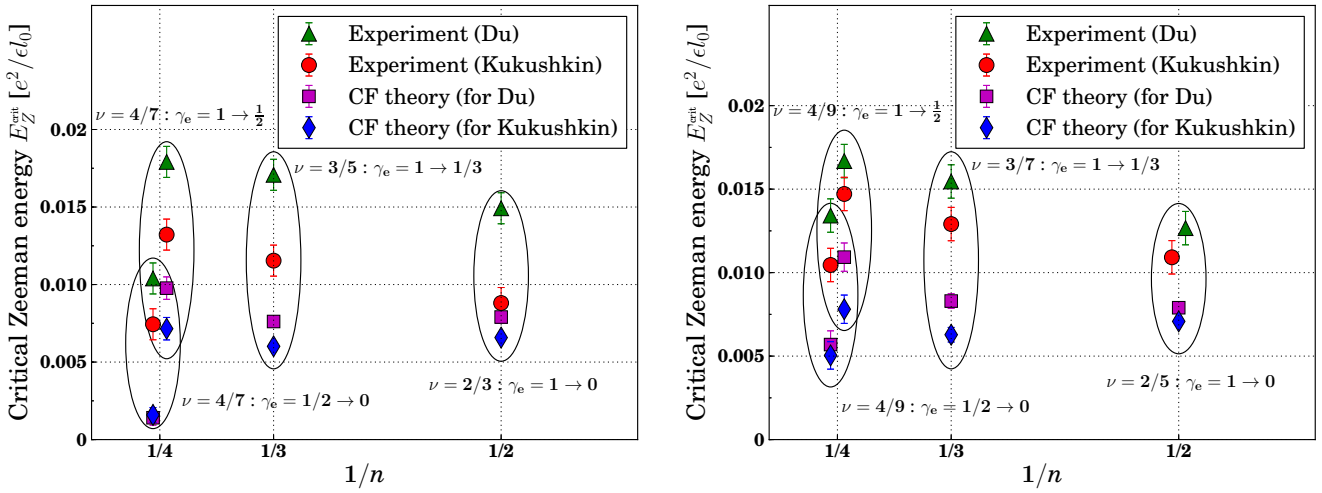

(a) Negative effective field

(b) Positive effective field

Figure 2.6: Predicted values for the critical Zeeman per electron modified by the inclusion of finite thickness effects and measured values for the critical Zeeman energy per electron from fig. 2.4 plotted against the reciprocal number of filled effective LLs, $1/n$. Transitions are labelled by their degree of spin polarization γ_e [defined in eq. (2.2)] and circled sets of points correspond to the same transition. In the text we explain how the theoretical predictions of the critical Zeeman energy per electron are calculated, taking into account a finite thickness correction to the potential appropriate to the conditions of the different experimental systems considered (all theoretical results presented in the figure are given in table 2.2). Experimental values are taken from Kukushkin *et al.* (ref. [14]) and from Du *et al.* (ref. [12]). We explain in the text how the experimental values are deduced. (Note that each set of points in the plots occur at an integer value of n and we have added in left/right shifts for clarity of presentation only.)

in the preceding two paragraphs and we also present the corresponding theoretical predictions for the critical Zeeman energy per electron calculated using the potential described in eq. (2.13). In fig. 2.6 we plot the modified results for the critical Zeeman energy per electron given in table 2.2 as a function of n as in fig. 2.4.

2.4 Conclusions

Comparing measurements from the different experiments (see fig. 2.4 and table 2.1), we conclude, firstly, that the Du *et al.* and Padmanabhan *et al.* data are in extremely good agreement with each other, as are the Kukushkin *et al.* and Feldman *et al.* data, although the two groups of experiments measure somewhat different values for the critical Zeeman energy (or critical valley splitting energy). Each study focused on a very different type of system (spin transitions in GaAs, valley transitions in AlAs and spin transitions in suspended graphene) and the excellent agreement between different the groups of experiments suggests that spin or valley transitions may not be very sensitive to the precise details of the system. The Du *et al.* / Padmanabhan *et al.* experiments studied particle-hole conjugate fractions of the Kukushkin *et*

al. / Feldman *et al.* experiments (e.g., 2/3 for Kukuhskin *et al.* we have assumed is equivalent to 4/3 for Du *et al.*). The apparent discrepancy in $E_Z^{\rm crit}$ between the two groups of experiments suggests that particle-hole symmetry is being broken. Further evidence for particle-hole asymmetry is indicated in measurements of AlAs valley transitions in ref. [134] (where the critical valley splitting energy for the 2/3 fraction in AlAs is measured to be ~ 0.004 compared to 0.013(1) for the 4/3 case). We notice a trend in all sets of experimental data for $E_Z^{\rm crit}$ to increase with increasing n (excluding the $\gamma_e = \frac{1}{2} \rightarrow 0$ transition). The CF theory results tend to underestimate most experimental measurements, especially for the negative effective field case and for the $\gamma_e = \frac{1}{2} \rightarrow 0$ transition at $\nu = 4/7$ and 4/9. Furthermore, the trend for $E_Z^{\rm crit}$ to increase with increasing n is somewhat weaker in the CF theory predictions than in the experimental data.

The potential impact of the finite thickness correction, for small values of the thickness parameter ($d < 0.5$) and for the negative effective field case, is to increase the differences in the predicted critical Zeeman energy per particle between the adjacent states typically by 20–30%. For larger values of the thickness parameter ($d > 0.5$) in the negative effective field case and for all values of d in the positive effective field case, the predicted critical Zeeman energy per particle decreases. Based on our estimates of the value of d, given in table 2.2, we conclude that the finite thickness correction typically lowers the predicted values for the critical Zeeman energy per electron. We correctly predict that the critical Zeeman energy should be greater under the experimental conditions of Du *et al.* compared to the conditions of Kukushkin *et al.*, with the exception of the $\gamma_e = \frac{1}{2} \rightarrow 0$ transition at $\nu = 4/7$ (see fig. 2.6) and therefore the finite thickness correction could partly explain the apparent particle-hole asymmetry. Nevertheless, the finite thickness correction clearly does not account for the discrepancy between the CF theory predictions and the experimental measurements. In particular it does not apply at all to spin transitions in graphene, where the Fang–Howard potential does not apply.

Other factors which have been neglected are LL mixing (which could also explain the apparent breaking of particle-hole symmetry seen in the experimental data), finite temperature effects, the effect of sample impurities and disorder. We note that in AlAs systems, the effective mass is known to be anisotropic and, further, it is differently anisotropic in the two lowest lying conduction band minima (in other words, the cyclotron orbitals in the two valleys are oval in shape, as opposed to the usual circular orbitals, such that the principle axis of the oval in one valley is perpendicular to the principle axis of the oval in the second valley).[85] We have completely neglected the band mass anisotropy in our study. For the $\nu = 1/3$ case,

it has been demonstrated that anisotropy has a significant impact on the form ground-state wave function and ground-state energy compared to a completely isotropic case.[144,145] These conclusions are also expected to hold in principle for the CF theory series of filling factors and for multicomponent systems, although detailed calculations have not yet been performed.[144] Similar modifications to the wave function are also anticipated for GaAs systems in the presence of tilted magnetic fields.[138] It is noteworthy that these anisotropy-related effects are anticipated for both the Du *et al.* and Padmanabhan *et al.* experiments, but not for the Kukushkin *et al.* and Feldman *et al.* experiments. Plainly, anisotropy constitutes a potential reason why the two groups of experiments are not quite in agreement and it merits further investigation.

Another potential source of error is that the precise value for the Coulomb energy in the thermodynamic limit depends on how one does the extrapolation: linear and quadratic regression, or regression taking into account the relative errors on each data point, or not. This issue is particularly acute for the $n = 4$ case because, according to eq. (2.12), we must multiply the differences in Coulomb energy by a factor of four to obtain the prediction for the critical Zeeman energy. We note that our results for the Coulomb energy in the positive effective field case differ marginally from those found in a previous study (ref. [16]), and the discrepancy appears to be down to a different extrapolation method used in in that work.

Perhaps the most prominent source of error is the use of CF theory to provide an approximation to the exact ground-state energy. In appendix D we present some comparisons between CF theory results for the Coulomb energy and exact results from numerical exact diagonalization for a number of finite-sized systems. The evidence suggests that CF wave functions calculated using the approximate LLL projection method outlined in sec. 2.2.3 provide a marginally better approximation to the exact ground-state when the spin is polarized, compared to when it is non-polarized. Therefore, the Coulomb energy differences, and hence the CF theory prediction for the critical Zeeman energy, are typically underestimates. This conclusion is consistent with what we find in our comparison of CF theory results against experimental measurements (fig. 2.4).

Turning to the results for the analogous states occurring in the 2nd LL, we can deduce an interesting prediction: it would appear that for $n = 4$ and $n = 3$ for both positive and negative effective field the fully polarized states ($^2\mathrm{CF}_{\pm 4}$ and $^2\mathrm{CF}_{\pm 3}$, respectively) lie lower in energy that any of the non spin-polarized states with the same filling factor. When $n = 2$, only the negative effective field case can favor a non spin-polarized ground state. Thus, for states at filling factors $2 + 2/5$, $2 + 3/5$,$2 + 3/7$, $2 + 4/7$ and $2 + 4/9$, the prediction of CF theory is that

it would not be energetically favorable to depolarize the spin as the field strength is reduced from its highest value and we would expect to observe no spin transitions at all in these cases. For the $2 + 2/3$ case, where a spin transition has been observed, the CF theory prediction for the critical Zeeman energy lies close to the experimentally measured value.[21] It is notable that a spin transition has been indicated at filling factor $2 + 2/5$, which is inconsistent with the CF theory prediction.[20] In other words, there may be an as yet unknown alternative ground-state wave function which provides a better approximation to the exact ground state in this case. An experimental observation of extensive non-polarized behavior at other 2nd LL CF filling factors might also suggest the existence of wave functions not encompased by CF theory.

Several experimental studies of the spin polarization of FQHE states have focused on the question of the spin polarization of the $\nu = 5/2$ state.[146,147] From the perspective of CF theory, the 5/2 state is described by CFs with zero effective magnetic field. Given our above conclusion that 2nd LL states described by CF theory would tend to favor a spin-polarized configuration, we speculate that a spin-polarized configuration may also be favorable at 5/2. [†] This would be in agreement with exact diagonalizations of smaller systems.[116,148]

[†]The limiting CF state is a gapless Fermi liquid type state, which is not thought to accurately describe the quantum Hall plateau at $\nu = 5/2$. On the other hand, the Moore–Read state, which is thought to describe $\nu = 5/2$, can be interpreted as BCS pairing of spin-polarized CFs.[27] This is consistent with our conclusion that, according to CF theory, $\nu = 5/2$ is a spin-polarized Fermi liquid.

CHAPTER 3

Multicomponent Multiparticle Pseudopotentials

The Haldane pseudopotential construction has been an extremely powerful concept in quantum Hall physics—it not only gives a minimal description of the space of Hamiltonians but also suggests special model Hamiltonians (those where certain pseudopotentials are set to zero) that may have exactly solvable ground states with interesting properties. In most discussions of fractional quantum Hall effect, one typically assumes that the interaction between particles is a pair-wise potential $V(|\mathbf{r_1} - \mathbf{r_2}|)$ and that the electrons have no additional degrees of freedom such as a spin or valley index. These two assumptions are ones we would like relax here. In this chapter,[†] we study multicomponent systems interacting via very general N-body potentials $V(\mathbf{r}_1, s_1; \mathbf{r_2}, s_2; \ldots \mathbf{r}_N, s_N)$ where here s_j represents the additional quantum number of the j^{th} particle. The purpose of this chapter is to generalize the pseudopotential construction to encompass such situations. Assuming a (spatially) rotationally invariant Hamiltonian, the essence of the problem is to obtain a full basis of wave functions for N particles with fixed relative angular momentum L. This basis decomposes into representations of $SU(n)$ with n the number of internal degrees of freedom. We give special attention to the case where the internal degree of freedom has $n = 2$ states, which encompasses the important cases such as spin-1/2 particles and quantum Hall bilayers.

In sec. 3.1 we review the idea of multiparticle pseudopotentials and we define our problem in more detail. Our main results for the multi particle multicomponent pseudopotentials are summarized in sec. 3.2. While our methods are generally applicable to any number of internal degrees of freedom per particle, we emphasize in particular the most experimentally relevant multicomponent cases, which are the cases where particles (fermions or bosons) have two, three, or four possible internal states for interactions between small numbers (2–4) particles. We present tables for these simple cases indicating the number p of linearly independent wave functions that exist for N particles having total relative angular momentum L. This specifies

[†]The material presented in this chapter is based on the publication S. C. Davenport and S. H. Simon, Phys. Rev. **B 85**, 075430 (see ref. [149]).

a $p \times p$ Hermitian matrix of pseudopotential parameters that can be defined for that value of angular momentum. In this same section we further give the explicit form of these linearly independent wave functions. Sec. 3.2.2 provides a brief primer on symmetry types and Young tableaux that is necessary for the description of the extension of this work to higher number of components, which we give in sec. 3.2.3. In sec. 3.2.4 we also briefly mention some specializations of our results to describe systems where the multicomponent degree of freedom arises from a spin-J particle, or from a combination of spin-1/2 and two-valley components present in systems such as graphene. Following the results section we give a brief discussion in sec. 3.3 of applications of our results as well as some simple examples.

The main mathematical formalism that derives the results presented here is relegated to the appendices.

3.1 Review of Multiparticle Pseudopotentials

The concept of two-body, single-component Haldane pseudopotentials is reviewed in chapter 1. It is worth pointing out again here that, as explained in chapter 1, pseudopotentials in higher LLs can always be defined directly in terms of the lowest Landau level (LLL) pseudopotentials using a LL raising operator.[122] This is the case for both Haldane's original two-body, single-component pseudopotentials and any multiparticle and multicomponent generalizations. Thus, by exclusively focusing on the LLL case we will always be able to construct pseudopotentials describing any higher LL also. Before we introduce multicomponent multiparticle pseudopotentials, it will be insightful to first consider the less general case of single component multiparticle pseudopotentials, first introduced in ref. [122].

In order to extend two-body pseudopotentials to multiparticle pseudopotentials, we extend the two-body interaction $V(|\mathbf{r_1} - \mathbf{r_2}|)$ discussed in chapter 1 to a general many body interaction potential $V(\mathbf{r}_1, \ldots, \mathbf{r}_N)$, and, for simplicity, we retain the restriction to a rotationally and translationally invariant system. Analogously to eq. (1.9) the interaction part of LLL Hamiltonian is written in terms of the N-particle potential as

$$H = \sum_{i_1 < i_2 < \ldots < i_N} V(\mathbf{r}_1, \ldots, \mathbf{r}_N) .$$

By analogy with Haldane's original pseudopotential construction, we decompose the wave function of the N particles into a centre-of-mass and a relative motion (see chapter 1). Further we would like to write a complete basis for the possible relative wave functions of the N particles which we will use for our pseudopotential construction.

Determining this complete basis turns out to be the tricky part of the N-body pseudopotential construction. As in the two-particle case we can use the total relative angular momentum L of the cluster of N particles as a useful parameter. Again by rotational invariance of the interaction, L will not be changed by the interaction V between the particles of the cluster. However, here the parameter L is not sufficient to fully describe the N-particle wave function as it is in the two-body case [see eq. (1.10)]. We must, therefore, instead write an orthonormal set of possible relative wave functions $|L, q\rangle$ all having the same total relative angular momentum between the N-particles. Here the index q runs from 1 to the number of states $p(N, L)$ in the basis for that given L and N. We will elaborate more on the structure of these wave functions below.

Given this basis of relative wave functions, we define N-particle pseudopotentials by:

$$V_{L,N}^{q,q'} = \langle L, q | \, V(\mathbf{r}_1, \ldots, \mathbf{r}_N) \, \big| L, q' \big\rangle \, . \tag{3.1}$$

As in the two-body case, by translational invariance of the interaction, we need not specify the centre-of-mass wave function, $|l\rangle$ in the definition of the pseudopotential. Again, by rotational invariance of the interaction, the relative angular momentum L must be conserved (the matrix element is diagonal in this variable). However, there is no need for the matrix element to be diagonal among the states q with the same angular momentum. Hence for each N and L we define a $p(N, L)$-dimensional Hermitian pseudopotential matrix with indices q and q'.

The Hamiltonian can be written in terms of these new pseudopotentials via a resolution of the identity (and making use of the fact that the interaction potential is rotationally invariant by construction):

$$H = \sum_{i_1 < \ldots < i_N} \sum_{L,l,q,q'} |L, q\rangle \, |l\rangle \, V_{L,N}^{q,q'} \, \langle l| \, \big\langle L, q' \big|, \tag{3.2}$$

where the sum over $i_1, \ldots, i_N$ indicates which N particles are considered in a particular term of the sum and it is implied that $|L, q\rangle$ is the relative wave function for that given set of particles (and $|l\rangle$ is the corresponding centre-of-mass wave function).

We now turn to the issue of determining the basis $|L, q\rangle$. These wave functions must be made of LLL variables and must be overall symmetric for boson wave functions or antisymmetric for fermion wave functions. Further, the basis states represent relative motion so they should be translationally invariant (i.e., the centre-of-mass coordinate should not appear).

To be more specific, let us factor out the Gaussian exponential factors throughout the discussion (indeed, these factors are geometry dependent anyway[119,122]). The remaining wave

function must be a homogenous analytic polynomial of degree L in the variables z_i analogous to eq. (1.10). Translational invariance of the wave function implies that the polynomial must be invariant under any global shift in all of the coordinates $z_i \to z_i + a$ for any complex number a. Finally, the wave function must be overall symmetric or antisymmetric for bosons or fermions respectively.

The enumeration of such polynomials is a task that turns out to be fairly straightforward.[122,150] First, we note that the problem of enumerating the antisymmetric wave functions is essentially equivalent to that of enumerating the symmetric wave functions. To see this we note that any antisymmetric polynomial in N variables can be written as a symmetric polynomial in N variables times a Jastrow factor (or Vandermonde determinant) as follows:

$$J_{1\ldots N} = \prod_{i,j=1;i<j}^{N} (z_i - z_j), \tag{3.3}$$

Thus, there is a precise isomorphism between homogeneous symmetric polynomials of overall degree L and homogeneous antisymmetric polynomials of degree $L + N(N-1)/2$.

To establish a complete basis of translationally invariant symmetric polynomials we use the basis of the elementary symmetric polynomials, which are defined in the following way:

$$e_{m,N}(x_1, \ldots, x_N) = \begin{cases} \sum_{0<i_1<i_2<\ldots<i_m\leq N} x_{i_1} \ldots x_{i_m} & m \leq N \\ 0 & \text{otherwise.} \end{cases} \tag{3.4}$$

All possible symmetric polynomials in N variables can be written as sums and products of these generators (i.e., these generate the *ring* of symmetric polynomials).

To impose the condition that the polynomials are translationally invariant we shift each variable by the overall centre-of-mass coordinate to give

$$\tilde{z}_i = z_i - \frac{1}{N}\sum_{j=1}^{N} z_j. \tag{3.5}$$

By writing elementary symmetric polynomials of the relative coordinates $\tilde{z}_i$, we then obtain generators for the ring of translationally invariant symmetric polynomials.[122,150] It is easy to check that

$$e_{1,N}(\tilde{z}_1, \tilde{z}_2 \ldots \tilde{z}_N) = 0. \tag{3.6}$$

therefore there is one generator fewer once we impose translational invariance. It can be shown that the remaining generators $e_{m,N}(\tilde{z}_1, \tilde{z}_2 \ldots \tilde{z}_N)$ for $1 < m \leq N$ do not vanish and are still linearly independent.[122,150]

Given that we know the generators, with some combinatorics, we can calculate the dimension $d_{\text{sym}}(L,N)$ of the space of translationally invariant symmetric polynomials in N variables and of degree L. The values of $d_{\text{sym}}(L,N)$ are listed in ref. [122]. The analytic formula for $d_{\text{sym}}(L,N)$ is reproduced here in eq. (H.2) in appendix H, and these values are identical to the spin polarized cases presented here in table 3.1 (see rows with the maximum S_{boson} value, i.e., the top row, for each value of N).

As an example, consider a translationally invariant symmetric polynomial of degree $L=4$ in $N=4$ variables. From our allowed generators, the only basis states we can construct of degree $L=4$ are given by $[e_{2,4}(\tilde{z}_1,\tilde{z}_2,\tilde{z}_3,\tilde{z}_4)]^2$ and $e_{4,4}(\tilde{z}_1,\tilde{z}_2,\tilde{z}_3,\tilde{z}_4)$. Hence, $d_{\text{sym}}(4,4)=2$ (cf. table 3.1).

Our objective was to determine a basis for the states $|L,q\rangle$. For bosonic wave functions, using combinations of these generators, we have found an appropriate basis of translationally invariant symmetric polynomial wave functions. The basis states given here are not orthonormal, but can easily be orthonormalized. For fermionic wave functions, we simply multiply these symmetric functions of degree L by a Jastrow factor $J_{1\ldots N}$ to give a basis for the space of translationally invariant antisymmetric polynomials of degree $L+[N(N-1)]/2$ in N variables.

Having determined our basis of states $|L,q\rangle$ it is then a straightforward matter to construct our pseudopotential representation of any given Hamiltonian using Eqs. 3.1 and 3.2.

3.2 Results for the Multicomponent Case

In this section, we present our main results for the multicomponent case. The essence of our objective in this section is, analogously to the single component case, to determine how many different linearly independent N-particle wave functions might exist with a fixed angular momentum L, and to form a complete basis for these states. For the multicomponent case, we may be able to classify these states by some additional quantum numbers (such as overall spin in the case where we are considering the multiple components to be multiple spin states). While some amount of formalism is necessary in this section, it will be minimized. The more detailed, and more formal, derivations are left to the appendices.

Very generally, we will consider an N-body interaction Hamiltonian that may depend on an internal degree of freedom s_i (such as spin) of each particle,

$$H=\sum_{i_1<i_2<\ldots<i_N} V(\mathbf{r}_1,s_1;\ldots;\mathbf{r}_N,s_N)\,. \tag{3.7}$$

We will assume that the interaction V is translationally invariant, and rotationally invariant in positional space (i.e., under rotation of the $\mathbf{r}$ variables), but we do not necessarily assume the interaction is invariant under any particular symmetry of the internal degree of freedom s_i (for example, if we are considering particles with spin, we do not assume rotational symmetry in spin space).

Analogously to the approach in the spinless case, to decompose this interaction into pseudopotentials, we need to construct a complete set of states for an N-particle cluster. Again factoring out the centre-of-mass degree of freedom of the cluster, let us write a complete set of relative wave functions as

$$|L, \mathfrak{q}\rangle, \tag{3.8}$$

where L is the relative orbital angular momentum of the cluster and $\mathfrak{q}$ enumerates all basis states with this value of L (note that the index $\mathfrak{q}$ indicates not only different spatial wave functions but also the different possible configurations of the internal degree of freedom, e.g., spin). Given such a complete basis, we can always define the corresponding pseudopotentials as the matrix elements of the form:

$$V_{L,N}^{\mathfrak{q},\mathfrak{q}'} = \langle L, \mathfrak{q}| \, V\left(\mathbf{r}_1, s_1; \ldots; \mathbf{r}_N, s_N\right) \left|L, \mathfrak{q}'\right\rangle . \tag{3.9}$$

Note that due to the rotational invariance of the potential, pseudopotentials are always diagonal in L and, due to the translational invariance of the potential, the centre-of-mass degree of freedom does not appear. This expression is analogous to eq. (3.1) above.

We can now use a resolution of the identity to rewrite the Hamiltonian, eq. (3.7), in the following general form:

$$H = \sum_{i_1<\ldots<i_N} \sum_{L,l,\mathfrak{q},\mathfrak{q}'} |L, \mathfrak{q}\rangle \, |l\rangle \, V_{L,N}^{\mathfrak{q},\mathfrak{q}'} \, \langle l| \left\langle L, \mathfrak{q}'\right|, \tag{3.10}$$

analogously to eq. (3.2).

Thus, our task in this section is simply to determine the complete linearly independent basis $|L, \mathfrak{q}\rangle$ when the particles have an internal degree of freedom.

3.2.1 Two Component Case: Spin 1/2, Bilayers, etc.

We begin with the simplest and most important multicomponent case: the two-component case. This case applies, for example, to spin-1/2 fermions, such as (unpolarized) electrons where each

fermion has two possible internal states (spin-up and spin-down). This case also applies to (spin-polarized) bilayers, where the layer index (or isospin) corresponds to the two-state system. We may also consider bosons with two internal states that are frequently referred to "spin-1/2 bosons" (although this nomenclature is not strictly correct). These two internal states could be two available hyperfine states or two possible layers or any other orbital index. Whatever the origin of the two possible states, we will use the nomenclature of spin for simplicity. (Note that in the case of more than two components which we discuss in sec. 3.2.3 below, the language of spins becomes somewhat less useful.)

In order to describe wave functions that depend on a spin degree of freedom, it is convenient to work with a basis of states that are eigenstates of spin angular momentum. These eigenstates are characterized by the spin quantum numbers S and S_z, which are the eigenvalues of the combined total spin angular-momentum operator for N particles, S^2, and of the combined z-component of spin angular-momentum operator for N particles, S_z, respectively.

Thus, we propose to write a complete basis of states for N spin-1/2 particles with total orbital relative angular momentum L, total spin angular momentum S^2, and z-component of spin angular momentum S_z. We denote this basis as

$$|L, S, S_z, q\rangle \,, \tag{3.11}$$

where q runs from 1 to the number of states in the basis (i.e., the total number of states of N particles having L, S^2, and S_z). In the language of eq. (3.8), the index $\mathfrak{q}$ here represents $\{S, S_z, q\}$.

Our first goal will be to determine the dimension of the space of the wave function basis (the number of q values for a given set of spin eigenvalues and a given N, L, S, and S_z), as has been documented for the spinless case (see eq. (H.2) below or ref. [122]). The results of our calculation of these parameters for fermionic and bosonic cases are shown in table 3.1. For each S, there are always $2S+1$ different possible values of S_z. The table presents the number of states for all possible values of S_z. (Note that some rows of the table are not labeled with a spin quantum number S_{boson} or S_{fermion}, for the bosonic or fermionic case, which means that the corresponding states cannot occur for a two-component system.)

Our second goal is to describe the forms of the basis wave functions. We shall now summarize our results, leaving the details of the derivation of the forms these wave functions take to Appendices F, G, and H. As in the spinless case, the basis wave functions, of the form $|L, S, S_z, q\rangle$, are equivalent to wave functions describing a small number of spin-1/2 particles.

N	λ	S_{fermion}	S_{boson}	L															
				0	1	2	3	4	5	6	7	8	9	10	11	12	13	14	15
2	[2]	0	1	1	0	1	0	1	0	1	0	1	0	1	0	1	0	1	0
	[1,1]	1	0	0	1	0	1	0	1	0	1	0	1	0	1	0	1	0	1
3	[3]	–	3/2	1	0	1	1	1	1	2	1	2	2	2	2	3	2	3	3
	[2,1]	1/2	1/2	0	1	1	1	2	2	2	3	3	3	4	4	4	5	5	5
	[1,1,1]	3/2	–	0	0	0	1	0	1	1	1	1	2	1	2	2	2	2	3
4	[4]	–	2	1	0	1	1	2	1	3	2	4	3	5	4	7	5	8	7
	[3,1]	–	1	0	1	1	2	2	4	4	6	6	9	9	12	12	16	16	20
	[2,2]	0	0	0	0	1	0	2	1	3	2	5	3	7	5	9	7	12	9
	[2,1,1]	1	–	0	0	0	1	1	2	2	4	4	6	6	9	9	12	12	16
	[1,1,1,1]	2	–	0	0	0	0	0	0	1	0	1	1	2	1	3	2	4	3
5	[5]	–	5/2	1	0	1	1	2	2	3	3	5	5	7	7	10	10	13	14
	[4,1]	–	3/2	0	1	1	2	3	4	6	8	10	13	16	20	24	29	34	40
	[3,2]	–	1/2	0	0	1	1	2	3	5	6	9	11	15	18	23	27	34	39
	[3,1,1]	1/2	–	0	0	0	1	1	3	3	6	7	11	13	18	21	28	32	41
	[2,1,1,1]	3/2	–	0	0	0	0	0	0	1	1	2	3	4	6	8	10	13	16
	[1,1,1,1,1]	5/2	–	0	0	0	0	0	0	0	0	0	0	1	0	1	1	2	2

Table 3.1: Dimensions of the polynomial spaces: the number of independent parameters occurring in the spatial part of the wave function at degree L for quantum Hall states containing N particles and with symmetry type λ. Where applicable to the two-component case, which is described in terms of spin eigenfunctions, we list the spin eigenvalues S corresponding to either a fermionic (S_{fermion}) or a bosonic (S_{boson}) wave function. For each S listed there will be $2S+1$ possible values of S_z. The symmetry types labeled by λ are introduced in sec. 3.2.2. We explain in the text that not all symmetry types λ correspond to a spin eigenvalue S_{fermion} or S_{boson}, and we indicate these cases by a dash in the table.

Compared to the spin-polarized case, these basis wave functions are now composed of both a spin part and a spatial part.

Once we have our complete basis, the set of spin pseudopotentials can be defined as in eq. (3.9):

$$V_{L,N}^{S,S_z,q;S',S'_z,q'} = \langle L,S,S_z,q|\, V\left(\mathbf{r}_1,s_1;\ldots;\mathbf{r}_N,s_N\right)\left|L,S',S'_z,q'\right\rangle .$$

Using these spin pseudopotentials we can now write down an expression for the Hamiltonian eq. (3.7) in the general form described by eq. (3.10).

As always, rotational invariance in the plane ensures that the Hamiltonian is diagonal in L. If the system is spin-rotationally invariant then the Hamiltonian is also diagonal in the eigenvalues S and S_z. For a more general interaction however, the Hamiltonian might not be spin-rotationally invariant, but, nonetheless, it is still convenient to decompose the interaction using the spin basis.

We now turn to the explicit construction of our complete set $|L, S, S_z, q\rangle$. A wave function for fermions must be overall antisymmetric, whereas a wave function for bosons must be overall symmetric. However, the wave functions we consider are a combination of both a spin and a spatial part, and only the combination of the two parts needs to have the overall fermionic or bosonic symmetry. The spatial and spin parts of the wave function can have more complicated symmetry as long as the two parts are appropriately sewn together and the combination has the correct overall symmetry. In fact, there is a direct correspondence between the type of symmetry and the spin quantum number S. The mathematical structure of forming this combination is discussed in detail in appendix F below. Here, however, we shall simply present the results of this procedure.

The presentation of our results is divided into two parts: first we shall introduce *primitive polynomials*, which are the lowest-degree polynomials corresponding to a particular type of spatial symmetry type for a set of N particles; second we shall describe how to use these primitive polynomials to construct a spatial function of arbitrary degree that still corresponds to a particular symmetry type. Each allowed spatial symmetry corresponds to a particular spin eigenvalue for the N particles. Merging a spatial wave function of a given symmetry type (a given spin quantum number) with a corresponding spin wave function will give an overall wave function with the appropriate fermionic or bosonic symmetry. In a moment we shall discuss how the spatial and spin wave functions are merged.

In Tables 3.2 and 3.3 we list what we have termed primitive polynomials, β_L, of degree L. These polynomials are written in terms of symmetric polynomials of the form of eq. (3.4) in terms of the relative coordinates as in eq. (3.5). Now, however, we frequently need to write symmetric polynomials in fewer than all N of the $\tilde{z}$ variables. For compactness, we shall use the following short-hand notation:

$$e_{m,i_1 i_2 i_3 \ldots i_p} \equiv e_{m,p}\left(\tilde{z}_{i_1}, \tilde{z}_{i_2}, \tilde{z}_{i_3}, \ldots, \tilde{z}_{i_p}\right). \tag{3.12}$$

Note that we will always take $\tilde{z}_i$ to have the centre of mass of all N particles subtracted off [as in eq. (3.5)] independent of the value of p. So, for example,

$$e_{2,245} \equiv e_{2,3}(\tilde{z}_2, \tilde{z}_4, \tilde{z}_5) = \tilde{z}_2\tilde{z}_4 + \tilde{z}_2\tilde{z}_5 + \tilde{z}_4\tilde{z}_5.$$

We also use the short-hand notation for Jastow factors,

$$J_{i_1 \ldots i_p} = \prod_{k,l \in \{i_1 \ldots i_p\}; k<l} (\tilde{z}_k - \tilde{z}_l), \tag{3.13}$$

λ	S_{fermion}	Primitive Polynomials
$[2]$	0	1
$[1,1]$	1	J_{12}

(a) $N = 2$

λ	S_{fermion}	Primitive Polynomials
$[3]$	–	1
$[2,1]$	1/2	$\beta_1 = J_{12}$ $\beta_2 = J_{12}(e_{1,12})$
$[1,1,1]$	3/2	J_{123}

(b) $N = 3$

λ	S_{fermion}	Primitive Polynomials
$[4]$	–	1
$[3,1]$	–	$\beta_1 = J_{12}$ $\beta_2 = J_{12}(e_{1,12})$ $\beta_3 = J_{12}\left(3\tilde{z}_3 e_{1,12} + e_{1,12}^2 - e_{2,12} + 3\tilde{z}_3^2\right)$
$[2,2]$	0	$\beta_2 = J_{12}J_{34}$ $\beta_4 = J_{12}J_{34}(e_{1,12}^2)$
$[2,1,1]$	1	$\beta_3 = J_{123}$ $\beta_4 = J_{123}(e_{1,123})$ $\beta_5 = J_{123}(e_{2,123})$
$[1,1,1,1]$	2	J_{1234}

(c) $N = 4$

Table 3.2: Primitive polynomials β_L of degree L for construction of *fermion* wave functions, listed by their symmetry type λ. Note that for compactness we use the notation $e_{m,i_1 i_2 \ldots i_p}$ defined in eq. (3.12) to be the elementary symmetric polynomial of degree m in the p variables $\tilde{z}_{i_1}, \ldots, \tilde{z}_{i_p}$, and we similarly write Jastrow factors on p variables as $J_{i_1 \ldots i_p}$ as defined in eq. (3.13). The column labeled S_{fermion} is in reference to the case of spin-1/2 (two component) particles only; entries labeled with a dash do not occur for the spin-1/2 case. The symmetry type λ pertains more generally.

so, for example,

$$J_{134} = (\tilde{z}_1 - \tilde{z}_3)(\tilde{z}_1 - \tilde{z}_4)(\tilde{z}_3 - \tilde{z}_4).$$

Multiplying an N-particle spatial wave function by any fully symmetric translationally invariant polynomial does not change its symmetry type. One can, thus, construct spatial wave functions with a given symmetry type and relative angular momentum L by multiplying a primitive polynomial by any fully symmetric (in all N variables) translationally invariant polynomial such that the combined polynomial degree of the resultant product is L. Thus, the most general spatial wave function of a particular symmetry and a particular relative angular momentum L is a linear combination of these products of translationally invariant polynomials times primitive polynomials giving a homogeneous polynomial of degree L.

We shall now demonstrate how to use the primitive polynomials via a simple example. Consider a three-particle electron wave function with total spin eigenvalue $S = 1/2$. For

λ	S_{boson}	Primitive Polynomials
$[2]$	1	1
$[1,1]$	0	J_{12}

(a) $N = 2$

λ	S_{boson}	Primitive Polynomials
$[3]$	3/2	1
$[2,1]$	1/2	$\beta_1 = e_{1,12}$ $\beta_2 = e_{1,12}^2 + 2e_{2,12}$
$[1,1,1]$	–	J_{123}

(b) $N = 3$

λ	S_{boson}	Primitive Polynomials
$[4]$	2	1
$[3,1]$	1	$\beta_1 = e_{1,123}$ $\beta_2 = \left(e_{1,123}^2 + e_{2,123}\right)$ $\beta_3 = \left(e_{1,123}e_{2,123} + 3e_{3,123}\right)$
$[2,2]$	0	$\beta_2 = \left(e_{1,12}^2 + 2e_{2,12} + 2e_{2,34}\right)$ $\beta_4 = \left(e_{1,12}^4 + 4e_{2,12}e_{1,12}^2 + 4e_{2,34}e_{1,12}^2 - 2e_{2,12}^2 - 2e_{2,34}^2 - 12e_{2,12}e_{2,34}\right)$
$[2,1,1]$	–	$\beta_3 = 3\tilde{z}_3^2 e_{1,12} - \tilde{z}_3 e_{1,12}^2 + 2\tilde{z}_3 e_{2,12} - e_{1,12}^3 + e_{1,12}e_{2,12} + 2\tilde{z}_3^3$ $\beta_4 = \tilde{z}_3^3 e_{1,12} - 3\tilde{z}_3^2 e_{1,12}^2 - \tilde{z}_3 e_{1,12}^3 + 6\tilde{z}_3 e_{1,12}e_{2,12} + 3e_{1,12}^2 e_{2,12}$ $\beta_5 = \tilde{z}_3 e_{1,12}^4 + 3\tilde{z}_3^2 e_{1,12}^3 + 2\tilde{z}_3^3 e_{1,12}^2 - 4\tilde{z}_3 e_{2,12}e_{1,12}^2$ $-6\tilde{z}_3^2 e_{2,12}e_{1,12} - 4\tilde{z}_3 e_{2,12}^2 - 4\tilde{z}_3^3 e_{2,12} - e_{2,12}e_{1,12}^3 - 2e_{2,12}^2 e_{1,12}$
$[1,1,1,1]$	–	J_{1234}

(c) $N = 4$

Table 3.3: Primitive polynomials β_L of degree L for construction of *boson* wave functions, listed by their symmetry type λ. As in table 3.2, the symbol $e_{m,i_1 i_2 \ldots i_p}$ is defined in eq. (3.12) and $J_{i_1 \ldots i_p}$ is defined in eq. (3.13). The column labeled S_{boson} is in reference to the case of spin-1/2 (two component) particles only; entries labeled with a dash do not occur for the spin-1/2 case. The symmetry type λ pertains more generally.

relative angular-momentum eigenvalue $L = 1$ we construct from the relevant entry in table 3.2 the only possible degree 1 polynomial conforming to this type of symmetry, namely

$$\beta_1 = J_{12} \equiv (\tilde{z}_1 - \tilde{z}_2)\,. \tag{3.14}$$

For $L = 2$ we can use the information in table 3.2 to construct the valid degree 2 polynomials conforming to this type of symmetry. Note that, due to eq. (3.6), $e_{1,123} = 0$, and so we cannot construct an degree 2 polynomial from J_{12} (which is degree 1) multiplied by any degree 1 translationally invariant fully symmetric polynomial. The only possibility according to table 3.2 is the second primitive polynomial:

$$\beta_2 = J_{12}e_{1,12} \equiv J_{12}\,(\tilde{z}_1 + \tilde{z}_2)\,.$$

For $L = 3$ we can have only the polynomial given by multiplying the $L = 1$ result by a fully symmetric translationally invariant polynomial of degree 2

$$(\tilde{z}_1 - \tilde{z}_2)\, e_{2,123}.$$

For $L = 4$ we can have either the $L = 1$ primitive polynomial multiplied by a translationally invariant fully symmetric polynomial of degree 3 or the $L = 2$ primitive polynomial multiplied by a translationally invariant fully symmetric polynomial of degree 2. The most general result is a linear combination,

$$(\tilde{z}_1 - \tilde{z}_2)\left[A_1 e_{3,123} + A_2\,(\tilde{z}_1 + \tilde{z}_2)\, e_{2,123}\right],$$

with two arbitrary coefficients, A_1 and A_2. Equivalently, we have two linearly independent basis states in the space of spatial wave functions. At each polynomial degree the number of linearly independent basis vectors appearing in these polynomials is precisely the dimension appearing in table 3.1: in this case $0, 1, 1, 1, 2, \ldots$, for polynomial degrees $L = 0, 1, 2, 3, 4, \ldots$, and so on. Since all fully symmetric translationally invariant polynomials are generated by $e_{2,123}$ and $e_{3,123}$, the most general spatial wave function with relative angular momentum L is, thus,

$$(\tilde{z}_1 - \tilde{z}_2)\left\{\sum_{2l+3m=L-1} A_{lm} e_{2,123}^{l} e_{3,123}^{m} + (\tilde{z}_1 + \tilde{z}_2) \sum_{2l'+3m'=L-2} A'_{l'm'} e_{2,123}^{l'} e_{3,123}^{m'}\right\},$$

where the total number of coefficients A_{lm} and $A'_{l'm'}$ appearing in the wave function takes the value given in table 3.1.

To generate the complete basis wave functions we must combine the spatial wave function with a spin wave function. In this procedure, we follow ref. [151]. We shall define a *primitive spin wave function* ϑ_i of a many-particle system to be an eigenfunction of the S_z operator of every particle in the system. For example, $|\uparrow\downarrow\uparrow\uparrow\downarrow\rangle$ is a primitive spin wave function for five particles. We imagine ordering all of the primitive spin wave functions in lexicographical order (an alphabetical, or last letter sequence ordering scheme), so the *first primitive spin wave function* (first in the sense of this ordering scheme) is given by

$$\vartheta_1\,(N, S_z) = |\uparrow\uparrow\uparrow \ldots \downarrow\downarrow\downarrow\rangle\,, \tag{3.15}$$

where the number of spin-up particles minus the number of spin-down particles times $1/2$ is equal to the total S_z eigenvalue:

$$S_z = \frac{1}{2}\,(N_\uparrow - N_\downarrow)\,.$$

To combine our spatial wave function with a spin wave function, we take a spatial wave function corresponding to the spin eigenvalue S (i.e., a primitive polynomial in table 3.2 or table 3.3 times any translationally invariant symmetric polynomial) and then multiply this by the first primitive spin wave function with any valid S_z eigenvalue for that particular S eigenvalue. To recover the complete basis wave function we simply antisymmetrize (for fermions) or symmetrize (for bosons) the resulting combination in all of the coordinates.

Continuing with our example, let us consider the case of $N = 3$ where the spin eigenvalue is $S_z = 1/2$. At degree 1, for example, we multiply the spatial wave function eq. (3.14) with the first primitive spin wave function $|\uparrow\uparrow\downarrow\rangle$ to construct

$$|\uparrow\uparrow\downarrow\rangle\,(\tilde{z}_1 - \tilde{z}_2)\,. \tag{3.16}$$

By antisymmetrizing in all the particle coordinates, we then find the three-body wave function,

$$|L = 1, S = 1/2, S_z = 1/2\rangle \propto 2\,|\uparrow\uparrow\downarrow\rangle\,(\tilde{z}_1 - \tilde{z}_2) - 2\,|\uparrow\downarrow\uparrow\rangle\,(\tilde{z}_1 - \tilde{z}_3) + 2\,|\downarrow\uparrow\uparrow\rangle\,(\tilde{z}_2 - \tilde{z}_3)\,. \tag{3.17}$$

Note that we do not write an additional q index here [as in eq. (3.11)] since there is a unique wave function with this value of N, L, S, S_z. Note also that this wave function is not normalized (and normalization depends on an inner product that depends on whether the geometry is on the sphere, plane, or torus). We can obtain a similar wave function with $S_z = -1/2$ by simply following the same procedure with the primitive spin wave function $|\uparrow\downarrow\downarrow\rangle$. An identical result is obtained by instead applying the spin lowering operator $\hat{S}^- = \sum_i \hat{S}_i^-$ to eq. (3.17).

To give another example briefly, to create a bosonic wave function of four particles with angular momentum $S = S_z = 1$ we look at table 3.3 under $N = 4, S = 1$. The listed spatial polynomials (such as $e_{1,123} = \tilde{z}_1 + \tilde{z}_2 + \tilde{z}_3$) can be multiplied by any overall symmetric polynomial (which does not change their symmetry). The spatial wave function must be then multiplied by the appropriate first primitive spin wave function $|\uparrow\uparrow\uparrow\downarrow\rangle$, and, finally, the entire wave function should be fully symmetrized over all particles.

The prescription laid out here so far is sufficient to construct a complete basis of states of a two-component system of N particles having overall relative (orbital) angular momentum L and spin quantum numbers S and S_z.

3.2.2 Introduction to Symmetry Types

In the above section we explained briefly how we take spatial and spin wave functions of certain symmetry types and sew them together to make a wave function with overall bosonic

or fermionic symmetry. In this section we briefly explain in more detail precisely what we mean by a symmetry type. While it is not essential to understand this material in order to follow the construction of the previous section, in the more complicated cases of the next two sections where there are more than two components to the wave function (e.g., spin-1, spin-3/2, graphene with spin and valley, etc.) it becomes more crucial to understand the concept of symmetry type. The information contained in this section is standard mathematics, reviewed here briefly for convenience. See, for example, ref. [152] for a more detailed discussion.

A key intellection we use to describe our basis wave functions is the concept of a symmetry type or antisymmetry type of a wave function (the original method was introduced in ref. [153]). These symmetry types are intimately related to irreducible representations of the symmetric group (the group of permutations of N objects). Such irreducible representations are visualized by *Young frames* (closely related to *Young tableaux*), a series of N boxes arranged in left-justified rows and columns (a more detailed description of the representation theory of the symmetric group and of Young tableaux is provided here in appendix E). We shall denote the shape of a frame containing N_i boxes in the ith row by $\lambda = [N_1, N_2, \ldots]$ with $N_i \geq N_j \geq 0$ if $i < j$ and $N = \sum_i N_i$. Thus, the shape of each frame represents a unique partition of the integer N into pieces $[N_1, N_2, \ldots]$.

We will use the term *conjugate* to refer to Young frames related by a reflection along the diagonal, for example, the following frame of shape $\lambda = [3, 1]$,

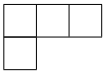

is conjugate to the following frame of shape $\tilde{\lambda} = [2, 1, 1]$,

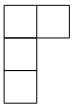

Representations of the symmetric group associated with conjugate Young frames are called *contragradient representations*. We will use the notation $\tilde{\lambda}$ to denote the conjugate Young frames (or integer partition) to λ.

We now explain how Young frames can be used to describe the permutation symmetry of a function. Given a Young frame $\lambda = [N_1, N_2, \ldots]$, being an integer partition of N, we say a function has *normal form* with symmetry λ if (a) it is symmetric in the first N_1 variables, symmetric in the next N_2 variables, symmetric in the next N_3 variables, and so forth, and (b) we cannot use permutation and linear combinations to construct a nonvanishing function that is symmetric in greater than N_1 variables, we cannot use permutation of the variables

$N_1+1, \ldots, N$ and linear combination to construct a nonvanishing function which is symmetric in greater than N_2 of these variables, we cannot use permutation of the variables $N_1+N_2+1, \ldots, N$ to construct a nonvanishing function symmetric in greater than N_3 of these variables, and so forth. In other words, permutations and linear combinations cannot make the function any more symmetric than it already is. By permutation and linear combination any function can be brought to normal form to clearly show its symmetry type (a detailed method of reduction to normal form is given in ref. [152]). Antisymmetry type is entirely analogous except that one should replace the word *symmetric* with *antisymmetric* in the above definition. A nontrivial theorem is that any function that has symmetry type λ also has the conjugate antisymmetry type, denoted by $\tilde{\lambda}$.[152]

One can check that the polynomials given in table 3.2 and table 3.3 are listed by symmetry type. For example, in table 3.3, the $N = 4$ primitive polynomials of symmetry type $[2, 2]$ are clearly symmetric in the first two variables [which are z_1 and z_2, bearing in mind the definitions given in eq. (3.5) and eq. (3.6)] and then also symmetric in second two variables (z_3 and z_4). Further, any attempt to symmetrize in four variables $(z_1, \ldots, z_4)$ will vanish [using eq. (3.5)]. Thus these entries are in normal form. For table 3.2 the symmetry type is sometimes less obvious (it is not in symmetric normal form), but the antisymmetry type is evident (the polynomials are listed in antisymmetric normal form). For example, symmetry type $\lambda = [2, 1, 1]$ must be equivalent to antisymmetry type $\tilde{\lambda} = [3, 1]$. The polynomials labeled by $\lambda = [2, 1, 1]$ in table 3.2 are indeed antisymmetric in the first three variables $(z_1, \ldots, z_3)$ and attempts to antisymmetrize in four variables $(z_1, \ldots, z_4)$ will fail.

Having defined symmetry type, the general procedure to create a wave function with bosonic symmetry involves sewing together a spin and a spatial wave function of the same symmetry type. Similarly to create wave functions of fermionic symmetry one must sew together spin and spatial wave functions with conjugate symmetries. The details of this procedure are presented in appendix F (see also ref. [151]). Here we shall simply state a few key results derived in that appendix. The first result is that, for a two-component system, the spin wave functions of a particular symmetry type are in one-to-one correspondence with spin eigenfunctions, that is, such functions are eigenfunctions of the $\hat{S}^2$ operator. For example, the following function is an eigenfunction of $\hat{S}^2$ with eigenvalue $S = S_z = 1/2$:

$$\tfrac{1}{\sqrt{6}} \left(2\,|\uparrow\uparrow\downarrow\rangle - |\uparrow\downarrow\uparrow\rangle - |\downarrow\uparrow\uparrow\rangle\right).$$

This can be shown by explicitly applying an $\hat{S}^2$ operator. One can also check that this function

has symmetry type $[2,1]$, since it is symmetric in the first two arguments. In order to generate a fully antisymmetric combined spin and spatial wave function, the procedure is to combine the above spin wave function with a spatial wave function of conjugate symmetry type and then antisymmerize the resulting construction. To generate a symmetric combined function, we associate that spin eigenfunction with a spatial function of the same symmetry type and then symmetrize that construction. If, for example, we wanted to generate a three-electron wave function then the corresponding spatial part would be a polynomial of conjugate symmetry type $[2,1]$ (note that $[2,1]$ is self-conjugate).

The second key result shown in appendix G and in ref. [151] is that, for a two-component system, the result of the construction procedure described in the previous paragraph can be obtained by using just the first primitive spin wave function [defined in eq. (3.15)] instead of the full spin eigenfunction. The simplest construction procedure is then to associate a spatial function of a given symmetry type with a first primitive spin wave function only, and then to (anti-) symmetrize or symmetrize that result to obtain an overall (anti-) symmetric combined spin and spatial wave function. The reason for this simplification lies with the (anti-) symmetrization operation: as long as the spatial part corresponds to a particular symmetry type, the (anti-) symmetrization procedure will automatically impose the correct symmetry type on the spin part.

Once we have more than two components in the wave function (higher spin, or multiple spins and valley degrees of freedom) this simplification no longer fully holds, nevertheless our guiding principle is to try to specify a (generalized) spin wave function of the simplest possible form, which can be associated with a spatial wave function of a particular symmetry such that the result of (anti-)symmetrizing that construction is an appropriate basis wave function.

A system built from N particles with n multiple components is described mathematically by the irreducible representations of the Lie algebra of the group SU(n). For example, we refer to spin-1/2 particles as being described by representations of the Lie algebra of SU(2). Irreducible representations of SU(n) are in correspondence with a subset of irreducible representations of the symmetric group of N objects[152] and, hence, the symmetry types. The simplest way to visualize this correspondence is via Young frames associated with these irreducible representations. The set of Young frames describing the irreducible representations of SU(n) corresponds precisely to the subset of symmetric group Young frames containing no more than n rows; the corresponding set of conjugate Young frames contain no more than n columns. There is a corresponding restriction on the possible symmetry types that can be used, for example, in the

case of a two-component system the possible symmetries of the spin and spatial wave function are restricted to being symmetric or antisymmetric in two subsets of particle indices. Hence, in table 3.3 where bosons are considered the only allowed symmetry type for the two-component case (spin-1/2 case) are those where there are only two columns of the frame λ, whereas in table 3.2 where fermions are considered the only allowed symmetry type for the two-component case (spin-1/2 case) are those where there are only two rows of the frame λ (or two columns of the conjugate frames).

3.2.3 Extension to Systems with n Components

Having described the general properties of symmetry types, we shall now turn our attention to systems containing n components. In this case the possible symmetries of the spin and spatial wave functions are symmetric or antisymmetric in up to n subsets of particle indices. The corresponding symmetry types are $\lambda = [N_1, N_2, \ldots, N_n]$ (for bosons) or conjugate symmetry types $\tilde{\lambda}$ (for fermions). In order to generate a complete basis for interactions with multicomponent symmetry, we have chosen to decompose the interparticle interaction into a basis of all the possible combinations of symmetry types that the spatial and spin wave functions can have. The forms of the spatial wave functions remain translationally invariant analytic polynomials.

In table 3.1 we have listed the dimensions of the space of polynomials for an n-component system (n possible values of the internal degree of freedom) for $N \leq 5$ particles. The dimensions are labeled by the symmetry type λ of the corresponding pseudopotential basis functions. Additionally, primitive polynomials for all symmetry types with $N \leq 4$ are listed in table 3.2 and table 3.3. We stress that not all symmetry types are available to a given n-component system—such a system can only be classified into symmetry types of the form $\lambda = [N_1, N_2, \ldots, N_n]$ (for bosons) or conjugate symmetry types $\tilde{\lambda}$ (for fermions). In particular, for the two-component case, one can see that only certain symmetry types are allowed depending on whether the system is bosonic or fermionic (e.g., the fully symmetric [3] type is not allowed for three fermions).

In order to construct complete basis wave functions, we also require a modified spin eigenfunction to describe the multiple internal degrees of freedom. We shall refer to this wave function as a *generalized spin wave function*. When a particle has an internal degree of freedom s, let us notate the different possible values of this degree of freedom by α, β, γ, and so on. The notation can be interpreted, for example, in the two-component case of spins as, $\alpha \equiv |\uparrow\rangle$ and $\beta \equiv |\downarrow\rangle$; but now there n possible values that our parameter can take. For a multiparticle system with multiple internal degrees of freedom, we similarly define primitive generalized spin

wave functions such as

$$\vartheta = |\alpha\zeta\beta\beta\alpha\rangle\,. \tag{3.18}$$

It is useful to define the index λ_z which represents the list $\{N_\alpha, N_\beta, \ldots, N_\zeta\}$ of how many times each type each component $(\alpha, \beta, \ldots)$ occurs in the primitive generalized spin wave function. So, for example, in the primitive generalized spin wave function $|\alpha\alpha\gamma\rangle$ for three particles we have the index $\lambda_z = \{2, 0, 1\}$.

A consequence of the increased number of component degrees of freedom is that the complete wave function can no longer be generated solely by using a so-called first primitive generalized spin wave function [first in the sense of a lexicographic ordering scheme, in analogy with eq. (3.15) for the two-component case]. Instead, we consult a list of the primitive components that occur for each symmetry type in order to generate a complete basis. These results are presented for the case of three-component and four-component systems in table 3.4.

As an example, consider the three-component $N = 3$, $\lambda = [2, 1]$, and $\lambda_z = \{1, 1, 1\}$ state. From table 3.4 we see that there is a choice of two possible primitive generalized spin wave functions, $|\alpha\beta\gamma\rangle$ or $|\alpha\gamma\beta\rangle$. Using these functions to construct a complete basis wave function will generate two orthogonal wave functions. (An interesting aside is that the three-component, $N = 3$, generalized spin wave functions are identical to the colour wave functions describing baryons in the SU(3) quark model; see, for example, ref. [154].)

The problem of constructing n-component N-particle wave functions with prescribed symmetry is equivalent to the problem of constructing tensor products of N fundamental irreducible representations of the Lie algebra of SU(n). We shall explain the mathematical details of that procedure in appendix E. Our general aim is to decompose our parameter space of wave functions into a basis of wave functions labeled by irreducible representations of the Lie algebra of SU(n). We shall describe the general method for selecting the appropriate primitive generalized spin wave functions in appendix G. Due to symmetry arguments, note that it is not possible to construct linear combinations of certain types of primitive generalized spin wave function corresponding to certain symmetry types. For example, it is clearly not possible to generate a fully antisymmetric generalized spin wave function from $|\alpha \ldots \alpha\rangle$.

The method to construct a full basis wave function is similar to the two-component case: first we choose a primitive generalized spin wave function from table 3.4, corresponding to a given symmetry type λ and having a given λ_z. For a boson wave function we construct a polynomial corresponding to a symmetry λ and at a given degree L using the primitive

polynomials in table 3.3. The full basis wave function is generated by putting these two parts together and then fully symmetrizing. To obtain a fermion wave function, we would instead construct a polynomial corresponding to a symmetry type $\tilde{\lambda}$ using the primitive polynomials given in table 3.2, and the complete basis function is given by fully antisymmetrizing. We shall explain how these results were derived in Appendices F, G, and H.

To obtain the total size $p(N, L)$ of the space of pseudopotentials, $|L, \mathfrak{q}\rangle$, for a given L, we need to include both the number of polynomials $p(N, L, \lambda)$ with a given symmetry type λ and the number of generalized spin wave functions for that same λ but with different values of λ_z (for example, in the two-component case the spin wave functions have $2S + 1$ values of S_z). For clarity, let us discuss an example: a system of $N = 4$ bosons with $n = 3$ components. Say that we want to construct the basis space of wave functions for an interaction at $L = 4$. The general form of the basis wave functions is $|L = 4, \mathfrak{q}\rangle$. In this case, the possible symmetry types that the wave function can have are $\lambda = [4], [3, 1], [2, 2]$, and $[2, 1, 1]$. Looking at table 3.1, the wave functions with these symmetry types have the respective polynomial space dimensions of $p(4, 4, [4]) = 2$, $p(4, 4, [3, 1]) = 2$, $p(4, 4, [2, 2]) = 2$, and $p(4, 4, [2, 1, 1]) = 1$. Further, the corresponding dimensions of the space of generalized spin wave functions are given by counting all of the primitive generalized spin wave functions in table 3.4, which are respectively 15, 15, 6, and 3. The total dimension of the space of $L = 4$ pseudopotentials, that is, the total number, $p(N, L)$, of possible values of $\mathfrak{q}$, is, thus, $15 \times 2 + 15 \times 2 + 6 \times 2 + 3 \times 1 = 75$. Each of these basis wave functions is obtained by multiplying the spatial part of the wave function by the generalized spin wave function and symmetrizing (for bosons in this case). The pseudopotential matrix at $L = 4$ would then be a 75-dimensional Hermitian matrix!

In a system with n components, if the Hamiltonian has full SU(n) symmetry, then the pseudopotential Hamiltonian, eq. (3.10), will be diagonal in both λ and λ_z variables.

3.2.4 Further Specializations: Spin-J and Spin+Valley in Graphene

Often when we consider particles with n internal states (components), these multiple states may have arisen from particles that had spin $J = (n - 1)/2$. If the Hamiltonian is spin-rotationally invariant, then it is very useful to consider a set of basis wave functions that are eigenfunctions of S^2 and S_z such that the Hamiltonian, eq. (3.10), is diagonal in these variables. More generally, a particle may have several different internal degrees of freedom. A particularly important example of this is graphene which has two spin states and two valley states resulting in four possible internal states. The Hamiltonian may have full SU(4) symmetry or, for example, it

could be symmetric only under the SU(2) rotations of the spin.[155–157] In the case where the system has an SU(2) spin rotational symmetry in each valley [but not the full SU(4) symmetry] it is useful to decompose these states into their S^2 eigenstates to exploit the symmetries of the problem as much as possible. Specializations of multicomponent pseudopotentials to both such systems are discussed in detail in ref. [149].

3.2.5 Tables

All of the results presented in the tables here have been generated using a MATHEMATICA-based computer program.[158] The program is capable of producing spatial and generalized spin wave functions for systems of up to $N = 6$ and for an arbitrary number of components, although we only have space to give a selection of results for the most relevant cases here.

3.3 Conclusions

The main result of this chapter is the enumeration of the space of N-particle wave functions for bosons or fermions with internal degrees of freedom such as spin (i.e., multiple components). These wave functions can be used as a basis for writing pseudopotential coefficients to parameterize physical problems, as, for example in refs. [117, 127, 159]. The formalism developed in this chapter has subsequently proved particularly useful in the development of analytical and, to some extent, numerical methods for determining Landau level mixing corrections to the pseudopotential coefficients in the LLL and second LL,[49–51] where it is found that pseudopotentials for two-body and three-body interactions in each spin channel (i.e., $S = 0, 1$ for two-body and $S = 1/2, 3/2$ for three-body) need to be taken into account (see chapter 1 for a brief definition of LL mixing). Most importantly, however, determining such a complete basis of pseudopotentials strongly suggests much of the physics of wave functions that can be generated with model interactions.

To elaborate on this last point, let us return to the spinless (single component) case for a moment, and for simplicity, let us consider bosons. In the case of $N = 3$ body interaction, there are three-body wave functions with $L = 0, 2, 3, 4, \ldots$ (this can be read off from the table in ref. [122], which is identical to the $N = 3$ fully symmetric $\lambda = [3]$ case of table 3.1 here). One can consider a family of model Hamiltonians that successively gives each of these terms some positive energy.[160] For example, if $L = 0$ is given positive energy (i.e., there is a nonzero pseudopotential coefficient $V_{L=0,N=3}$) and no other potential energy term is in the Hamiltonian,

then it can be demonstrated that the highest density zero-energy ground state is the Moore–Read Pfaffian wave function, which has the property that when three particles approach each other, the wave function vanishes as $L = 2$ powers (since $L = 1$ is forbidden).[5] One can then consider adding a positive energy for $L = 2$ as well (a positive pseudopotential $V_{L=2,N=3}$), which results in the gaffnian as its ground-state wave function,[120] where the wave function vanishes as $L = 3$ powers when three particles approach each other. One can continue by adding positive energy for $L = 3$, resulting in the Haffnian,[121] which then vanishes as $L = 4$ powers when three particles approach each other. [†]

For higher L the situation becomes somewhat more complicated for several reasons (see refs. [160] and [162]). First, there can be several wave functions with the same value of L (e.g., two such $N = 3$ wave functions at $L = 6$), so specifying L alone does not fully characterize the wave function. Second, it is possible that a Hamiltonian that forbids all $L < L_0$ for clusters of N particles can have a ground-state wave function where $L > L_0$ for clusters of N particles rather than $L = L_0$ (see, for example, the discussion in ref. [160]). Nonetheless, the general idea that one can dictate the vanishing properties of a wave function by appropriately choosing nonzero pseudopotentials remains a powerful approach both to understanding the properties of quantum Hall wave functions and to generating new and interesting trial states.

To generalize this approach to the multicomponent case, if one is interested in two component (spin-1/2) quantum Hall states, for, say, bosons, we can look at table 3.1 and quickly see what kind of pseudopotentials are possible, which then also suggests what kind of wave functions might occur. In the simplest case we might consider two-body interactions. Trivially, in this case (looking in the $N = 2$ rows of the table), we see that even L occurs in the triplet channel ($S_{\text{boson}} = 1$), whereas odd L occurs in the singlet channel ($S_{\text{boson}} = 0$). Choosing to give positive energy (positive pseudopotential coefficient) to all $L < m$ (triplet) even and all $L < n$ (singlet) odd generates the Halperin ground state (ref. [15] and see also chapter 1).

Let us now move on to three-body interactions and, for simplicity, let us still consider spin-1/2 bosons. In the spin polarized ($S_{\text{boson}} = 3/2$) channel we see exactly the same structure we did for spinless bosons; wave functions occurring at $L = 0, 2, 3, 4, \ldots$ ($N = 3, S = 3/2$ line of table 3.1). In the $S_{\text{boson}} = 1/2$ channel, on the other hand, we see wave functions at $L = 1, 2, 3, \ldots$. A simple example of a three-body Hamiltonian is one that forbids $L = 0$ in the

[†]The nomenclature for these wave functions has an interesting history. While *Paffian* is named after a person (Johann Friedrich Pfaff), and *Haffnian* (a misspelling with two fs) is named after the latin name, "Hafnia", for Copenhagen, a name given to it in ref. [161] (the same origin as the element Hafnium), the word *gaffnian* is an alphabetical interpolation between these according to the wave function's vanishing power, i.e., P**f**affian, **g**affnian, **H**affnian (see ref. [122]).

polarized ($S_{\text{boson}} = 3/2$) channel (a positive $V^{S=3/2}_{L=0,N=3}$ only); such a Hamiltonian generates the $k = 2$ NASS state as its ground state.[17,101] As one might suspect, this wave function vanishes as $L = 2$ powers when three particles come together in the $S_{\text{boson}} = 3/2$ channel and vanishes as $L = 1$ power in the $S_{\text{boson}} = 1/2$ channel. These are the lowest powers on the table that are not explicitly forbidden by the Hamiltonian.

By similarly examining the tables we can easily propose new wave functions that generalize those already discussed, and we may even be able to guess at the model Hamiltonians that generate these wave functions as their ground states. For example, generalizing the $k = 2$ NASS state we might propose to forbid the lowest powers that are not forbidden by the NASS Hamiltonian, i.e., we choose to forbid $N = 3, S = 3/2, L = 2$ and the $N = 3, S = 1/2, L = 1$ in addition to the $N = 3, S = 3/2, L = 0$ of the NASS wave function. We might guess that the resulting wave function should vanish $L = 3$ powers when three particles come together in the $S = 3/2$ channel and as $L = 2$ powers when three come together in the $S = 1/2$ channel. Such a wave function, a spin-singlet generalisation of the gaffnian, will be the subject of chapter 4 (see also refs. [163] and [159]). Another possible direction is the generation of wave functions that mix N and N' body multicomponent interactions; for example, the double Pfaffian wave function discussed in ref. [99] is the ground state of the sum of a three body interaction and a two body interaction.

The examples discussed here are only a fraction of the model Hamiltonians that have been discussed in the literature.[5,17,99,101–104,119–121,125] Since the language of multicomponent pseudopotentials is arbitrarily general, all of these model Hamiltonians can be rephrased into this language. In many cases it is quite obvious from looking at our tables what vanishing behaviors for N-particle cluster are being forbidden and what the resulting properties of the corresponding ground-state wave functions should, therefore, be (albeit rigorous proofs of these correspondences may be more tricky). Because of the added richness of the multicomponent case over the single component case there are certainly a far wider variety of possible model Hamiltonians and model wave functions to be explored. Potentially we may even find some new physically realizable multicomponent wave functions with interesting braiding properties that can be exploited for quantum information processing.[3]

λ	Set of Primitive Generalized Spin Wave Functions	Counting
[2]	$\|\alpha\alpha\rangle, \|\alpha\beta\rangle, \|\alpha\gamma\rangle, \|\beta\beta\rangle, \|\beta\gamma\rangle, \|\gamma\gamma\rangle$	6
[1, 1]	$\|\alpha\beta\rangle, \|\alpha\gamma\rangle, \|\beta\gamma\rangle$	3

(a) Three-component $N = 2$

λ	Set of Primitive Generalized Spin Wave Functions	Counting
[3]	$\|\alpha\alpha\alpha\rangle, \|\alpha\alpha\beta\rangle, \|\alpha\alpha\gamma\rangle, \|\alpha\beta\beta\rangle, \|\alpha\beta\gamma\rangle, \|\alpha\gamma\gamma\rangle, \|\beta\beta\beta\rangle, \|\beta\beta\gamma\rangle, \|\beta\gamma\gamma\rangle, \|\gamma\gamma\gamma\rangle$	10
[2, 1]	$\|\alpha\alpha\beta\rangle, \|\alpha\alpha\gamma\rangle, \|\alpha\beta\beta\rangle, \|\alpha\beta\gamma\rangle, \|\alpha\gamma\beta\rangle, \|\alpha\gamma\gamma\rangle, \|\beta\beta\gamma\rangle, \|\beta\gamma\gamma\rangle$	$16 = 8 \times 2$
[1, 1, 1]	$\|\alpha\beta\gamma\rangle$	1

(b) Three-component $N = 3$

λ	Set of Primitive Generalized Spin Wave Functions	Counting
[4]	$\|\alpha\alpha\alpha\alpha\rangle, \|\alpha\alpha\alpha\beta\rangle, \|\alpha\alpha\alpha\gamma\rangle, \|\alpha\alpha\beta\beta\rangle, \|\alpha\alpha\beta\gamma\rangle, \|\alpha\alpha\gamma\gamma\rangle, \|\alpha\beta\beta\beta\rangle,$ $\|\alpha\beta\beta\gamma\rangle, \|\alpha\beta\gamma\gamma\rangle, \|\alpha\gamma\gamma\gamma\rangle, \|\beta\beta\beta\beta\rangle, \|\beta\beta\beta\gamma\rangle, \|\beta\beta\gamma\gamma\rangle, \|\beta\gamma\gamma\gamma\rangle, \|\gamma\gamma\gamma\gamma\rangle$	15
[3, 1]	$\|\alpha\alpha\alpha\beta\rangle, \|\alpha\alpha\alpha\gamma\rangle, \|\alpha\alpha\beta\beta\rangle, \|\alpha\alpha\beta\gamma\rangle, \|\alpha\alpha\gamma\beta\rangle, \|\alpha\alpha\gamma\gamma\rangle, \|\alpha\beta\beta\beta\rangle, \|\alpha\beta\beta\gamma\rangle,$ $\|\alpha\beta\gamma\beta\rangle, \|\alpha\beta\gamma\gamma\rangle, \|\alpha\gamma\gamma\beta\rangle, \|\alpha\gamma\gamma\gamma\rangle, \|\beta\beta\beta\gamma\rangle, \|\beta\beta\gamma\gamma\rangle, \|\beta\gamma\gamma\gamma\rangle$	$45 = 15 \times 3$
[2, 2]	$\|\alpha\alpha\beta\beta\rangle, \|\alpha\alpha\beta\gamma\rangle, \|\alpha\alpha\gamma\gamma\rangle, \|\alpha\beta\beta\gamma\rangle, \|\alpha\beta\gamma\gamma\rangle, \|\beta\beta\gamma\gamma\rangle$	$12 = 6 \times 2$
[2, 1, 1]	$\|\alpha\alpha\beta\gamma\rangle, \|\alpha\beta\beta\gamma\rangle, \|\alpha\beta\gamma\gamma\rangle$	$9 = 3 \times 3$

(c) Three-component $N = 4$

λ	Set of Primitive Generalized Spin Wave Functions	Counting
[2]	$\|\alpha\alpha\rangle, \|\alpha\beta\rangle, \|\alpha\gamma\rangle, \|\alpha\delta\rangle, \|\beta\beta\rangle, \|\beta\gamma\rangle, \|\beta\delta\rangle \|\gamma\gamma\rangle, \|\gamma\delta\rangle, \|\delta\delta\rangle$	10
[1, 1]	$\|\alpha\beta\rangle, \|\alpha\gamma\rangle, \|\alpha\delta\rangle, \|\beta\gamma\rangle, \|\beta\delta\rangle \|\gamma\delta\rangle$	6

(d) Four-component $N = 2$

λ	Set of Primitive Generalized Spin Wave Functions	Counting
[3]	$\|\alpha\alpha\alpha\rangle, \|\alpha\alpha\beta\rangle, \|\alpha\alpha\gamma\rangle, \|\alpha\alpha\delta\rangle, \|\alpha\beta\beta\rangle, \|\alpha\beta\gamma\rangle, \|\alpha\beta\delta\rangle, \|\alpha\gamma\gamma\rangle, \|\alpha\gamma\delta\rangle, \|\alpha\delta\delta\rangle,$ $\|\beta\beta\beta\rangle, \|\beta\beta\gamma\rangle, \|\beta\beta\delta\rangle, \|\beta\gamma\gamma\rangle, \|\beta\gamma\delta\rangle, \|\beta\delta\delta\rangle, \|\gamma\gamma\gamma\rangle, \|\gamma\gamma\delta\rangle, \|\gamma\delta\delta\rangle, \|\delta\delta\delta\rangle$	20
[2, 1]	$\|\alpha\alpha\beta\rangle, \|\alpha\alpha\gamma\rangle, \|\alpha\alpha\delta\rangle, \|\alpha\beta\beta\rangle, \|\alpha\beta\gamma\rangle, \|\alpha\beta\delta\rangle, \|\alpha\gamma\beta\rangle, \|\alpha\gamma\gamma\rangle, \|\alpha\gamma\delta\rangle, \|\alpha\delta\beta\rangle,$ $\|\alpha\delta\gamma\rangle, \|\alpha\delta\delta\rangle, \|\beta\beta\gamma\rangle, \|\beta\beta\delta\rangle, \|\beta\gamma\gamma\rangle, \|\beta\gamma\delta\rangle, \|\beta\delta\gamma\rangle, \|\beta\delta\delta\rangle, \|\gamma\gamma\delta\rangle, \|\gamma\delta\delta\rangle$	$40 = 20 \times 2$
[1, 1, 1]	$\|\alpha\beta\gamma\rangle, \|\alpha\beta\delta\rangle, \|\alpha\gamma\delta\rangle, \|\beta\gamma\delta\rangle$	4

(e) Four-component $N = 3$

Table 3.4: The minimal set of primitive generalized spin wave functions specifying a complete basis, classified by symmetry type λ. In order to count the number of states, we count the number of primitive generalized spin wave functions in each symmetry type, multiplied by the dimension of the corresponding symmetric group representation (see appendix G for details). The total number should be equal to n^N for an n component system of N particles.

CHAPTER 4

Putting a Spin on the Gaffnian

In this chapter,[†] we characterize in detail a wave function conceivable in fractional quantum Hall systems where a spin or equivalent degree of freedom is present. This wave function combines the properties of two previously proposed quantum Hall wave functions, namely the non-Abelian spin-singlet (NASS) state and the nonunitary gaffnian wave function. This is a spin-singlet generalization of the spin-polarized gaffnian, which we call the "spin-singlet gaffnian" (SSG). [‡] Most notably, we argue that the wave function can be written as a special polynomial and that it corresponds to the highest density zero energy state of a certain local Hamiltonian.

In sec. 4.1 we shall explain how the proposed SSG Hamiltonian can be written in terms of the generalized Haldane pseudopotentials discussed in chapter 3. In sec. 4.2 we shall present the results of numerical exact diagonalization of the SSG Hamiltonian in the sphere geometry (see appendix B for a definition of the sphere geometry). We have determined that the proposed SSG wave function is the unique, highest density zero energy ground state of that model Hamiltonian at $\nu = 4/5$ (for bosons) and shift $\delta = 3$ (the shift is defined in appendix B such that the flux N_Φ for a given number of particles N is given by $N_\Phi = N/\nu - \delta$). We shall discuss an explicit form of the wave function in sec. 4.3.

4.1 Pseudopotential Construction of the SSG Hamiltonian

In previous investigations, most notably for the Laughlin and Moore–Read wave functions, it has been determined that trial quantum Hall wave functions correspond to unique, zero energy ground states of certain model Hamiltonians.[52,164] Often, these model Hamiltonians are most simply expressible in terms of Haldane pseudopotentials[52] and their generalizations.[122,149] Given a system with a certain N-body interaction potential $V(\mathbf{r_1}, s_1; \mathbf{r_2}, s_2; \ldots; \mathbf{r}_N, s_N)$, where, in general, s_j represents any additional quantum number of the j^{th} particle (if present), the action of a pseudopotential is to project out a particular component of that interaction. Those

[†]This chapter is based on my contribution to the publication S. C. Davenport, E. Ardonne, N. Regnault, and S.H Simon, PRB **87**, 045310 (see ref. [159]).

[‡]Throughout the chapter, we shall describe how the wave function corresponds to a spin degree of freedom, however, note that all of what follows applies equally well to any other type of multicomponent degree of freedom such as valley or layer index.

components are labelled by a convenient set of quantum numbers, which describe all possible few-particle interactions. The vector space of few-particle interactions is spanned by specifying both the relative angular momentum L and, if we consider a spin degree of freedom as well, the spin quantum number S also. In general it is necessary to further distinguish between distinct interaction components with the same L, S. In other words, there exists in general a subvector space of dimension $d_{L,S}$ for each L and S sector (see chapter 3). In this chapter, however, we shall only be concerned with subspaces of dimension $d_{L,S}$=1 or 0, and so, for clarity, we omit any additional notation.

Pseudopotentials specify projection operators in the Hamiltonian and are thus labelled by two distinct sets of such quantum numbers L, S and L', S' in general. The pseudopotential $V^{S;S'}_{L;L',N}$ is expressed in terms of the vector space $|L, S\rangle$ and the N-body interaction potential as

$$V^{S;S'}_{L;L',N} = \langle L, S|\, V(\mathbf{r_1}, s_1; \mathbf{r_2}, s_2; \ldots; \mathbf{r}_N, s_N)\, \big|L', S'\big\rangle\,, \tag{4.1}$$

[cf. eq. (3.9)]. Such a basis of pseudopotentials is particularly convenient when the interaction potential is rotationally and/or spin rotationally invariant, since in that case the pseudopotentials then are diagonal in L, S, or both. In this chapter we will only need to consider situations where the pseudopotentials are diagonal:

$$V^{S;S}_{L;L,N} \equiv V^{S}_{L,N} = \langle L, S|\, V(\mathbf{r_1}, s_1; \mathbf{r_2}, s_2; \ldots; \mathbf{r}_N, s_N)\, |L, S\rangle\,. \tag{4.2}$$

The most general form of the Hamiltonian, assuming both spatial and spin rotational invariance, is then given by the following [cf. eq. (3.10)]:

$$H = \sum_{L,l,S} |L, S\rangle\, |l\rangle\, V^{S}_{L,N}\, \langle l|\, \langle L, S|\,. \tag{4.3}$$

At our convenience, we can pick certain special many-body interactions (such as δ-function-type interactions) for which only a small set of pseudopotentials remain nonzero. The impact of specifying a positive value of a given pseudopotential in a model Hamiltonian is to assign energy to the corresponding component of the interaction, therefore, if such a component is present in a given trial wave function, then that wave function will not be a zero energy state of our Hamiltonian. Conversely, if a component is not present in a given trial wave function, then we can include the corresponding pseudopotential in the Hamiltonian without introducing an extra energy cost. In this way we can tailor the Hamiltonian to correspond to the desired properties of a given trial ground-state wave function. These properties might come, for instance, from a

conformal field theory (CFT) description of the state; see, e.g., ref. [5].

To give an example, briefly, it is known that the Moore–Read wave function for bosons at $\nu = 1$ is the unique, highest density zero energy ground state of a spin-polarized three-body contact interaction.[164] The space of pseudopotentials for spin-polarized three-body interactions is spanned by a relative angular momentum L. S takes only its maximal value for a three-body interaction, $S = 3/2$.[122] † In the language of pseudopotentials, the Moore–Read state corresponds to the spinless pseudopotential $V_{L=0,N=3}$ being positive and all other pseudopotentials being zero and, in addition, the corresponding Hilbert space is restricted to only spin-polarized sectors. Along similar lines, the spin-polarized gaffnian wave function for bosons corresponds to $V_{L=0,N=3}$ and $V_{L=2,N=3}$ being positive and all other pseudopotentials being zero, and again the Hilbert space is restricted to spin-polarized sectors (note that for $L = 1$, $S = 3/2$, and $N = 3$, we have a 0-dimensional vector space of wave functions, so no corresponding $L = 1$, $S = 3/2$, and $N = 3$ pseudopotential can occur; see table 3.1 in chapter 3). The (bosonic) NASS state, like the (bosonic) Moore–Read state, corresponds to a spin-polarized three-body contact interaction, however the Hilbert space now includes additional spin sectors (not just the spin-polarized sector).[17] In the language of pseudopotentials, the bosonic NASS state is the highest density zero energy ground state of a Hamiltonian with the positive pseudopotential $V^{S=3/2}_{L=0,N=3}$.

Motivated by the generalization of the Moore–Read Hamiltonian to the gaffnian Hamiltonian, our proposal for the SSG Hamiltonian is to keep $V^{S=3/2}_{L=0,N=3}$, $V^{S=3/2}_{L=2,N=3}$, and $V^{S=1/2}_{L=1,N=3}$ positive (for the bosonic case). The proposed Hamiltonian for the SSG wave function is thus expressed as

$$H_{\mathrm{SSG}} = |0,3/2\rangle\, V^{S=3/2}_{L=0,N=3}\, \langle 0,3/2| + |2,3/2\rangle\, V^{S=3/2}_{L=2,N=3}\, \langle 2,3/2| + |1,1/2\rangle\, V^{S=1/2}_{L=1,N=3}\, \langle 1,1/2|\,, \quad (4.4)$$

[not writing the centre of mass part, $|l\rangle$, see eq. (4.3)]. To obtain a fermionic version, one simply includes an additional two-body term $V^{S=0}_{L=0,N=2}$, precisely as in the NASS case.[101]

From this pseudopotential Hamiltonian, we can already infer some properties of its zero energy eigenstates. Because the three-body interaction in the $S = 3/2$ channel is identical to the Hamiltonian generating the (polarized) gaffnian, the zero energy eigenstates will vanish as at least a third power when three particles with the same spin are brought to the same point. In addition, when three particles have overall spin $S = 1/2$, the wave functions vanish

† Note a slight abuse of notation here: as in chapter 3, we are denoting bosons as if they are spin-1/2 objects, e.g., three bosons can have $S = 3/2$ and $S = 1/2$ interaction channels. In actual fact we are describing systems such as cold atomic gasses for which bosons can be engineered to have internal two-state degrees of freedom, and we have simply mapped that two-state degree of freedom onto a spin degree of freedom.

at least quadratically. These are indeed the vanishing properties consistent with the CFT description of the SSG, as explained in refs. [163] and [159]. It is worth stating here that the SSG wave function likely also corresponds to the ground state of other, more complicated, local Hamiltonians involving N-body terms with $N > 3$, following the line of reasoning in ref. [122].

4.2 Energy Spectrum

The energy spectrum is determined by numerical exact diagonalization of the Hamiltonian for finite-sized systems in the sphere geometry. This is done for a variety of system sizes, N, and for a variety of fluxes N_Φ. Eigenstates are labelled by the quantum numbers L_z and S_z and fall into (L, S) multiplets. (Note that these quantum numbers are completely separate from the N, L and S describing the pseudopotentials, unless one has only N particles with an N-body interaction.) Given practical constraints due to the dimension of the spinful Hilbert space, we were able to study systems of up to $N = 12$ bosons and $N_\Phi = 12$ flux. An example of such a spectrum is plotted in fig. 4.1. All the numerical results were calculated using the freely available *DiagHam* package.[54]

Our key observations are as follows: first, there is a unique zero energy state occurring only in the $L = 0$, $S = 0$ sector for $N = 4$ at $N_\Phi = 2$, for $N = 8$ at $N_\Phi = 7$ (see fig. 4.1) and for $N = 12$ at $N_\Phi = 12$, which all correspond to $\nu = 4/5$ and shift $\delta = 3$ (see appendix B for the definition of the shift). We have further determined for $N = 4$ and $N = 8$ that the ground-state monomial expansion of the Hilbert space, that is, the eigenvector corresponding to the zero-energy eigenstate, generated by exact diagonalization of eq. (4.4), precisely matches that of the proposed analytic form of the ground-state SSG wave function (we shall discuss the analytical form of the ground-state wave function in sec. 4.3).

With the evidence presented in this section in mind, we conclude that the proposed SSG Hamiltonian in eq. (4.4) generates the correct zero energy Hilbert space for the SSG wave function, at least for system sizes up to $N = 12$ bosons. Based on this evidence, and on significant further evidence presented in ref. [159], we also expect our conclusion to hold for any other system size.

An important question, left unanswered by our numerical calculations here, is what is the size of the gap for quasiparticle excitations in the thermodynamic limit? For finite-sized systems, looking at fig. 4.1, the gap is clearly finite (as it is in the gaffnian case). There is good reason, however, to argue that the gap does in fact vanish in the thermodynamic limit, and

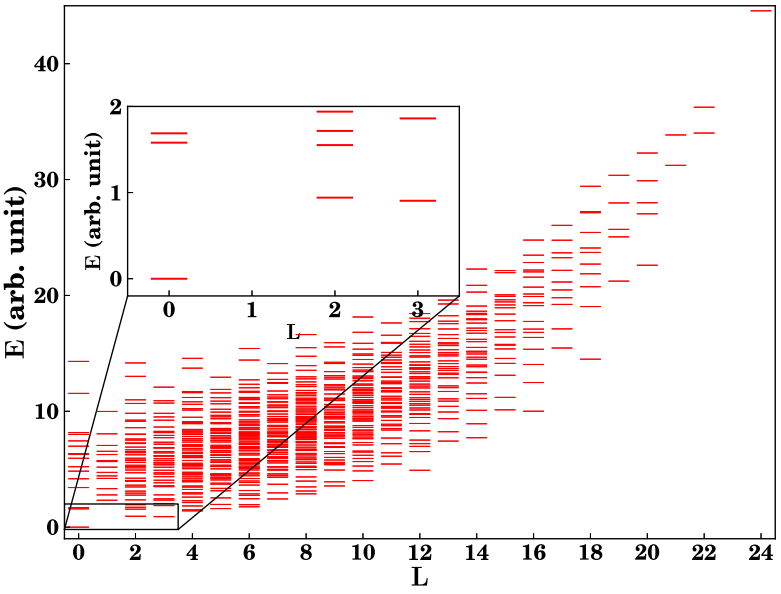

Figure 4.1: The $S = 0$ sector of the energy spectrum of the Hamiltonian H_{SSG}, defined in eq. (4.4), for $N = 8$ and $N_\Phi = 7$, obtained by numerical exact diagonalization in the sphere geometry. The inset zooms in on the bottom left corner of the spectrum and shows the unique zero energy state located in the $L = 0$, $S = 0$ sector.

hence the SSG corresponds to a compressible phase of matter.[165] That argument is based on the fact that the CFT corresponding to the SSG is nonunitary.[159,163]

4.3 Ground-State SSG Wave Function

In this section we shall present an explicit construction for the ground-state SSG wave function. Our construction is conjectured with the view to satisfying the vanishing properties imposed by the corresponding CFT (vanishing as at least a third power when three particles with the same spin are brought to the same point, and vanishing at least quadratically when three particles have overall spin $S = 1/2$; see refs. [163] and [159]) as well as the constraints of filling factor $\nu = 4/5$ (and shift $\delta = 3$ when constructed in the sphere geometry). In addition, the wave function must describe a spin-singlet state. That condition specifies the requirement to satisfy the Fock cyclic symmetry conditions.[152]

Before we describe how to construct the SSG, it will be useful to motivate our methodology by briefly reviewing the construction of the spin-polarized gaffnian wave function.[120] For the gaffnian, the required vanishing properties are that for any three particles coincident the wave function must vanish as three powers and that the wave function must not vanish for any two particles coincident [the CFT describing the gaffnian, which imposes these vanishing properties, is the nonunitary minimal model $\mathcal{M}(3, 5)$]. Further, it was determined that in its bosonic form, the gaffnian occurs at filling 2/3 and $\delta = 3$.

To give the expression of the gaffnian wave function that can be generalized to the SSG, we divide the particles into two groups A and B of equal size. The gaffnian wave function can then be written as

$$\Psi_{\text{gaffnian}} = \hat{S}\left[\prod_{i<j\in A}(z_i^A - z_j^A)^2 \prod_{i<j\in B}(z_i^B - z_j^B)^2 \prod_{i\in A, j\in B}(z_i^A - z_j^B)\,\mathbf{Per}\left(\frac{1}{z_i^A - z_j^B}\right)\right],$$

where $\hat{S}$ represents a symmetrization operation over all N particle coordinates, and $\mathbf{Per}(M_{ij})$ denotes the "permanent" of a matrix M whose elements are in this case given by $M_{ij} = (z_i^A - z_j^B)^{-1}$ if $i \neq j$ and 0 otherwise. On its own, this permanent factor contains a certain pattern of poles. When placed within the full construction, these poles conspire to ensure that the overall wave function does not vanish as two particles become coincident. Thus the polynomial vanishes only when three particles are coincident. The vanishing power can be tuned, if desired, by adjusting the exponents of each Jastrow-type factor in the construction. For example, $\prod_{i<j\in A}(z_i^A - z_j^A)^2$ could be adjusted to, say, $\prod_{i<j\in A}(z_i^A - z_j^A)^4$ (and similar for the particles in group B) to alter the vanishing power from 3 to 5 in this example. An entirely nontrivial step is to determine whether or not these vanishing properties are retained once the overall symmetrization operation has been completed. For the gaffnian, it was found that the vanishing properties are retained.

Now let us turn to the construction of the ground-state SSG wave function. We have determined that the following construction, written in eq. (4.5), gives a wave function at filling factor $\nu = 4/5$ and $\delta = 3$ that satisfies the vanishing constraints for $N = 4, 8, 12$. We have reason to believe that it will also work for all other values of N (i.e., 16, 20, etc.), although an explicit check is not possible. In the construction, we have used a clustering principle: the particle coordinates are first divided into equal sets of spin up and spin down, and then each of these sets is further subdivided into two equal subsets labelled by either A or B, giving four sets in total ($A\uparrow$, $A\downarrow$, $B\uparrow$, $B\downarrow$). With the label A or B on its own, we refer to the two subsets with either spin direction,

$$\Psi_{\text{SSG}} = \hat{Y}_{S=0}\left[\prod_{a=A,B}\left\{\prod_{i<j\in a\uparrow}(z_i^{a\uparrow} - z_j^{a\uparrow})^2 \prod_{i<j\in a\downarrow}(z_i^{a\downarrow} - z_j^{a\downarrow})^2 \prod_{i\in a\uparrow, j\in a\downarrow}(z_i^{a\uparrow} - z_j^{a\downarrow})\right\}\right.$$
$$\left.\times \prod_{i\in A, j\in B}(z_i^A - z_j^B)\,\mathbf{Per}\left(\frac{1}{z_i^A - z_j^B}\right)\right], \tag{4.5}$$

where and $\mathbf{Per}(M_{ij})$ denotes the "permanent" of a matrix M whose elements are in this case given by $M_{ij} = (z_i^A - z_j^B)^{-1}$ if $i \neq j$ and 0 otherwise, and $\hat{Y}_{S=0}$ is the Young operator for a spin-singlet representation of the symmetric group—this operation is required in order to

guarantee that the wave function satisfies the correct Fock cyclic symmetry conditions for a spin-singlet state (see appendix I).

$$\hat{Y}_{S=0} = \hat{S}_{z_1^\uparrow \ldots z_{N/2}^\uparrow} \hat{S}_{z_1^\downarrow \ldots z_{N/2}^\downarrow} \hat{A}_{z_1^\uparrow z_1^\downarrow} \ldots \hat{A}_{z_{N/2}^\uparrow z_{N/2}^\downarrow}, \tag{4.6}$$

that is, the Young operator for a spin-singlet representation corresponds to the operation of antisymmetrizing over ordered pairs of spin-up and spin-down coordinates, followed by symmetrizating over all spin-down and then all spin-up coordinates. Crucially, it is important to note that the wave function does not completely vanish when $\hat{Y}_{S=0}$ is applied! To obtain a fermionic version of this wave function, one can simply multiply the bosonic version by a Jastrow factor $\prod_{i<j}(z_i - z_j)$. The fermionic version occurs at $\nu = 4/9$ and $\delta = 4$.

In sec. 4.2 we provided strong evidence showing that the spectrum of the Hamiltonian for the SSG contains a unique zero energy state with $L = 0$ and $S = 0$ with an eigenvector proportional to eq. (4.5), for precisely the values of particle number and flux corresponding to filling $\nu = 4/5$ and $\delta = 3$. Therefore we conclude that this trial ground-state wave function is unique, and further, it is precisely the highest density zero energy ground state of the SSG Hamiltonian proposed in eq. (4.4).

4.4 Conclusions

We have presented evidence to demonstrate that the proposed SSG wave function satisfies many of the ingredients of an ideal theory of a FQHE state: a local Hamiltonian and a relatively simple analytic expression for the wave function, at least for the ground state. For the spin-polarized gaffnian it is also possible to construct exact quasihole wave functions [120]; the main stumbling block to achieving the same goal with the SSG is the additional complexity due to the spin degree of freedom. Significant further evidence supporting the validity of the SSG wave function construction is presented in ref. [159].

To briefly summarize that additional evidence: first, it has also been determined that a certain nonunitary, rational conformal field theory provides an underlying description of the SSG [the SSG wave function can be constructed from conformal blocks in a CFT associated with the semidirect product of nonunitary minimal models expressible as $\mathcal{M}(3,5) \ltimes \mathcal{M}(5,7)$], which indicates that the SSG possesses a vanishing energy gap in the thermodynamic limit. Second, the wave function construction presented here can be compared to two independent techniques for the analysis of fractional quantum Hall trial states: the "spin dressed squeezing algorithm", [166,167] and the "generalized Pauli principle". [168] One finds that the counting of zero

energy eigenstates in the energy spectrum precisely matches the counting predicted by the squeezing algorithm. The counting of zero energy eigenstates is also found to be identical to the result generated by the spinful version of the generalized Pauli principle. Finally, it can be checked that the structure of quasihole eigenstates in the energy spectrum of the Hamiltonian is identical to the structure of the entanglement eigenstates of a reduced density matrix given by partitioning the system into two groups of particles (the so-called particle entanglement spectrum[169–172]). Similar results have been determined for other exact FQH wave functions.[172]

In sec. 4.1 we described how to generate the SSG wave functions by means of a local Hamiltonian written in terms of spin-dependent pseudopotentials. An interesting question left unaddressed is whether other states could be constructed with faster vanishing properties than the SSG. For instance, in the spin-polarized case, adding the next highest L pseudopotential to the gaffnian Hamiltonian is known to produce the Haffnian Hamiltonian.[121] Might we be able to generate a "spin-Haffnian" state with a Hamiltonian containing positive $V^{S=3/2}_{L=0,N=3}$, $V^{S=3/2}_{L=2,N=3}$, $V^{S=1/2}_{L=1,N=3}$ and now, in addition, $V^{S=3/2}_{L=3,N=3}$ (and possibly $V^{S=1/2}_{L=2,N=3}$)? Wave functions of this type were also considered in ref. [163].

Presently, we lack a corresponding CFT description with which to conduct the same checks as for the SSG. For nonunitary coset constructions, such as the CFT corresponding to the SSG and, perhaps, generalizations such as the "spin-Haffnian", no general procedure exists to fully determine the contents of the theory, and each CFT must be constructed on a case-by-case basis (for unitary CFTs on the other hand, there is a standard procedure for constructing the required so-called simple current extensions).[73,173,174]

CHAPTER 5

Summary

One conclusion that we can draw from all of the topics studied in this thesis is that the multicomponent degrees of freedom play an important role in determining several particularly interesting properties of fractional quantum Hall systems.

On the topic of spin and valley transitions there is still much scope for further progress to be made. Can we go beyond the mean field theory approach of the composite fermion model in order to obtain even more accurate predictions for the critical Zeeman energy? Experimental measurements in anisotropic AlAs systems have indicated the presence of particle-hole symmetry breaking. Some further modifications to the theory would be to take into account the anisotropy and Landau level mixing corrections that could lead to these results. In systems such as AlAs and graphene, where there are both spin and valley degrees of freedom, the interplay between these degrees of freedom merits further investigation; for instance the question over whether experiments observe a spin or valley transition, or some combination. We did not even begin to study anything beyond the most basic aspects of these phase transitions, for instance, the scaling behaviour in transport quantities. Other aspects that have not been studied extensively are the edge modes that would be associated with these multicomponent systems.

Much of this thesis has concentrated on the topic of methodology for constructing new and interesting analytic models to describe potential fractional quantum Hall phases, continuing in line with previous tradition. Although the generalization of the pseudopotentials to the multicomponent case appears at first sight to be a rather academic issue, nevertheless it provides a valuable toolbox with which to further the understanding of the quantum Hall problem. The scope of its implications may well end up going beyond what was originally intended—indeed the generalization to multicomponent pseudopotentials was not principally motivated by applications to calculation of Landau level mixing perturbations, even though it has been a useful tool forming part of the solution to that problem.

An ideal theoretical description of a FQHE state comprises at least the following three ingredients: a local Hamiltonian that describes the ground state and excitation spectrum of the Hilbert space; relatively simple analytic wave functions that are the highest density zero

energy states corresponding to the Hilbert space of that Hamiltonian; and a (rational) two-dimensional conformal field theory (CFT) that generates these wave functions. If a plasma analogy is available, then a gapped state is associated with the analogous plasma being in a screening phase.[64] In general, the quantum Hall Hilbert space is built from a basis of monomials in the complex particle coordinates z_i. In certain instances—the Laughlin series,[64] the Read–Rezayi series,[119] the gaffnian and Haffnian wave functions,[120,121] the Halperin wave functions,[15] and the non-Abelian spin-singlet (NASS) states,[17,101,102]—it has been possible to i) determine simple analytical expressions for the polynomial wave functions, and ii) construct a local Hamiltonian whose zero energy eigenstates are in one-to-one correspondence with those polynomial wave functions. We have found that this is also possible for the spin-singlet gaffnian wave function, at least for the ground state.

A key feature in each of these special cases is that the wave functions are uniquely defined by their vanishing properties. A prime example is the wave function of the Moore–Read state for spinless bosons, which vanishes quadratically when three of the constituent bosons are coincident. The gaffnian wave function is obtained by changing this behaviour, such that the wave function vanishes as a third power, when three constituent particles are coincident.[120] This simple change, however, results in a wave function corresponding to a nonunitary CFT, for which the quasiparticle excitations are expected to be gapless (in the thermodynamic limit) and which, therefore, does not describe a topological phase. Nevertheless wave functions such as the gaffnian are still of interest as they are thought to correspond to critical points between other, incompressible topological phases. This scenario is well understood in the case of the Haldane–Rezayi wave function,[125] which describes the phase transition between a d-wave spin-singlet phase and a strongly paired state.[6,121] Similar scenarios have been suggested for the gaffnian.[120] It is noteworthy that the gaffnian wave function has large overlap with an incompressible composite fermion state thus suggesting that the gaffnian is a critical point between the composite fermion phase and some other phase.[120,168,175,176] A similar overlap calculation can be performed between the fermionic version of the SSG with the spin-singlet composite fermion phase at $\nu = 4/9$. In this case, however, we have determined that the overlaps are vanishingly small. An interesting question still to be addressed is whether or not the Hilbert spaces associated with multiparticle pseudopotential Hamiltonians with the restriction $L > 1$ always correspond to nonunitary CFTs, as has been found so far for the gaffnian, Haffnian and now the SSG.

Of the wave functions discussed above, the single-component ones turn out to be special

cases of a very broad set of so-called Jack polynomial wave functions.[163,166] The Jack polynomials provide a convenient basis in which to describe polynomial wave functions with precisely defined vanishing properties. It has been further realized that special cases such as the Moore–Read state are rather atypical: out of all the Jacks, there exist only a handful of special cases where the polynomial wave function can be written in a relatively simple form and which correspond to unitary CFTs. While there is a general belief that local N-body Hamiltonians may exist for all of the Jacks, only limited further cases have actually been explored.[162,177] Such Hamiltonians, should they be constructed, can be phrased in the general language of pseudopotentials.[122,162]

Where might we look to for further insights into multicomponent fractional quantum Hall effects? Some interesting places to search for new physics are undoubtedly the 2nd LL, because CF theory does not appear to describe well the 8/3 and particularly the $\nu = 12/5$ states. It is noteworthy that the polarized $\nu = 12/5$ state might possibly be described by a certain wave function construction of the Read–Rezayi type (raised to the 2nd LL), a state that is anticipated to exhibit non-Abelian quasiparticles and that also corresponds to a Hamiltonian constructed from multiparticle pseudopotentials.[119] It seems that the most significant and exciting open question to ask is about the nature of the spin-singlet state indicated at $\nu = 12/5$. Is it possible write a exactly solvable model in terms of multicomponent pseudopotentials to describe it? Unlike for the SSG this would require a gapped phase of matter (in the thermodynamic limit). The corresponding wave function would also need to provide a lower energy bound than the alternative CF wave function describing the $\nu = 12/5$ spin-singlet state. The methodology for the investigation of such a new wave function will otherwise be along precisely the same lines explored in this thesis.

Appendices for Chapter 2

A Monte Carlo Algorithm for a Quantum Hall Fluid

In this work we apply the Metropolis Monte Carlo algorithm[178] to evaluate the ground-state energy of various trial wave functions. We wish to evaluate expectation values of operators $\hat{A}$ with respect to the co-ordinate wave functions $\psi(\mathbf{r}_1, \ldots, \mathbf{r}_N)$:

$$\left\langle \hat{A} \right\rangle = \frac{\int d\mathbf{r}_1 \ldots d\mathbf{r}_N \psi^*(\mathbf{r}_1, \ldots, \mathbf{r}_N)\, \hat{A}\psi(\mathbf{r}_1, \ldots, \mathbf{r}_N)}{\int d\mathbf{r}_1 \ldots d\mathbf{r}_N \left|\psi(\mathbf{r}_1, \ldots, \mathbf{r}_N)\right|^2}.$$

The Metropolis Monte Carlo procedure works by statistically sampling configurations of the co-ordinates $\{\mathbf{r}_1, \ldots, \mathbf{r}_N\}$ drawn from the probability distribution

$$\rho_N(\mathbf{r}_1, \ldots, \mathbf{r}_N) = \frac{\left|\psi(\mathbf{r}_1, \ldots, \mathbf{r}_N)\right|^2}{\int d\mathbf{r}_1 \ldots d\mathbf{r}_N \left|\psi(\mathbf{r}_1, \ldots, \mathbf{r}_N)\right|^2}.$$

The expectation value of the operator is then estimated using N_S sets of co-ordinate samples:

$$\left\langle \hat{A} \right\rangle = \frac{1}{N_\mathrm{S}} \sum_{i=1}^{N_\mathrm{s}} \psi(\mathbf{r}_1, \ldots, \mathbf{r}_N)^*\, \hat{A}\psi(\mathbf{r}_1, \ldots, \mathbf{r}_N).$$

It can be shown that the standard deviation behaves as $\sigma / < \hat{A} > \sim 1/\sqrt{N_\mathrm{S}}$. In our simulations we typically used $N_\mathrm{S} \sim \mathcal{O}(10^7)$.

B The Sphere Geometry

The fractional quantum Hall effect (FQHE) occurs in two-dimensional (2D) systems in a perpendicular magnetic field. Real systems are, of course, finite in size and, thus will have edges; however, for our investigation, we are concerned only with the bulk properties of the ground-state and do not want to take into account edge effects. One method to eliminate edge effects, from a theoretical perspective,[52] is to place the quantum Hall system on the surface of a hypothetical sphere of radius R_S. The surface of a sphere is described by a spherical co-ordinate system $\Omega \equiv (\theta, \phi)$ with a fixed radius R_S. Out of convenience we choose to write wave functions in this geometry using a pair of complex spinor co-ordinates u, v such that

$$u = \cos\left(\tfrac{\theta}{2}\right) e^{i\phi/2} \quad , \quad v = \sin\left(\tfrac{\theta}{2}\right) e^{-i\phi/2}.$$

A magnetic field B perpendicular to the surface of the sphere can be realized by placing a magnetic monopole at the centre of the sphere: the total magnetic flux is $N_\Phi \phi_0 = 4\pi R_S^2 B$ (here ϕ_0 is the flux quantum $\phi_0 = hc/e$). The radius of the sphere is then $R_S = \sqrt{N_\Phi/2}$, in

units of the magnetic length. The flux is related to the filling factor by $N_\Phi = N/\nu - \delta$, where N is the number of electrons and δ is called the *shift*.

For spin-polarized composite fermion (CF) states we derived (in sec. 2.2) the result $N_\Phi = 2p(N-1) + 2Q$, where $Q = \pm\frac{N-n^2}{2n}$. For the non spin-polarized CF states we use eq. (2.8), along with the definition $N = N_\uparrow + N_\downarrow$, to find an expression for Q in terms of N,

$$Q = \pm\frac{N - n_\uparrow^2 - n_\downarrow^2}{2(n_\uparrow + n_\downarrow)}. \tag{B.1}$$

The total flux is then again given by $N_\Phi = 2p(N-1)+2Q$. In each case, in the thermodynamic limit, the sphere radius tends to infinity and so we recover a 2D plane geometry but without edge effects. The length scale set by the magnetic length l_0 is generally much smaller than the sphere radius, and so we argue that the physics remains independent of the system size and, therefore, taking the thermodynamic limit is valid.

C Algorithm for Numerical Evaluation of Composite Fermion States in Negative Effective Field

The principal difficulty in using the Metropolis algorithm (appendix A) for our calculation of the Coulomb energy associated with composite fermion (CF) wave functions is that the value of the wave function must be re-calculated for many millions of different sample particle configurations and, for CF trial wave functions, this process can be very computationally demanding. In order to make the procedure viable we require an efficient algorithm with which to evaluate the wave functions. A previously described algorithm to evaluate CF wave functions for the negative effective field case is most computationally efficient for larger values of the effective Landau level (LL) number n and very inefficient for the smallest values of n, e.g $n = 2$ or $n_\uparrow$ or $n_\downarrow = 1$ or 2.[63] For the purposes of studying the spin CF states we have seen that we often need to consider small values of $n_\uparrow$ or $n_\downarrow$ and, consequently, until now, accurate calculation of energies for the spin CF states has not been computationally feasible. We were able to design an alternative algorithm that is *most* efficient for smallest n and less efficient for larger values of n.

Composite fermion wave functions have been intensely scrutinized using MC methods.[16,62,63] The principal difficulty for CF wave functions is the procedure for lowest Landau level (LLL) projection. The method for doing this projection for CF states in negative effective field was introduced in ref. [63], and the resulting form of the generalized spherical harmonics is repeated here in eq. (2.6). Once written in this form, the key difficulty lies in the evaluation of

the multiple derivatives of the Jastrow factor,

$$\left[\left(\frac{\partial}{\partial u_i}\right)^{|Q|+m+s}\left(\frac{\partial}{\partial v_i}\right)^{|Q|-m+n-s} J_i^p\right] \qquad \text{with} \qquad J_i = \prod_{j\neq i}(u_i v_j - u_j v_i)\,.$$

A procedure for evaluating these derivatives is given in ref. [179] (see also ref. [27]), and this method is also used in ref. [63]. Briefly, the method is as follows: first, we pull the Jastrow factor through the derivatives and write

$$J_i^p\left[\hat{U}_i^{|Q|+m+s}\hat{V}_i^{|Q|-m+n-s}1\right] \qquad \text{where} \qquad \hat{U}_i = J_i^{-p}\frac{\partial}{\partial u_i}J_i^p \quad , \quad \hat{V}_i = J_i^{-p}\frac{\partial}{\partial v_i}J_i^p;$$

we then introduce

$$f_i(\alpha,\beta) = \sum_{k=1}^{N}\left(\frac{v_k}{u_i v_k - v_i u_k}\right)^{\alpha}\left(\frac{-u_k}{u_i v_k - v_i u_k}\right)^{\beta},$$

from which one can deduce the recursion relations

$$\frac{\partial}{\partial u_i}f_i(\alpha,\beta) = -(\alpha+\beta)f_i(\alpha+1,\beta) \quad , \quad \frac{\partial}{\partial v_i}f_i(\alpha,\beta) = -(\alpha+\beta)f_i(\alpha,\beta+1). \tag{C.1}$$

Using these results, one can calculate a series of relations, for example,

$$\hat{U}_i 1 = p f_i(1,0) \;\; , \hat{U}_i^2 1 = p^2 f_i(1,0)^2 - p f_i(2,0) \;\; , \ldots .$$

For CF wave functions in negative effective field we must take up to $2|Q|+n = \left(\frac{N}{n}\right) - 2n$ derivatives with respect to both u_j and v_j. As we take more derivatives, the results of this method become increasingly complicated, particularly for smaller values of n.

We have determined an alternative method to evaluate the derivatives, which is at its most effective in precisely the regime where the current method runs into difficulties. We shall present our result for the case of $p = 1$ only; however, higher p cases could be constructed along the same lines.

Let us restate exactly what we need to evaluate, leaving out the unimportant constant factors as they can be absorbed into the normalization. For each element of a N-by-N Slater matrix we need to evaluate

$$\hat{Y}^{Q}_{n',m}(u_i,v_i)J_i \propto$$
$$\sum_{s=0}^{n'}(-1)^s\binom{n'}{s}\binom{2\,|Q|+n'}{|Q|+m+s}u_i^s v_i^{n'-s}\left(\frac{\partial}{\partial u_i}\right)^{|Q|+m+s}\left(\frac{\partial}{\partial v_i}\right)^{|Q|-m+n'-s}\prod_{j\neq i}(u_i v_j - u_j v_i)\,.$$

It is insightful to expand out the J_i product into a sum as follows:

$$J_i = v_i^{N-1}\prod_{j\neq i}^{N}u_j - u_i v_i^{N-2}\sum_{j\neq i}^{N}\left(v_j\prod_{k\neq i,j}u_k\right) + \ldots = \left(\prod_{j\neq i}^{N}u_j\right)\left(\sum_{t=0}^{N-1}(-1)^t e_t^i v_i^{N-1-t}u_i^t\right),$$

where e_t^i denotes the degree t elementary symmetric polynomial in the $N-1$ variables v_j/u_j for $j \neq i$,

$$e_t^i \equiv e_{t,N-1}(v_1/u_1, \ldots, v_j/u_j, \ldots, v_N/u_N),$$

for $j \neq i$. The elementary symmetric polynomials are defined in eq. (3.4) in chapter 3. With this form for J_i we now evaluate all of the necessary derivatives, which leaves us with:

$$\hat{Y}^Q_{n',m}(u_i, v_i)J_i \propto \sum_{s=0}^{n'}(-1)^s\binom{n'}{s}\binom{2|Q|+n'}{|Q|+m+s}\left(\prod_{j\neq i}^N u_j\right) \times \sum_{t=|Q|+m+s}^{N-1-(|Q|-m+n'-s)} e_t^i(-1)^t \frac{(N-1-t)!}{[N-1-t-(|Q|-m+n'-s)]!} v_i^{N-1-t-(|Q|-m)} \frac{t!}{[t-(|Q|+m+s)]!} u_i^{t-(|Q|+m)}. \tag{C.2}$$

The expression in eq. (C.2) appears complicated at first sight, but notice that the sum over t contains at most $N-1-\binom{N}{n}+2n$ terms (note that we use the convention for binomial coefficients that $\binom{a}{b}=0$ if $a<b$). If the CF state only fills a small number of effective LLs (i.e., $n=1,2,\ldots$), then the number of terms in the sum is actually quite small.

A key result is that the elementary symmetric polynomials can be calculated recursively using one of Newton's identities,[180]

$$e_{m,N}(x_1,\ldots,x_N) = \frac{1}{m}\sum_{r=1}^{m}(-1)^{[r-1]}p_{r,N}(x_1,\ldots,x_N)\,e_{m-r,N}(x_1,\ldots,x_N),$$

where $p_{r,N}(x_1,\ldots,x_N) = \sum_{i=1}^N x_i^r$ are the power-sum polynomials. Also, note the following recursive identity:

$$e_{m,N-1}(x_1,\ldots,x_{j\neq i},\ldots,x_N) = e_{m,N}(x_1,\ldots,x_N) - x_i e_{m-1,N-1}(x_1,\ldots,x_{j\neq i},\ldots,x_N).$$

Wielding these two identities it is possible to build an efficient algorithm to generate the full set of e_t^i for $i=1,\ldots,N$ that is required to calculate the elements of the form $\hat{Y}^Q_{n',m}(u_i,v_i)J_i$ for the $N\times N$ Slater matrix. Once the Slater matrix is populated, the remainder of the work is involved in calculating its determinant. The full algorithm evaluates the probability density of a given CF state for a given set of co-ordinates. Based on the times recorded when running the program, our full algorithm evaluation time scales roughly as $N^{2.2}$–$N^{2.75}$, the better figure occurring for $n=1$ and the worse figure for $n=4$, which confirms our assertion that our algorithm is more efficient for smaller values of n.

We note that the evaluation of the CF wave functions tends to suffer from a numerical precision issue, particularly for large N. To overcome the issue we simply store all numerical values to a higher precision—although this slows down the algorithm considerably, we are able to obtain accurate results up to around $N=40$, which is high enough for our purposes.

D Comparison of CF theory with Exact Diagonalization

In this appendix we compare lowest Landau level (LLL) Coulomb energies calculated using spinful composite fermion (CF) wave functions and using numerical exact diagonalization (ED) of the Coulomb interaction in the sphere geometry. The purpose of the comparison is to demonstrate that CF trial wave functions represent a very good approximation to the ground-state energy for each spin and flux sector we want to consider. The numerical EDs were performed for the most computationally tractable cases using the freely available *DiagHam* package.[54] The CF calculations were performed using the LLL projection procedure outlined in sec. 2.2.3 and the Monte Carlo procedure outline in appendix A. Note that most of the ED results collected here are presented in ref. [27] and references therein.

The comparison of the results for the ground-state Coulomb energy is presented in table D.1. We conclude that, although CF trial wave functions indubitably provide an excellent approximation to the exact ground-state energies in the LLL, the energy bound is typically marginally better for the spin polarized cases compared to the spin non-polarized cases. It is also worth noting that with exactly projected CF wave functions, the bounds on the ground-state energy are expected to be better than for the approximate projection method we have used.[27] However, as was pointed out in sec. 2.2.3, the exactly projected CF wave functions are also numerically intractable for all but the smallest system sizes.

For the $\nu = 2/3$ case there are sufficient exact results available to perform a rough extrapolation to the thermodynamic limit. Using linear or quadratic extrapolation the thermodynamic limit, the critical Zeeman energy, E_Z^{crit}, obtained from the exact results is 0.0097(15) or 0.017(5) respectively, in units of $e^2/\epsilon l_0$. The wide range of results and large error bars are due to finite-sized effects heavily influencing the extrapolation. These results can be compared to an E_Z^{crit} of 0.0073(1) obtained with CF theory for the $\nu = 2/3$ case, which suggests that CF theory underestimates the critical Zeeman energy by roughly 25–60%. Since we cannot reliably extrapolate the exact diagonalization results or exactly projected CF wave function results to the thermodynamic limit in all cases, it is not possible to ascertain to what extent our conclusion would hold for all filling factors considered in this work. From the evidence presented here, we expect that CF theory does typically underestimate the critical Zeeman energy by a significant amount. This conclusion is consistent with the theoretical predictions underestimating the experimental measurements, as discussed in sec. 2.3.

Fraction	CF Wave Function	N	CF E_C	Exact ground state E_C	Difference
2/3	${}^2CF_{-2}$ $(\gamma = 1)$	6	$-0.53899(4)$	$-0.539636\ldots$	0.12%
		8	$-0.53376(8)$	$-0.534148\ldots$	0.07%
		10	$-0.53047(3)$	$-0.531017\ldots$	0.10%
		12	$-0.52819(7)$	$-0.528878\ldots$	0.13%
		14	$-0.52675(3)$	$-0.5273653\ldots$	0.12%
		16	$-0.52556(6)$	$-0.5262384\ldots$	0.13%
2/3	${}^2CF_{(-1,-1)}$ $(\gamma = 1/2)$	4	$-0.5975(1)$	$-0.601017\ldots$	0.59%
		6	$-0.57025(4)$	$-0.574384\ldots$	0.72%
		8	$-0.55748(4)$	$-0.561821\ldots$	0.78%
		10	$-0.5498(1)$	$-0.5544872\ldots$	0.85%
3/5	${}^2CF_{-3}$ $(\gamma = 1)$	12	$-0.49843(3)$	$-0.498718\ldots$	0.06%
		15	$-0.49810(3)$	$-0.498432\ldots$	0.07%
3/5	${}^2CF_{(-2,-1)}$ $(\gamma = 1/3)$	8	$-0.52139(5)$	$-0.523037\ldots$	0.32%
2/5	${}^2CF_2$ $(\gamma = 1)$	6	$-0.50040(4)$	$-0.500400\ldots$	$< 0.008\%$
		8	$-0.48025(3)$	$-0.480244\ldots$	0.001%
		10	$-0.46941(2)$	$-0.469450\ldots$	0.009%
		12	$-0.46259(2)$	$-0.462652\ldots$	0.013%
2/5	${}^2CF_{(1,1)}$ $(\gamma = 1/2)$	4	$-0.52656(3)$	$-0.527243\ldots$	0.13%
		6	$-0.49198(3)$	$-0.492544\ldots$	0.11%
		8	$-0.47677(2)$	$-0.477497\ldots$	0.15%
3/7	${}^2CF_3$ $(\gamma = 1)$	12	$-0.48259(2)$	$-0.482639\ldots$	0.01%
		15	$-0.47343(2)$	$-0.473529\ldots$	0.02%
3/7	${}^2CF_{(2,1)}$ $(\gamma = 1/3)$	8	$-0.49581(2)$	$-0.496249\ldots$	0.09%

Table D.1: Collected values of the Coulomb energy per particle E_C calculated for spin polarized and spin non-polarized positive and negative effective field composite fermion trial wave functions alongside equivalent results for the exact ground-state energy per particle for a numerically diagonalized Coulomb interaction in the LLL. All values are given in units of the Coulomb energy, $e^2/\epsilon l_0$. CF wave functions are labeled using the notation introduced in sec. 2.2.3 and by their degree of spin polarization, γ, introduced in eq. (2.2). We conclude that CF theory provides an excellent approximation to the ground-state energy in all cases in the LLL, however the energy bound is marginally better for the spin polarized cases ($\gamma = 1$) compared to the spin non-polarized cases ($\gamma < 1$).

Appendices for Chapter 3

In this set of appendices we shall set out to provide a detailed exposition of the linear vector space inhabited by (multicomponent) Haldane pseudopotentials, that is, the vector space defined in eq. (3.8), $|L, \mathfrak{q}\rangle$. In doing so, the key realization is that vector space of multicomponent pseudopotentials is *identical* to the vector space of coordinate wave functions describing a multicomponent quantum Hall system. We can, thus, map the problem of discovering a suitable basis in which to describe pseudopotentials in the lowest Landau level (LLL) to a problem of constructing multiparticle coordinate wave functions in the LLL with an internal degree of freedom. The properties required of these wave functions are that they should be homogeneous of degree L, translationally invariant, and overall (anti-) symmetric for (fermions) bosons. These conditions are equivalent to the statement that each wave function would be a rotationally invariant state on an appropriately sized sphere.

In these appendices we shall provide a description of how to construct such wave functions $\psi \equiv |L, \mathfrak{q}\rangle$. Very generally, systems with n internal degrees of freedom are characterized by irreducible representations of the special unitary group $\mathrm{SU}(n)$. The fundamental objective of this work is, thus, to decompose the space of wave functions ψ in terms of a basis of wave functions corresponding to irreducible representations of $\mathrm{SU}(n)$.

The layout of the appendices will be as follows: in appendix E we shall allude to some important mathematical preliminaries, which are to be employed in the remaining appendices; in appendix F we shall describe the general procedure for the construction of the basis of wave functions from a combination of spatial functions and generalized spin wave functions; in appendix G we shall concentrate on the details of the generalized spin wave functions and we shall derive the results presented in table 3.4; in appendix H we shall concentrate on the details of the spatial parts of the wave functions; in particular, we shall apply the procedure of appendix F in the context of quantum Hall wave functions, and we shall derive the coordinate wave functions listed in table 3.2 and table 3.3 and the dimensions of the vector space of polynomials listed in table 3.1; finally, appendix I deals with some more advanced mathematical underpinnings of these ideas.

E Mathematical Prelimaries

Our goal in this appendix will be to deal with the underlying mathematical concepts and theorems that are to be employed in later appendices. The underlying mathematics is that of integer partitions, of Young tableaux and of the representation theory of the symmetric group and special unitary group SU(n).

E.1 Integer Partitions

The concept of an *integer partition* is frequently used in this work. An integer partition λ is defined as follows[181]: for a positive integer N, an integer partition is a way of writing N as a list of k positive integer summands $\lambda = [N_1, N_2, \ldots, N_k]$ for which $\sum_{i=1}^{k} N_i = N$. The list of summands is typically presented in weakly descending order (that is, $N_1 \geq N_2 \geq N_3 \ldots \geq N_k$). For example, the set of integer partitions for the integer 5 are $[5]$, $[4,1]$, $[3,2]$, $[3,1,1]$, $[2,2,1]$, $[2,1,1,1]$, $[1,1,1,1,1]$.

When writing down a set of integer partitions such as that given in the above example, it is clearly important to specify an ordering system. In this thesis we shall make use of *lexicographic ordering*[181]: when comparing two integer partitions λ and μ we say that λ occurs before μ, denoted $\lambda \geq \mu$, if $\lambda_i = \mu_i$ for $i = 1, \ldots, j$ for some integer j between 1 and $k-1$, and then $\lambda_{j+1} > \mu_{j+1}$. In the above example we have used lexicographic ordering, for instance, $[3,2]$ occurs before $[3,1,1]$. In appendix I we shall discuss a more general ordering method known as *dominance ordering*.

E.2 Young Tableaux

The concept of *Young tableaux* is an important tool for categorizing group representations, which we shall need to do shortly. Before discussing specific group representations, let us, first, explain how to construct Young tableaux in general.

To draw a Young tableau, one first draws a *Young frame* or diagram. A Young frame is constructed as follows: given an integer partition λ, we build a frame by placing a series of empty boxes in rows and columns. There is one row for each of the k summands in the integer partition: the ith row contains λ_i boxes. We shall use the convention that a new row is started beneath the previous row and that the rows are in the order specified by the integer partition; hence, the length of a row will always be less than or equal to the length of the row above. In addition, the rows are to be left justified (we conform to the English notation). For example,

the Young frame corresponding to the integer partition $\lambda = [3, 2, 1, 1]$ would be

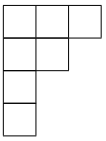

A Young tableau can be constructed from a Young frame by placing a series of N integers in the boxes. The set of integers can be chosen in several ways; of particular significance to our work are the arrangements called *standard tableaux* and the arrangements called *semistandard tableaux*.

In a standard tableau, the integers 1 to N are placed in the boxes of a Young frame of size N, with each number occurring precisely once. Further, we place the numbers such that the integer placed in any box is strictly less than both the integer placed in the box immediately to the right and the integer placed in the box immediately below. For example, here is a possible standard tableau constructed from the Young frame given above:

1	2	3
4	5	
6		
7		

There can, of course, be multiple ways to satisfy these conditions, in other words, if the shape of a Young tableau is specified by an integer partition λ then there is a corresponding set of size f^λ of admissible standard tableaux. We introduce an index r, which runs from 1 to f^λ, to distinguish between the possible standard tableaux T_r in the set.

In order to specify one particular standard tableau in the set of T_r we must first order that set: to do so we shall again employ a kind of lexicographic ordering system. For a given standard tableau we generate a list of numbers starting with the number in the top left box (for the above tableau that would be 1), then working along each row from left to right taking the numbers from these boxes and then adjoining the numbers from each subsequent row in the same fashion. Doing so will generate a list of N numbers N_1 to N_N (in the above tableau that would be $[1, 2, 3, 4, 5, 6, 7]$) and we then simply apply the procedure of lexicographic ordering to these lists.

Let us demonstrate the definitions given in the last two paragraphs via the following example: the integer partition $\lambda = [3, 1]$ has $f^{[3,1]} = 3$, and the lexicographically ordered set of standard tableaux are

1	3	4
2		

1	2	4
3		

1	2	3
4		

A semistandard tableau is constructed along similar lines: in this case, however, one is

allowed to place any of the numbers 1 to n in the boxes of a Young frame of size N, where N does not have to equal to n. It is not necessary to include every number from 1 to n and the numbers can also be repeated. Further, we place the numbers such that they are nondecreasing from left to right and strictly increasing from top to bottom. For example, here is a possible semistandard tableau of type $n = 4$ and $N = 8$:

1	1	4	4
2	2		
3	3		

The complete set of semistandard tableaux for a given λ is enumerated by listing every possible arrangement of subsets of the numbers 1 to n in the N boxes and satisfying the conditions described above. As with the standard tableaux, there are multiple ways to satisfy these conditions and we, therefore, have a set of h^λ admissible semistandard tableaux. Semistandard tableaux can also be ordered lexicographically, using the same procedure as for the standard tableaux. For example, with $\lambda = [2, 1]$ and with $n = 3$ we have $h^{[2,1]} = 8$ and the set of lexicographically ordered semistandard tableaux are

1	1	1	2	1	3	1	1	1	2	1	3	2	2	2	3
2		2		2		3		3		3		3		3	

Finally, we shall introduce the term *conjugate* to refer to any tableaux related by a reflection along the diagonal, for example, the following tableau of shape $\lambda = [3, 1]$:

1	3	4
2		

is conjugate to the following tableau of shape $\tilde{\lambda} = [2, 1, 1]$:

1	2
3	
4	

E.3 Irreducible Representations of the Symmetric Group

The *symmetric group* S_N is the group of permutations on N objects, $\{\pi_1, \ldots, \pi_{N!}\}$. A permutation π_i of labels $(123 \ldots N)$ to $(\mathrm{i}_1\mathrm{i}_2\mathrm{i}_3 \ldots \mathrm{i}_N)$ is denoted by $(\mathrm{i}_1\mathrm{i}_2\mathrm{i}_3 \ldots \mathrm{i}_N)$. A transposition (pair interchange) of label i and label j with all other labels unchanged is denoted by $(\mathrm{i}; \mathrm{j})$.

The classification of multicomponent wave functions depends essentially on the properties of S_N and, in particular, on the understanding of irreducible representations of S_N. Throughout this appendix we shall assume that the reader is familiar with the fundamental concepts of representation theory; a more detailed discussion can be found in ref. [152]. The correspondence

between wave functions and representations of the symmetric group manifests itself in the concept of a symmetry type, as described in sec. 3.2.2. †

In order to construct multicomponent wave functions, we will find that we need to construct an appropriate *symmetric group algebra*. A well-known example of a symmetric group algebra is the algebra of Young operators (for their definition, see appendix I). There is, very generally, a direct correspondence between a representation of a group and a representation of the group algebra[152]. For our purposes it will be convenient to construct the symmetric group algebra corresponding to the *orthogonal* representation of the symmetric group (the reasoning behind this choice is explained in appendix I; essentially it will give rise to multicomponent wave functions with convenient orthogonality properties). We shall define the orthogonal representation of the symmetric group shortly. In order to construct such an algebra we will then make use of the *matric* basis of the symmetric group algebra, which is a very general method to construct a basis directly from a group representation.[151,182]

E.3.1 Young's Orthogonal Representation of the Symmetric Group

A fundamental principle of the representation theory of the symmetric group is that the irreducible representations of the symmetric group are in one-to-one correspondence with the standard tableaux.[152] Given the set of Young tableaux of shape λ we can always construct some kind of irreducible representation matrices $U(\pi_i)^{\lambda}$ of dimension f^{λ} for $\pi_i \in \mathrm{S}_N$. In order for the representation to be an orthogonal representation, all that is required is that the representation matrices are themselves orthogonal matrices, meaning that they satisfy $U\left(\pi_i^{-1}\right)_{rs} = U(\pi_i)_{sr}$.

In fact, orthogonal representation matrices can be constructed directly from standard tableaux using a measure called the *axial distance*.[182] Suppose that the number p appears in the i_{p}th row and the j_{p}th column of a given standard tableau and that the number q appears in the i_{q}th row and the j_{q}th column. The axial distance from p to q in tableau T_r is defined as

$$d^r_{\mathrm{p,q}} = (i_{\mathrm{p}} - j_{\mathrm{p}}) - (i_{\mathrm{q}} - j_{\mathrm{q}})\,.$$

Using this definition one can construct orthogonal representation matrices $U(\pi_i)$ for $\pi_i \in \mathrm{S}_N$ as follows: first, we define the elements of the representation matrix $U[(\mathrm{k}-1;\mathrm{k})]$ of transpositions

† The interpretation in terms of symmetry types is said to be the physicists' interpretation of the mathematics of the irreducible representations.[152]

$(\mathrm{k}-1;\mathrm{k})$ for $\mathrm{k}=1\ldots N$:

$$U\left[(\mathrm{k}-1;\mathrm{k})\right]_{rs} = -1/d^{r}_{\mathrm{k}-1,\mathrm{k}} = \rho_r\,,$$

$$U\left[(\mathrm{k}-1;\mathrm{k})\right]_{rs} = \begin{cases} 0 & \text{if } T_s \neq (\mathrm{k}-1;\mathrm{k})\,T_r \\ \left(1-\rho_r^2\right)^{1/2} & \text{if } T_r = (\mathrm{k}-1;\mathrm{k})\,T_r \end{cases}$$

We then note that every permutation can be expressed as a product of transpositions of the form $(\mathrm{k}-1;\mathrm{k})$; the proof is given in ref. [182], for example. Using this result we can generate the representation matrices corresponding to every other element of the symmetric group by simple matrix multiplication. This is Young's orthogonal representation. Some of these orthogonal matrices are tabulated in ref. [152].

Representations of the symmetric group corresponding to conjugate Young tableau shapes are known as *contragradient* (or dual) representations (see ref. [151]). We can explicitly construct contragradient orthogonal representation matrices $V\left(\pi_i\right)^{\tilde{\lambda}}$, which are related to the original orthogonal representation matrices $U\left(\pi_i\right)^{\lambda}$ by

$$V\left(\pi_i\right)^{\tilde{\lambda}}_{rs} = \mathrm{sgn}\left(\pi_i\right) U\left(\pi_i\right)^{\lambda}_{rs}\,.$$

Here we have used the sign of a permutation, $\mathrm{sgn}\left(\pi_i\right)$, which is defined as follows: writing a permutation as a product of transpositions, if there are m transpositions in the product then the sign of the permutation is $\mathrm{sgn}\left(\pi_i\right) = (-1)^m$.

E.3.2 The Matric Basis of the Symmetric Group Algebra

For any given set of symmetric group representation matrices $U\left(\pi_i\right)^{\lambda}$ of dimension f^{λ} we can, in general, form the following elements of the corresponding symmetric group algebra, called *matric units*[151] or *seminormal units*[182]:

$$\hat{e}^{\lambda}_{rs} = \frac{f^{\lambda}}{N!}\sum_{i=1}^{N!} U\left(\pi_i^{-1}\right)^{\lambda}_{sr}\,\pi_i \qquad r,s=1,\ldots,f^{\lambda}. \tag{E.1}$$

These elements are linearly independent (the proof of which is given in ref. [182]) and can be chosen as a basis for the symmetric group algebra (see ref. [151]). They satisfy the orthogonality condition (with no summation implied):

$$\hat{e}^{\lambda}_{rs}\hat{e}^{\mu}_{uv} = \delta_{\lambda\mu}\delta_{su}\hat{e}^{\lambda}_{rv}. \tag{E.2}$$

The diagonal elements, $\hat{e}_{rr}$, are idempotent and mutually orthogonal. Some explicit forms of these operators are tabulated in ref. [149].

Using the matric units, we can also define a basis for the group algebra of a cotragradient representation,

$$\hat{e}_{rs}^{\tilde{\lambda}} = \frac{f^{\lambda}}{N!} \sum_{i=1}^{N!} V\left(\pi_i\right)_{rs}^{\tilde{\lambda}} \pi_i \,. \tag{E.3}$$

and these elements satisfy the same condition as above, namely

$$\hat{e}_{rs}^{\tilde{\lambda}} \hat{e}_{uv}^{\tilde{\mu}} = \delta_{\tilde{\lambda}\tilde{\mu}} \delta_{su} \hat{e}_{rv}^{\tilde{\lambda}}.$$

E.4 Irreducible Representations of SU(n)

The special unitary group, denoted SU(n), is the group of $n \times n$ unitary matrices with determinant 1. SU(n) also describes the structure of multicomponent systems. Irreducible representations of SU(n) are in one-to-one correspondence with certain subsets of the irreducible representations of the symmetric group; specifically, those representations associated with the set of standard Young tableaux restricted to having at most n rows (see ref. [152] for more details).

E.5 The Lie algebra of SU(n)

In this work we describe wave functions with internal degrees of freedom such as spin. The reader will likely be familiar with the fact that quantum states labeled by spins are classified by the irreducible representations of the Lie algebra of SU(2), that is, the algebra of the $\hat{S}^2$ and $\hat{S}_z$ operators. More generally, a generalized spin wave function will be classified by representations of the Lie algebra of SU(n). Irreducible representations of the Lie algebra of SU(n) are sometimes called *multiplets* and each multiplet contains a vector space of associated functions or states.[183] For example, for SU(2) the multiplets correspond to the values of the quantum numbers S and the states within each multiplet are labeled by the possible values of S_z; for SU(3) the multiplets correspond to the classification of baryonic particles in the quark model.[154] The general form of the SU(n) multiplets is described in detail in ref. [183]. Since the multiplets correspond to the irreducible representations of SU(n), they are labeled in accordance with the set of Young tableaux of shape λ. In other words, a multiplet labeled by λ corresponds to a particular symmetry type λ.

In order to label a particular state in a given multiplet, one must specify the component content of that state: for example, in the two-component case, the number of spin-up and spin-down particles (or, alternatively, the S_z eigenvalue); in the three-component case, the quark content of the state, and so on. We shall introduce the notation λ_z, which will specify the

component content of a given state and, thus, distinguish between different states in the same multiplet (the nomenclature is inspired by S_z). In addition, there can be multiple states that occur for the same value of λ_z; the number of such states is called the multiplicity $M(\lambda, \lambda_z)$.

There is a one-to-one correspondence between the states of a SU(n) multiplet and the set of semistandard tableaux.[152] For a given λ we construct the set of semistandard tableaux containing up to n different numbers; these can be interpreted as the set of components λ_z for that state. Recall our earlier example of the set of SU(3) semistandard tableaux:

corresponds to $\lambda_z = \{2, 1, 0\}$, and since there is only one occurrence of this type of tableau we have $M([2, 1], \{2, 1, 0\}) = 1$. Similarly, we have

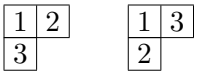

which both correspond to $\lambda_z = \{1, 1, 1\}$. In this case we clearly have $M([2, 1], \{1, 1, 1\}) = 2$ for SU(3). The total number of states in each multiplet, including the multiplicity, is the SU(n) dimension of the representation; it is calculated by enumerating the complete set of semistandard Young tableaux for a given λ, for example, with $\lambda = [2, 1]$ and $n = 3$, the dimension is 8.

A more complete description of the Lie algebras of SU(n) and their representations can be found in ref. [183].

E.6 Tensor Products of SU(n) Multiplets

The problem of constructing a vector space of all possible N-particle generalized spin wave functions is equivalent to the mathematical problem of forming tensor products of N *fundamental* multiplets. A fundamental multiplet is the irreducible representation corresponding to a Young tableau containing a single box—so for SU(n) the dimension of the fundamental multiplet is equal to n. Such tensor products can be decomposed into a direct sum of multiplets.[183] An important feature is that in this direct sum it is possible to have multiple occurrences of the same multiplet (we shall give an example shortly). In our general construction we shall therefore introduce an index r which will distinguish between such repeated multiplets. This decomposition enables us to determine the possible multiplets and multiplet states which fully span our vector space.

For illustrative purposes we shall go through the three-component case in detail here. A three-component system can be decomposed into SU(3) multiplets. We can determine the allowed set of generalized spin wave functions by forming tensor products of SU(3) representations of a single-particle state.

We start with a single-particle state with three components, which corresponds to the fundamental SU(3) multiplet. To deduce the vector space of two-particle generalized spin wave functions we form a tensor product of two fundamental multiplets (here we label the multiplets by the shapes of the corresponding young frames):

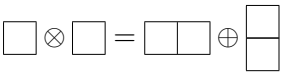

This product is evaluated according to the Littlewood-Richardson rule (see, for example, ref. [152]) to give a direct product of SU(3) multiplets. The [2] representation is six-dimensional, while the [1,1] representation is three-dimensional (cf. the $N = 2$ case in table 3.4).

If we want to include a third particle then we construct

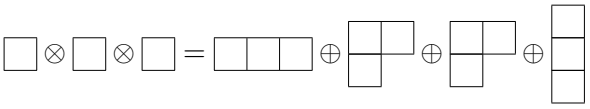

We see that there are two copies of the [2,1] multiplet, which has dimension 8. The two copies are distinguished by the index r and the states within the two multiplets are mutually orthogonal to each other (so in this example we can have $r = 1$ or $r = 2$). The [3] multiplet has dimension 10, and the [1,1,1] has dimension 1: so we see that the total dimension is $10+2\times8+1 = 27 = 3^3$ (cf. the $N = 3$ case in table 3.4). The total dimensions calculated in this way are consistent with the counting of states listed in table 3.4.

We can also apply the Littlewood–Richardson rule to the construction of standard tableaux, thus, we observe

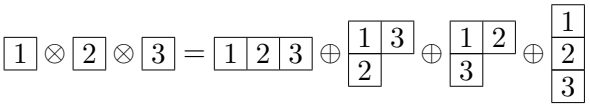

We see that the two copies of the [2,1] multiplet can be distinguished by their association to standard Young tableaux. This result comes about because of the underlying connection between tensor representations of groups and irreducible representations of the symmetric group: specifically the symmetry property of the indices of the tensor itself forms a representation of the symmetric group.

More generally, therefore, the number of repeated occurrences of a particular Young tableau shape λ simply corresponds to the dimension f^λ of the symmetric group representation that

would also be denoted by a Young tableau of that shape (a proof of this result is given, for example, in ref. [152]). For example, the symmetric group representation dimension of the [2,1] tableau is 2 (recall that the symmetric group representation dimension is given by the number of standard tableaux for a given tableau shape). Thus, one can associate a specific standard Young tableau shape with each occurrence of an SU(n) multiplet in our decomposition.

To summarize, the tensor product of N fundamental multiplets will contain every admissible irreducible representation of the Lie algebra of SU(n), that is, the irreducible representations corresponding to every possible standard tableaux of shape λ with size N and with no more than n rows,[152] and in such a decomposition the multiplet described by λ will occur f^λ times, with the occurrences being distinguished by an association to standard Young tableaux.

F Construction of Multicomponent Wave Functions

In this appendix we shall describe the solution to the very general problem of constructing wave functions for multicomponent systems by decomposing into a basis of spatial wave functions and generalized spin wave functions. In the following appendix, appendix G, we shall describe the forms of the generalized spin wave functions in more detail. Finally, in appendix H, we shall describe how to apply the general arguments for construction of spatial wave functions presented in the current appendix to the special case of construction of translationally invariant LLL quantum Hall wave functions with fixed relative angular momentum.

The vector space of wave functions describing a system of identical particles with internal degrees of freedom can always be written as a tensor product of the spaces of spatial and generalized spin wave functions:

$$|\psi\rangle \;\in\; |\Phi_{\text{spatial}}\rangle \otimes |X_{\text{gsw}}\rangle \,.$$

Thus, the dimension of the Hilbert space (with no symmetry restriction) is equal to the product of the dimensions of the space of spatial and generalized spin wave functions. Additionally, such a wave function must conform to the symmetry condition required for a system of identical fermions (bosons)—namely the wave function must be antisymmetric (symmetric) under any exchanges of the particle labels.

If we are trying to determine the dimension of the space of wave functions with N particles of some degree L that obeys the proper symmetry condition, we can, in principle, start with the most general spatial function Φ_{spatial} of this degree and the most general generalized spin wave function X_{gsw} (where a "most general wave function" contains one arbitrary coefficient

multiplying each of the basis functions in the space). The most general Φ_{spatial} is given by a linear combination of all possible arrangements of N particles into N_{orbitals} single-particle orbitals $\phi_1 \ldots \phi_N$ (including multiple occupancy) with a fixed combined degree:

$$\Phi_{\text{spatial}} = \sum_{i_1,\ldots,i_N=1}^{N_{\text{orbitals}}} a_{i_1,\ldots,i_N} \left[\phi_{i_1}(r_1) \ldots \phi_{i_N}(r_N)\right], \tag{F.1}$$

where $a_{i_1,\ldots,i_N}$ are arbitrary coefficients. Similarly the most general X_{gsw} is given by

$$X_{\text{gsw}} = \sum_{j=1}^{n^N} x_j \vartheta_j,$$

where x_j are arbitrary coefficients and where ϑ_j are the complete set of primitive generalized spin wave functions of the form given in eq. (3.18), of which there are n^N for an N-particle, n-component system. The most general combined wave function is given by the product of the generalized spin wave function and spatial wave function: $X_{\text{gsw}}\Phi_{\text{spatial}}$.

Next, we impose that the wave function ψ is overall antisymmetric (for fermions) by applying an antisymmetrizer $\hat{\mathcal{A}}$ to the most general construction,

$$\psi = \hat{\mathcal{A}}\Phi_{\text{spatial}}X_{\text{gsw}}, \tag{F.2}$$

where

$$\hat{\mathcal{A}} = \frac{1}{\sqrt{N!}} \sum_{i=1}^{N!} \text{sgn}\,(\pi_i)\pi_i.$$

For bosons we simply replace the antisymmetrizer by a symmetrizer $\hat{\mathcal{S}}$:

$$\hat{\mathcal{S}} = \frac{1}{\sqrt{N!}} \sum_{i=1}^{N!} \pi_i.$$

After applying one of these symmetry operators to the most general construction we will be left with a wave function containing a certain number of linearly independent coefficients: the total number of those coefficients is the size of the Hilbert space. One can always deduce by brute force the number of linearly independent coefficients in ψ by determining the linearly independent combinations of the $a_{i_1,\ldots,i_N}$ and x_j coefficients remaining after the symmetry operator is applied. In general, however, this method is extremely inefficient and becomes essentially algebraically impossible for more than a very few particles and very low degrees. A much cleaner approach is to fully exploit the symmetries of the problem, which is what we shall do.

We explained in appendix E that generalized spin wave functions are classified by irreducible representations of the Lie algebra of SU(n) given by forming tensor products of N fundamental

multiplets. Specifically, we can decompose the vector space of generalized spin wave functions into subspaces labeled by Young tableaux of shape λ and in such a decomposition the multiplet labeled by λ occurs f^λ times. We can, thus, write a basis of generalized spin wave functions $X_{\text{gsw}}(N, \lambda, \lambda_z, r)$ labeled in the same way as states within SU(n) multiplets, where N is the number of particles, λ is the symmetry type, and where r runs from 1 to f^λ and distinguishes between SU(n) multiplets occurring in the tensor product with the same λ. We shall use the convention that wave functions with different r values are mutually orthogonal. Recall from sec. 3.2.3 (and see below in sec. F.1) that λ_z describes how many particles in the generalized spin wave function are of each type α, β, γ, ... Note that it may or may not be possible to construct a wave function in representation λ given a particular N and λ_z as we will describe further in sec. F.1 below.

Given the above decomposition of the generalized spin wave function into representations, we can analogously decompose the combined wave function ψ based on the same irreducible representation of $SU(n)$. This follows because the spatial function is independent of the component values. Thus, without loss of generality, we may divide the space of possible N-particle wave functions ψ into subspaces indexed by λ and λ_z. In order to decompose our wave functions into a basis of irreducible representations while remaining of the general form given in eq. (F.2), we propose the following alternative general form for a basis for ψ, which loses no generality:

$$\psi(N, \lambda, \lambda_z) = \sum_{r=1}^{f^\lambda} c_r \hat{\mathcal{A}} \, \Phi_{\text{spatial}} X_{\text{gsw}}(N, \lambda, \lambda_z, r), \tag{F.3}$$

where c_r are arbitrary coefficients. For bosons we simply use a symmetrization operator $\hat{\mathcal{S}}$ instead of an antisymmetrization operator $\hat{\mathcal{A}}$.

In this expression we are free to choose the most general possible Φ_{spatial}. However, here not all different choices of Φ_{spatial} will correspond to different wave functions ψ. In sec. F.1 we will first construct the generalized spin wave functions $X_{\text{gsw}}(N, \lambda, \lambda_z, r)$, then, in sec. F.2 we will (use group theory to) determine how to construct a complete (but not over-complete) basis for the spatial wave functions Φ_{spatial}.

F.1 Introduction to Generalized Spin Wave Functions

The generalized spin wave functions $X_{\text{gsw}}(N, \lambda, \lambda_z, r)$ describing a system with n components correspond to particular irreducible representations of SU(n): those given by forming tensor products of N fundamental multiplets. Such representations are in correspondence with the

standard tableaux of shape λ and, hence, with a subset of the symmetric group. We must specify the tableau shape λ, where λ is a partition of the integer N into at most n parts, the standard tableau index r, and the component composition of the function, which is denoted by λ_z. In order to enforce that $X_{\mathrm{gsw}}(N, \lambda, \lambda_z, r)$ are mutually orthogonal in λ, λ_z and r, we shall construct our SU(n) representations based on the orthogonal representation of the symmetric group.

The generalized spin wave functions can be written as linear combinations of primitive generalized spin wave functions: these are defined by specifying a list of the values that each component can take; α, β, γ, and so on. For example, $\vartheta_j = |\alpha\gamma\beta\beta\alpha\rangle$ is a primitive generalized spin wave function. One can order these wave functions according to a lexicographic ordering scheme, so the first primitive generalized spin wave function would be

$$\vartheta_1(N, \lambda_z) = |\alpha\alpha\alpha\ldots\beta\beta\ldots\zeta\zeta\rangle\,.$$

The index λ_z represents the list $\{N_\alpha, N_\beta, \ldots, N_\zeta\}$ of N that corresponds to the number of times each type of component value occurs in the primitive generalized spin wave function. In general, we have wave functions ϑ_j, where j runs from 1 to the number of primitive generalized spin wave functions $d(\lambda_z)$ of all possible orderings of the components and indexes the position of ϑ_j within an ordered list of those wave functions.

The explicit forms of the generalized spin wave functions can be deduced as follows: first, we write down the orthogonal representation matrices $U(\pi_i)^\lambda$ corresponding to the subset of standard tableaux of shape λ; from this orthogonal representation we then construct a corresponding group algebra using the matric basis, defined in eq. (E.1). As the elements of the group algebra are expressed as a linear combination of permutation operators, one can apply the matric unit operator $\hat{e}^\lambda_{ss}$ to any primitive generalized spin wave function to give either zero or a linear combination of permuted primitive generalized spin wave functions. A key result of this construction is that there is an irreducible representation of the symmetric group associated with each λ and that representations associated with different λ are inequivalent.[182] Thus, the generalized spin wave functions constructed in this way are in one-to-one correspondence with the irreducible representations of SU(n) and with the SU(n) multiplets occurring in the tensor product of N fundamental multiplets. In other words, the operator $\hat{e}^\lambda_{ss}$ acts as a projector on the primitive generalized spin wave functions to give a particular representation of SU(n).

A further key result is that the wave functions $\hat{e}^\lambda_{rs}\vartheta_j(N, \lambda_z)$ are either zero or, independently of the choice of r and s, they belong to the same symmetry type λ. Due to the orthogonality

of the matric unit operators, defined in eq. (E.2), two such wave functions $\hat{e}^{\lambda}_{rs}\vartheta_j(N,\lambda_z)$ and $\hat{e}^{\lambda}_{r's}\vartheta_j(N,\lambda_z)$ are orthogonal if $r \neq r'$. The operators $\hat{e}^{\lambda}_{rs}$ act as shift operators in the sense that

$$\hat{e}^{\lambda}_{rs}\left[\hat{e}^{\lambda}_{ss}\vartheta_j(N,\lambda_z)\right] = \hat{e}^{\lambda}_{rs}\vartheta_j(N,\lambda_z),$$

and so operating on the first projected function $\hat{e}^{\lambda}_{ss}\vartheta_j$ yields a set of orthogonal functions belonging to the same symmetry type and, further, by acting with all such possible shift operators on all possible ϑ_j, we obtain a complete basis of states having the same λ and λ_z.

For the SU(2) case it is possible to prove further that $\hat{S}^2\hat{e}^{\lambda}_{ss}\vartheta_j(N,S_z) = S(S+1)\hat{e}^{\lambda}_{ss}\vartheta_j(N,S_z)$ with λ the representation corresponding to spin S (the proof is given in ref. [151]). In other words, for the two-component case, the generalized spin wave functions are precisely spin eigenfunctions.

Thus, we may decompose the complete space of generalized spin wave functions X_{gsw} in terms of the multiplet label λ and r, and the multiplet state label λ_z. Most generally, we write

$$X_{\text{gsw}}\,(N,\lambda,\lambda_z,r) = \sum_{s=1}^{f^{\lambda}}\sum_{j=1}^{d(\lambda_z)} b_{s,j}\,\hat{e}^{\lambda}_{rs}\vartheta_j(N,\lambda_z), \tag{F.4}$$

where $b_{s,j}$ are arbitrary coefficients. Since these wave functions are constructed in correspondence with the multiplets of SU(n), the number of linearly independent values of $b_{s,j}$ is precisely the multiplicity, $M(\lambda,\lambda_z)$, of the SU(n) multiplet state (this can be explicitly checked). It can be shown that these wave functions are mutually orthogonal in λ, λ_z, and r due to the orthogonality relations satisfied by the matric unit operators (see ref. [151] for the proof in the SU(2) case).

The mapping to representations of the symmetric group manifests itself in the permutation symmetry of the wave function, for example, $X_{\text{gsw}}\,(N,\lambda,\lambda_z,1)$, independent of λ_z, must be symmetric in labels 1 to N_1, in labels N_1+1 to N_2 and so on where N_i are the integers describing the partition λ. We shall describe the explicit forms of the generalized spin wave functions in more detail in appendix G.

F.2 Combination of Generalized Spin and Spatial Wave Functions

In this section of the appendix we shall now describe the procedure for sewing together the spatial and generalized spin wave functions to give a combined wave function with the correct symmetry property. We shall then focus on the explicit form of the spatial part of the wave function. We aim to determine the dimension of the vector space of spatial wave functions.

So far we have shown that the most general expression for the basis of combined generalized spin wave functions is given in eq. (F.3). It is insightful to split up the antisymmetrization operator into parts acting separately on either the spatial or spin functions—a permutation π_i is equivalent to identical permutations π_i^{Φ} acting on the spatial wave function and π_i^{X} acting on the generalized spin wave function. Thus, eq. (F.3) can be written in the equivalent form:

$$\psi\left(N,\lambda,\lambda_z\right)=\frac{1}{\sqrt{N!}}\sum_{r=1}^{f^{\lambda}}c_r\sum_{i=1}^{N!}\mathrm{sgn}\left(\pi_i\right)\pi_i^{\Phi}\Phi_{\mathrm{spatial}}\pi_i^{X}X_{\mathrm{gsw}}\left(N,\lambda,\lambda_z,r\right).$$

Now, the most general expression for the generalized spin wave functions is given in eq. (F.4). An important result, which follows from the definition of the matric unit operators, is that the action of an arbitrary permutation operator π_i^{X} on a generalized spin wave function is

$$\pi_i^{X}X_{\mathrm{gsw}}\left(N,\lambda,\lambda_z,r\right)=\sum_{s=1}^{f^{\lambda}}X_{\mathrm{gsw}}\left(N,\lambda,\lambda_z,s\right)U(\pi_i)_{sr}^{\lambda} \tag{F.5}$$

Using this result, we can write eq. (F.3) without the antisymmetrization operator in the form

$$\psi\left(N,\lambda,\lambda_z\right)=\frac{1}{\sqrt{f^{\lambda}}}\sum_{r=1}^{f^{\lambda}}X_{\mathrm{gsw}}\left(N,\lambda,\lambda_z,r\right)\sum_{s=1}^{f^{\lambda}}c_s\Phi_{rs},$$

where we have introduced the spatial wave function Φ_{rs}, which is defined as

$$\Phi_{rs}=\left(\frac{f^{\lambda}}{N!}\right)^{1/2}\sum_{i=1}^{N!}U(\pi_i)_{rs}^{\lambda}\mathrm{sgn}\left(\pi_i\right)\pi_i^{\Phi}\Phi_{\mathrm{spatial}}.$$

Finally, using the definition of the contragradient matric unit operators, we can write the spatial wave function in the form

$$\Phi_{rs}=\left(\frac{N!}{f^{\lambda}}\right)^{1/2}\hat{e}_{rs}^{\tilde{\lambda}}\Phi_{\mathrm{spatial}}.$$

In the boson case, where we require the wave function to be fully symmetric [thus removing the $\mathrm{sgn}\left(\pi_i\right)$ factor], it clearly follows that $\tilde{\lambda}$ is replaced by λ. Note that Φ_{spatial} is still given by eq. (F.1).

Now, in order to simplify our presentation, we shall define the rth part of spatial wave function to be the spatial wave function associated with the rth generalized spin wave function, in other words,

$$\Phi\left(N,\lambda,r\right)=\sum_{s=1}^{f^{\lambda}}c_s\hat{e}_{rs}^{\tilde{\lambda}}\Phi_{\mathrm{spatial}}, \tag{F.6}$$

or with $\tilde{\lambda}$ replaced with λ for the boson case. These spatial wave functions are mutually orthogonal in λ and in r due to the othogonality relations satisfied by the matric unit operators.

Note that the explicit form of $\Phi(N,\lambda,r)$ will be

$$\Phi(N,\lambda,r) = \sum_{i_1,\ldots,i_N=1}^{N_{\text{orbitals}}} a'_{i_1,\ldots,i_N}\left[\phi_{i_1}(r_1)\ldots\phi_{i_N}(r_N)\right]. \tag{F.7}$$

where now the coefficients a' depend on the combinations of the a coefficients [from eq. (F.1)] and the c coefficients [introduced in eq. (F.3)] and, in particular, they must contain linear dependencies.

Thus, the most general form of the basis wave functions is

$$\psi(N,\lambda,\lambda_z) \propto \sum_{r=1}^{f^\lambda} X_{\text{gsw}}(N,\lambda,\lambda_z,r)\,\Phi(N,\lambda,r). \tag{F.8}$$

Since both $X_{\text{gsw}}(N,\lambda,\lambda_z,r)$ and $\psi(N,\lambda,r)$ are mutually orthogonal in λ, λ_z and in r, the wave function $\psi(N,\lambda,\lambda_z)$ is itself othogonal to wave functions with different λ and λ_z values. We now propose to simplify this result using the following theorem.

Theorem 1: *The wave function $\psi(N,\lambda,\lambda_z)$ in eq. (F.8) can be written in the form $\hat{\mathcal{A}}\Phi(N,\lambda,1)\,X_{\text{gsw}}(N,\lambda,\lambda_z,1)$ for fermions or $\hat{\mathcal{S}}\Phi(N,\lambda,1)\,X_{\text{gsw}}(N,\lambda,\lambda_z,1)$ for bosons.*

Proof: Let us demonstrate the proof in the fermion case only, since the boson case follows along very similar lines. The proof uses the following additional results: first, from eq. (F.4), using the orthogonality condition for the matric unit operators, we have:

$$X_{\text{gsw}}(N,\lambda,\lambda_z,r) = \sum_{s=1,j=1}^{f^\lambda,\,d(\lambda_z)} b_{s,j}\,\hat{e}^\lambda_{rs}\vartheta_j(N,\lambda_z) = \hat{e}^\lambda_{r1}\sum_{s=1,j=1}^{f^\lambda,\,d(\lambda_z)} b_{s,j}\,\hat{e}^\lambda_{1s}\vartheta_j(N,\lambda_z) = \hat{e}^\lambda_{r1}X_{\text{gsw}}(N,\lambda,\lambda_z,1).$$

Thus, all coefficients in $X_{\text{gsw}}(N,\lambda,\lambda_z,r)$ are linearly dependent on the set of coefficients in $X_{\text{gsw}}(N,\lambda,\lambda_z,1)$.

Similarly, the second result is that

$$\sum_{s=1}^{f^\lambda} c_s\hat{e}^{\tilde{\lambda}}_{rs}\Phi_{\text{spatial}} = \hat{e}^{\tilde{\lambda}}_{r1}\sum_{s=1}^{f^\lambda} c_s\hat{e}^{\tilde{\lambda}}_{1s}\Phi_{\text{spatial}},$$

or, alternatively,

$$\Phi(N,\lambda,r) = \hat{e}^{\tilde{\lambda}}_{r1}\Phi(N,\lambda,1), \tag{F.9}$$

and so the coefficients in $\Phi(N,\lambda,r)$ are linearly dependent on the coefficients in $\Phi(N,\lambda,1)$.

Now consider the following construction

$$\psi(N,\lambda,\lambda_z) \propto \hat{\mathcal{A}}\Phi(N,\lambda,1)\,X_{\text{gsw}}(N,\lambda,\lambda_z,1). \tag{F.10}$$

Writing the sum over permutations in the antisymmetrization explicitly, this becomes

$$\psi(N,\lambda,\lambda_z) \propto \sum_{i=1}^{N!} \mathrm{sgn}\,(\pi_i)\pi_i \left\{\Phi\,(N,\lambda,1)\,X_{\mathrm{gsw}}(N,\lambda,\lambda_z,1)\right\}.$$

Then we can use that the permutation π_i is equivalent to identical permutations π_i^{Φ} acting on the spatial wave function and π_i^{X} acting on the generalized spin wave function to write instead

$$\psi(N,\lambda,\lambda_z) \propto \sum_{i=1}^{N!} \mathrm{sgn}\,(\pi_i)\pi_i^{\Phi}\Phi\,(N,\lambda,1)\,\pi_i^{X} X_{\mathrm{gsw}}(N,\lambda,\lambda_z,1).$$

Now, using eq. (F.5), we have, equivalently,

$$\psi(N,\lambda,\lambda_z) \propto \sum_{s=1}^{f^{\lambda}} \sum_{i=1}^{N!} \mathrm{sgn}\,(\pi_i)\pi_i^{\Phi}\Phi\,(N,\lambda,1)\,U(\pi_i)^{\lambda}_{s1} X_{\mathrm{gsw}}\,(N,\lambda,\lambda_z,s)\,.$$

Then, using the definition of the contragradient matric unit operator in eq. (E.3), we have

$$\psi(N,\lambda,\lambda_z) \propto \sum_{s=1}^{f^{\lambda}} \hat{e}^{\tilde{\lambda}}_{s1}\Phi\,(N,\lambda,1)\,X_{\mathrm{gsw}}\,(N,\lambda,\lambda_z,s)\,.$$

Finally, using eq. (F.9), we obtain

$$\psi(N,\lambda,\lambda_z) \propto \sum_{s=1}^{f^{\lambda}} \Phi\,(N,\lambda,s)\,X_{\mathrm{gsw}}\,(N,\lambda,\lambda_z,s)\,,$$

which is proportional to eq. (F.8), as required. Thus, we have proved theorem 1.

For the boson case, we should start with a symmetrizer $\hat{\mathcal{S}}$ instead of the antisymmetrizer in the expression for $\psi(N,\lambda,\lambda_z)$ and we must, consequently, replace the contragradient representations $\tilde{\lambda}$ by λ.

Corollary: We have expressed all of the linearly independent terms in the basis wave functions $\psi(N,\lambda,\lambda_z)$ in terms of the product $\Phi\,(N,\lambda,1)\,X_{\mathrm{gsw}}(N,\lambda,\lambda_z,1)$; the entire basis wave function can then be recovered from this single term by simply antisymmetrizing or symmetrizing in all the particle coordinates, and, further, this antisymmetrization procedure does not reduce the number of linearly independent terms. In other words, the dimension of the space of multicomponent basis wave functions $\psi\,(N,\lambda,\lambda_z)$ is given by the dimension of the space of generalized spin wave functions $X_{\mathrm{gsw}}\,(N,\lambda,\lambda_z,1)$ multiplied by the dimension of the space of spatial wave functions $\Phi\,(N,\lambda,1)$. Our task now is to determine the dimensions of these vector spaces. We shall discuss the generalized spin wave functions $X_{\mathrm{gsw}}(N,\lambda,\lambda_z,1)$ in appendix G and we shall discuss the spatial wave functions $\Phi\,(N,\lambda,1)$ in appendix H.

G Vector Space of Generalized Spin Wave Functions

In this appendix we shall explain how to derive the space of generalized spin wave functions $X_{\mathrm{gsw}}(N, \lambda, \lambda_z, r)$. First, we shall explain the simplifications that arise in the description of the two-component case (spin-1/2 eigenfunctions); we shall then explain the most general n-component case. In each case, we shall describe how the procedure described in appendix F is applied to generate the vector space of generalized spin wave functions.

G.1 Two-Component Systems

An important observation is that any two-component multiparticle system can be mapped onto a system with a spin-1/2 degree of freedom regardless of whether it contains fermionic or bosonic particles. The procedure of decomposing into SU(2) representations is then identical to the problem of the construction of spin eigenfunctions—a well studied problem in theoretical chemistry.[151] Note that, in general, a wave function need only be an eigenfunction of spin if the system is invariant under spin rotations. Nonetheless, since a decomposition in terms of spin eigenfunctions is akin to a decomposition in terms of SU(2), the spin eigenfunctions will always provide a complete basis in which to describe any two-component system.

Spin eigenfunctions for a multiparticle system are defined to be eigenfunctions of the total spin operator $\hat{S}^2$ and total z-component of spin operator $\hat{S}_z$. Such functions can be expressed as linear combinations of *primitive spin wave functions*: to repeat the definition given in sec. 3.2.1, a primitive spin wave function ϑ_i of a many particle system is an eigenfunction of the S_z operator of every particle in the system. (They are effectively two-component generalized spin wave functions where $\alpha \equiv |\uparrow\rangle$ and $\beta \equiv |\downarrow\rangle$.)

Spin eigenfunctions $X(N, S, S_z, r)$ are constructed from linear combinations of these primitive spin wave functions. For a system of N particles with spin eigenvalue S, there is a one-to-one correspondence between the spin eigenfunctions and the subset of orthogonal irreducible representations of the symmetric group denoted by Young tableaux of the shape $\lambda = \left[\frac{1}{2}N + S, \frac{1}{2}N - S\right]$; see ref. [151].

The following results apply specifically to the two-component case. For any primitive spin wave function ϑ_j it can be shown that

$$\hat{e}^{\lambda}_{rr}\vartheta_j \propto \hat{e}^{\lambda}_{r1}\vartheta_1, \text{ or } 0.$$

A corollary is that one can generate the entire space of spin eigenfunctions from only the first primitive spin wave function ϑ_1. The key expression for the construction of spin eigenfunctions is then

$$X\left(N, S, S_z, r\right) \propto \hat{e}^{\lambda}_{r1}\vartheta_1. \tag{G.1}$$

Let us demonstrate these ideas with a simple example: the three particle state with eigenvalues $S = 1/2$ and $S_z = 1/2$. The associated Young tableaux are of the shape $\lambda = [2, 1]$:

There are two possible arrangements of standard tableau:

and there are correspondingly two eigenfunctions with the same spin eigenvalue, each of which is generated by one of the group algebra basis operators

$$X\left(3, \tfrac{1}{2}, \tfrac{1}{2}, 1\right) = \hat{e}^{[2,1]}_{11}\vartheta_1\left(3, 1/2\right) \propto \tfrac{1}{\sqrt{6}}\left(2\left|\uparrow\uparrow\downarrow\right\rangle - \left|\uparrow\downarrow\uparrow\right\rangle - \left|\downarrow\uparrow\uparrow\right\rangle\right)$$
$$X\left(3, \tfrac{1}{2}, \tfrac{1}{2}, 2\right) = \hat{e}^{[2,1]}_{21}\vartheta_1\left(3, 1/2\right) \propto \tfrac{1}{\sqrt{2}}\left(\left|\uparrow\downarrow\uparrow\right\rangle - \left|\downarrow\uparrow\uparrow\right\rangle\right).$$

On inspection we see that $X\left(3, \frac{1}{2}, \frac{1}{2}, 1\right)$ is symmetric under exchange of indices 1 and 2 with no particular symmetry conditions for index 3; moreover $X\left(3, \frac{1}{2}, \frac{1}{2}, 2\right)$ is antisymmetric under exchange of the same indices.

Recall the most general expression for the wave function given in eq. (F.10). In the two-component case, since $X(N, \lambda, \lambda_z, 1) \equiv X(N, S, S_z, 1) = \hat{e}^{\lambda}_{11}\vartheta_1(N, S_z)$, we need only specify the first primitive spin wave function in order to describe the full wave function. Thus, in the two-component case the wave function (for fermions) can be succinctly expressed as

$$\psi(N, S, S_z) \propto \hat{\mathcal{A}}\Phi\left(N, S, 1\right)\vartheta_1(N, S_z). \tag{G.2}$$

G.2 Non Spin-Rotationally Invariant n-Component Systems

In the most general n-component case, the system may not be invariant under spin rotations, or, if there is no spin degree of freedom present, rotations within the generalized spin space. The most general set of generalized spin wave functions in this case are simply those specified by the decomposition into tensor products of N fundamental SU(n) multiplets. The irreducible representations occurring in the decomposition are labeled by λ and r, with no additional constraints—these are the functions described by eq. (F.4). We note that n-component systems

of this type have previously been conceived in ref. [184]; however, the explicit wave functions have not been calculated.

Since primitive generalized spin wave functions at different positions in the ordered set are related by permutations, it is possible to write eq. (F.4) [i.e., $X_{\mathrm{gsw}}(N, \lambda, \lambda_z, r)$] in the form:

$$\sum_{s=1,j=1}^{f^\lambda,\, d(\lambda_z)} b_{s,j}\, \hat{e}^\lambda_{rs} \vartheta_j(N, \lambda_z) \equiv \sum_{p=1}^{M(\lambda,\lambda_z)} b_p \hat{e}^\lambda_{r1} \vartheta_p(N, \lambda_z), \tag{G.3}$$

where p runs from 1 up to the multiplicity, $M(\lambda,\, \lambda_z)$, of the SU(n) multiplet state; recall that this is given by the number of semistandard tableaux of shape λ and component content λ_z. Note that since p can be greater than 1 but is always less than or equal to $d(\lambda_z)$ (that is, the total number of primitive generalized spin wave functions including, all possible orderings of components), we include only a certain subset of the lexicographically ordered primitive generalized spin wave functions in the basis; these correspond precisely to the semistandard tableau shapes. For example, in the $\lambda = [3, 1]$ state of SU(3) the semistandard tableaux are

1 1 1 2	1 1 1 3	1 1 2 2	1 1 2 3	1 1 3 2
1 1 3 3	1 2 2 2	1 2 2 3	1 2 3 2	1 2 3 3
1 3 3 2	1 3 3 3	2 2 2 3	2 2 3 3	2 3 3 3

The corresponding primitive generalized spin wave functions are given by interpreting the placement of the numbers 1 to n in the semistandard tableau as the placement of the components $\alpha, \beta, \gamma, \ldots$ in the primitive generalized spin wave functions. The corresponding set of primitive generalized spin wave functions that can occur in this state are then:

$$|\alpha\alpha\alpha\beta\rangle\,, |\alpha\alpha\alpha\gamma\rangle\,, |\alpha\alpha\beta\beta\rangle\,, |\alpha\alpha\beta\gamma\rangle\,, |\alpha\alpha\gamma\beta\rangle\,,$$

$$|\alpha\alpha\gamma\gamma\rangle\,, |\alpha\beta\beta\beta\rangle\,, |\alpha\beta\beta\gamma\rangle\,, |\alpha\beta\gamma\beta\rangle\,, |\alpha\beta\gamma\gamma\rangle\,,$$

$$|\alpha\gamma\gamma\beta\rangle\,, |\alpha\gamma\gamma\gamma\rangle\,, |\beta\beta\beta\gamma\rangle\,, |\beta\beta\gamma\gamma\rangle\,, |\beta\gamma\gamma\gamma\rangle\,.$$

The set of $\vartheta_p(N, \lambda_z)$ for N up to 4 and for SU(3) and SU(4) are listed in table 3.4. The results presented in table 3.4 have been checked by explicitly applying the matric unit operators to all possible primitive generalized spin wave functions and then determining the linearly independent combinations algebraically. The results of this brute-force approach for the numbers of linearly independent state precisely match with the multiplicities and multiplet dimensions deduced by the decomposition into irreducible representations of the Lie algebra of SU(n) according to appendix E.

Recall that in the tensor product of N fundamental SU(n) multiplets there are f^λ irreducible representations associated with each symmetry type λ, for example with $\lambda = [2,1]$ we have $f^\lambda = 2$, and, thus, there are f^λ generalized spin wave functions of the form $X_{\rm gsw}\,(N,\lambda,\lambda_z,r)$. When we construct the fully symmetric or antisymmetric basis wave function by sewing together spin and spatial parts [eq. (F.3)], any orthogonal generalized spin wave functions of the same symmetry type and generated by the same root primitive generalized spin wave function will appear in the same basis wave function. Thus, when counting the number of generalized spin wave functions we include this degeneracy (see table 3.4), but when counting the size of the vector space of generalized spin wave functions we do not .

Recalling eq. (F.10), we aim to determine the most general form for $X_{\rm gsw}(N,\lambda,\lambda_z,1)$. We can use eq. (G.3) to write the basis of $X_{\rm gsw}(N,\lambda,\lambda_z,1)$ in terms of $\hat{e}^\lambda_{11}$ applied to the set of primitive generalized spin wave functions given in table 3.4. Thus, the minimal information to reconstruct the wave function is contained within that set of primitive generalized spin wave functions. In the multicomponent case the wave function (for fermions) can then be succinctly expressed as

$$\psi(N,\lambda,\lambda_z,p) \propto \hat{\mathcal{A}}\Phi\,(N,\lambda,1)\,\vartheta_p(N,\lambda_z), \tag{G.4}$$

where the set of functions $\vartheta_p(N,\lambda_z)$ are taken from table 3.4.

H Spatial Wave Functions for Quantum Hall Systems

In this appendix we will apply the general techniques for the construction of spatial wave functions derived in appendix F to the specific case of translationally invariant lowest Landau level (LLL) wave functions of fixed degree L. Specifically, our task is to determine the functions $\Phi\,(N,\lambda,1)$ which will provide the minimal information required to reconstruct the complete wave function. The enumeration of these functions will lead us to a derivation of the dimension of the space of spatial wave functions. In sec. H.1 we shall describe how to construct appropriate LLL wave functions in general, and we shall explain how the vector space of LLL spatial wave functions can be enumerated algebraically using a set of projection operators. In sec. H.2 we shall explain a more general procedure to calculate the dimensions of the vector space of LLL spatial wave functions.

H.1 Procedure for Construction of Spatial Wave Functions in the LLL

Spatial wave functions describing multiparticle LLL states are built from sums of products of single particle LLL wave functions and, as we argued in chapter 1, it follows that the spatial wave functions must be (translationally invariant) analytic polynomials of a fixed degree in the complex relative coordinates $\tilde{z}_i$. For a state with fixed relative angular-momentum eigenvalue L the most general form of spatial wave function is given by

$$\Phi_{\text{spatial}} = \sum_{i_1,\ldots,i_N} a_{i_1\ldots i_N} \tilde{z}_1^{i_1} \ldots \tilde{z}_N^{i_N} \qquad \text{with} \qquad \sum_{m=1}^{N} i_m = L.$$

with arbitrary coefficients $a_{i_1\ldots i_N}$ [cf. eq. (F.1)]. For example, for $N = 3$ and $L = 2$ the most general spatial wave function is

$$\Phi_{\text{spatial}} = a_{200}\tilde{z}_1^2 + a_{020}\tilde{z}_2^2 + a_{002}\tilde{z}_3^2 + a_{110}\tilde{z}_1\tilde{z}_2 + a_{011}\tilde{z}_2\tilde{z}_3 + a_{101}\tilde{z}_1\tilde{z}_3.$$

Using this definition, we could, in principle, now use eq. (F.6) to produce an expression for $\Phi(N, \lambda, 1)$ in the form given in eq. (F.7). In practice, we can employ a further short cut to this procedure that reproduces exactly the same result. Recalling the proof of theorem 1, we showed that

$$\Phi(N, \lambda, r) = \hat{e}_{r1}^{\tilde{\lambda}} \Phi(N, \lambda, 1).$$

This result implies the following idempotency relation:

$$\Phi(N, \lambda, 1) = \hat{e}_{11}^{\tilde{\lambda}} \Phi(N, \lambda, 1).$$

Thus, we see that if we start by writing $\Phi(N, S, 1)$ as the most general form of spatial wave function Φ_{spatial} given above, then the action of applying $\hat{e}_{11}^{\tilde{\lambda}}$ will automatically project out the most general form of the first spatial wave function, given in eq. (F.7). We can interpret this process of applying the symmetric group algebra basis operator as a process of introducing many linear dependencies between the original set of linearly independent coefficients $a_{i_1\ldots i_N}$. The result will be a polynomial of a particular symmetry imposed by the representation of the symmetric group λ, which may still contain some linearly independent coefficients $a'_{i_1\ldots i_N}$, the number of which is the dimension of the space of spatial wave functions.

We have now deduced that the vector space of LLL spatial wave functions can be projected out from the space of most general LLL wave functions. In principle, this method can be employed to determine the dimensions of the basis (listed in table 3.1) and the explicit forms of the basis functions. However, due to the algebraic complexity of constructing the most general

form of the spatial wave functions, and the fact that the number of terms in $\hat{e}_{11}^{\lambda}$ grows as $N!$ with the number of particles N, this brute-force approach is not viable in general. In the next section we shall describe a method to calculate the dimensions of the space of LLL spatial wave functions in general.

H.2 Calculating the Dimension of the Vector Space of Spatial Wave Functions

In this section we shall explain the method used to calculate the values listed in table 3.1. Using these results we shall then reinterpret the form of the spatial wave functions $\Phi(N, \lambda, 1)$ and in doing so we shall complete our explanation of the results presented in table 3.2.

The spatial wave function $\Phi(N, \lambda, 1)$ takes the form of a translationally invariant, analytic polynomial in the coordinates z_i, satisfying a particular set of permutation symmetries imposed by the underlying symmetric group representation. In general, it contains many linearly independent coefficients, the number of which depends on the degree of the polynomial. This is called the dimension of the polynomial space. In order to determine how many independent parameters occur at a given degree we construct generating functions for the polynomial space dimension, and to do this we first need to construct a linearly independent basis in which to describe the polynomials.

Recall from sec. 3.1 that any antisymmetric polynomial in N variables can always be written as a symmetric polynomial by factoring out a Jastrow factor, eq. (3.3). There are many ways to construct a basis of symmetric polynomials; the one we utilize is the basis of elementary symmetric polynomials, which we defined in eq. (3.4). If we impose the condition that the polynomials must be translationally invariant then we must write elementary symmetric polynomials in terms of relative coordinates $\tilde{z}_i$, which we defined in eq. (3.5). Recall also that translational invariance results in eq. (3.6). These modified elementary symmetric polynomials form a basis of translationally invariant symmetric polynomials, in other words we can form any translationally invariant symmetric polynomial from a sum of products of the modified elementary symmetric polynomials. (More precisely, these polynomials form what is called a ring of translationally invariant symmetric polynomials.)[150]

The polynomials such as $\Phi(N, \lambda, 1)$ are not fully symmetric but, instead, they have symmetries in subsets of particle indices as dictated by the shape λ of their associated Young tableaux. As a starting point we shall try to use the basis of elementary symmetric polynomials to span the space of polynomials with subsets of symmetries. We require, in addition that

the polynomials are translationally invariant and this places a restriction on the basis,

$$e_{1,1\ldots N} = 0. \tag{H.1}$$

The dimension $d_{\text{sym}}(L,N)$ of the space of translationally invariant symmetric polynomials in N variables and of degree L is defined in terms of the generating function

$$Z_N(q) = \prod_{m=2}^{N} \frac{1}{1-q^m} = \sum_{L=0}^{\infty} q^L d_{\text{sym}}(L,N),$$

so

$$d_{\text{sym}}(L,N) = \left[\frac{1}{L!}\left(\frac{d}{dq}\right)^L Z_N(q)\right]_{q=0}. \tag{H.2}$$

We can write down a generating function for the space of polynomials with subsets of symmetries by multiplying the generating functions of the subsets (for proof, see appendix I.2).

Our task now is to construct a basis of partially symmetric polynomials that reflects the symmetric group representations. It happens that the two component case is the simplest to explain, and so we shall discuss that case first before generalizing our result to the multicomponent case.

H.2.1 Two-Component Case

The basis of two-component wave functions is identical to the basis of spin eigenfunctions. We shall, thus, consider the spatial functions associated with an N-particle state of spin S.

For bosons the particular case of interest is a translationally invariant polynomial that is symmetric in arguments 1 to $\frac{1}{2}N+S$ and in the arguments $\frac{1}{2}N+S+1$ to N. Due to eq. (H.1) we must eliminate elementary symmetric polynomials of degree 1 from the generating function of one subset. The generating function for translationally invariant, symmetric polynomials with two symmetry subsets is then

$$Z^{\text{boson}}_{N,S}(q) = \prod_{m=1}^{\frac{N}{2}+S} \frac{1}{1-q^m} \prod_{n=2}^{\frac{N}{2}-S} \frac{1}{1-q^n}. \tag{H.3}$$

For example, we might consider polynomials of degree $L=3$ in $N=5$ indices that are symmetric in indices 1, 2, and 3 and separately symmetric in indices 4 and 5. In terms of elementary symmetric polynomials we can construct: $e_{1,123}e_{2,123}$, $e_{1,123}e_{2,45}$, $e_{3,123}$, $e^3_{1,123}$. This number, 4, is precisely given by appropriately differentiating the generating function given in eq. (H.3), for the case of $N=5$ and $S=1/2$.

For fermions we require that the polynomial is separately antisymmetric in the two symmetry subsets instead of separately symmetric in the two subsets, and so the space of symmetric polynomials only comes into play at polynomial degrees higher than the degree of the associated Jastrow factor. To start the generating function at a particular degree, J, we must multiply by q^J (for a proof, see appendix I.2). In order to take into account the Jastrow factors associated with each of the symmetry subsets we must have

$$J = \frac{1}{2}\left(\frac{N}{2} - S\right)\left(\frac{N}{2} - S - 1\right) + \frac{1}{2}\left(\frac{N}{2} + S\right)\left(\frac{N}{2} + S - 1\right) = \frac{N^2}{4} - \frac{N}{2} + S^2. \tag{H.4}$$

The generating function for translationally invariant, antisymmetric polynomials with two symmetry subsets is then

$$Z^{\text{fermion}}_{N,S}(q) = q^J \prod_{m=1}^{\frac{N}{2}+S} \frac{1}{1-q^m} \prod_{n=2}^{\frac{N}{2}-S} \frac{1}{1-q^n}. \tag{H.5}$$

More precisely these generating functions actually account for polynomials with this type of symmetry *or greater symmetry*. For example, a polynomial which is fully symmetric is also, by definition, symmetric in any subset of its arguments. A polynomial that is symmetric in two subsets of its arguments is also symmetric in any further subdivision of those subsets. What we really require is a generating function for polynomials of one particular symmetry only, which we shall denote by $\tilde{Z}_{N,S}$, and we emphasize that Eqs. H.3 and H.5 fail to do this. In appendix I.3 we make the statement "greater symmetry" more precise; in particular, we show that for tableaux containing the same number of boxes, a tableau λ is of "greater symmetry" than a tableau μ if and only if $S_\lambda \geq S_\mu$, where S is the corresponding spin eigenvalue of the tableau.

What we call $\tilde{Z}_{N,S}$ is the generating function for polynomials that are eigenfunctions of S^2 (note that this is independent of S_z eigenvalue). Below, $Z_{N,S}(q)$ represents either $Z^{\text{fermion}}_{N,S}(q)$ defined in eq. (H.5) or $Z^{\text{boson}}_{N,S}(q)$ defined in eq. (H.3). Our derivation of the generating function $\tilde{Z}_{N,S}$ is as follows. First, it is easy to see that

$$Z_{N,\frac{N}{2}}(q) = \tilde{Z}_{N,\frac{N}{2}}(q),$$

which is simply the statement that for the state where $S = N/2$, the wave function is fully symmetric (bosons) or fully antisymmetric (fermions). For the next highest state we have

$$Z_{N,\frac{N}{2}-1}(q) = \tilde{Z}_{N,\frac{N}{2}}(q) + \tilde{Z}_{N,\frac{N}{2}-1}(q),$$

that is, the polynomial space whose dimension is generated by either eq. (H.3) or eq. (H.5)

with $S = N/2 - 1$, is composed of both fully symmetric polynomials and polynomials that are symmetric in $N - 1$ indices. We can rearrange this equation to give an expression for the generating function that we want to get at:

$$\tilde{Z}_{N,\frac{N}{2}-1}(q) = Z_{N,\frac{N}{2}-1}(q) - Z_{N,\frac{N}{2}}(q).$$

In general, we have

$$Z_{N,S}(q) = \sum_{i=0}^{\frac{N}{2}-S} \tilde{Z}_{N,\frac{N}{2}-i}(q),$$

and so

$$\tilde{Z}_{N,S}(q) = Z_{N,S}(q) - Z_{N,S+1}(q). \tag{H.6}$$

These generating functions are used to calculate the results displayed in table 3.1. A more rigorous proof of this result is given in appendix I.3.

Although the generating functions provide us with a means to calculate the dimension of the space of polynomials at a given degree, they shed no light on the explicit form of the polynomials. An insight into the forms of the polynomials can be obtained by first rewriting the generating function using the following result (see appendix I.2):

$$\tilde{Z}_{N,S}(q) = q^J \prod_{n=2}^{N} \frac{1}{1-q^n} \sum_{k=0}^{k_{\max}} b'_k q^k, \tag{H.7}$$

where b'_k are positive integer coefficients and

$$k_{\max} = \left(\tfrac{N}{2} - S\right)\left(\tfrac{N}{2} + S\right).$$

We interpret the expression for the generating function in eq. (H.7) as describing a polynomial basis comprising *primitive polynomials* at degrees J up to $J + k_{\max}$, each of which has b'_k linearly independent coefficients. In order to indicate the polynomial degrees at which the primitive polynomials occur, we include the following functions, $Y_{N,S}$, in table H.1:

$$Y_{N,S} = \frac{\tilde{Z}_{N,S}(q)}{\prod_{l=2}^{N} \frac{1}{1-q^l}} = q^J \sum_{k=0}^{k_{\max}} b'_k q^k. \tag{H.8}$$

Some examples of the b'_k thus can be read off from table H.1.

The conclusion of this section is the following key statement: the most general polynomial of a given symmetry type is a linear combination of the primitive polynomials multiplied by any valid translationally invariant fully symmetric polynomial.

λ	$Y_{N,S}$
$[2]$	1
$[1,1]$	q
$[3]$	1
$[2,1]$	$q+q^2$
$[1,1,1]$	q^3
$[4]$	1
$[3,1]$	$q+q^2+q^3$
$[2,2]$	q^2+q^4
$[2,1,1]$	$q^3+q^4+q^5$
$[1,1,1,1]$	q^5

λ	$Y_{N,S}$
$[5]$	1
$[4,1]$	$q+q^2+q^3+q^4$
$[3,2]$	$q^2+q^3+q^4+q^5+q^6$
$[3,1,1]$	$q^3+q^4+2q^5+q^6+q^7$
$[2,2,1]$	$q^4+q^5+q^6+q^7+q^8$
$[2,1,1,1]$	$q^6+q^7+q^8+q^9$
$[1,1,1,1,1]$	q^{10}

Table H.1: These functions, $Y_{N,S}$, are calculated as in eq. (H.8), by taking the ratios of the generating functions for polynomials of a particular symmetry type λ in eq. (H.12) [or eq. (H.6) for the two-component case], to the generating function of a fully symmetric polynomial for the same number of particles. As explained in the text, the q polynomial degree of each term indicates the presence of a primitive polynomial at that degree in the spatial wave function and the value of the coefficient in the q polynomial indicates the number of linearly independent parameters constituting the primitive polynomial at that degree (cf. Tables 3.2 and 3.3).

H.2.2 Generlization to the Multicomponent Case

In the multicomponent case, we have already shown that the full spatial wave function can be reconstructed from just the first part, $\Phi(N,\lambda,1)$. In this section we aim to describe the form of this first part of the spatial wave function, a translationally invariant analytic polynomial of a particular symmetry, in terms of the elementary symmetric polynomials. We would like to derive an expression for the dimensions of the spaces of such polynomials, as we did for the two-component case, by constructing a set of generating functions.

We start by writing down a generating function for the space of polynomials with an arbitrary number of symmetry subsets, and we do this by simply multiplying together the generating functions corresponding to each of the different subsets (previously we only needed to consider two subsets). To take into account the translational invariance of the polynomial, we use the relative coordinates also defined in sec. 3.1. This introduces the constraint given in eq. (H.1). To enforce this constraint, we remove one of the sets of e_1 terms by starting one of the generating functions from a lower bound of 2 rather than 1 (similar to the argument given in for the two-component case),

$$Z_\lambda^{\text{boson}} = \prod_{m_1=1}^{N_1} \frac{1}{1-q^{m_1}} \prod_{m_2=1}^{N_2} \frac{1}{1-q^{m_2}} \cdots \prod_{m_n=2}^{N_n} \frac{1}{1-q^{m_n}} \tag{H.9}$$

or for conjugate tableaux we would have to take out an appropriate Jastrow factor of degree

$$J = \sum_{i=1}^{n} \frac{1}{2} N_i \left(N_i - 1\right).$$

The generating function in this case is

$$Z_\lambda^{\text{fermion}} = q^J \prod_{m_1=1}^{N_1} \frac{1}{1-q^{m_1}} \prod_{m_2=1}^{N_2} \frac{1}{1-q^{m_2}} \cdots \prod_{m_n=2}^{N_n} \frac{1}{1-q^{m_n}}. \tag{H.10}$$

In fact, the generating functions written down here describe a space of polynomials that has a certain symmetry type or a greater symmetry. For example, the generating function $Z^{\text{boson}}_{\lambda=[2,1]}$ gives the dimension of the vector space of polynomials of symmetry type $\lambda = [2,1]$ added to the dimension of the vector space of polynomials of symmetry type $\lambda = [3]$. More precisely, we say that the vector space generated by Z_λ^{boson} contains two subvector spaces, each of which corresponds to a particular irreducible representation of the symmetric group. It follows that, for our purposes, determining the vector spaces of polynomials associated with irreducible representations of the symmetric group, we are looking for the dimensions of these subvector spaces. If we wish to perform this decomposition of vector spaces for any arbitrary shape of tableau then an important question to address is which subvector spaces are included, in general, and how many times is each subvector space included (as there is no reason, in principle, why a subvector space cannot be included multiple times in the decomposition). The answer to this question can be found in the underlying mathematical structure of the construction of polynomial spaces corresponding to representations of the symmetric group (objects known as modules in the mathematical nomenclature); we shall simply state the result here, leaving the details of the underlying mathematics to appendix I.3. In order to state the result we must, first, introduce a notation that makes precise the statement "greater symmetry" [185]: when comparing two Young tableaux shapes $\mu = [\mu_1, \mu_2, \ldots \mu_n]$ and $\lambda = [\lambda_1, \lambda_2, \ldots \lambda_l]$, we say that μ dominates (has "greater symmetry" than) λ, written $\mu \trianglerighteq \lambda$ if

$$\mu_1 + \mu_2 + \ldots + \mu_i \geq \lambda_1 + \lambda_2 + \ldots + \lambda_i \quad \forall\, i \geq 1, \qquad \text{with} \qquad \mu_{i>l} = \lambda_{i>n} = 0.$$

For example, $[3,3] \trianglerighteq [2,2,1,1]$. Note that there are cases when tableaux are incomparable, such as $[3,3]$ and $[4,1,1]$. One way to avoid such incomparable tableau shapes by restricting possible shapes to tableaux having no more than two rows, which is precisely the two-component case. For proof of this result, see appendix I.3. Below, $Z_\lambda(q)$ represents either $Z_\lambda^{\text{fermion}}(q)$ defined in eq. (H.10) or $Z_\lambda^{\text{boson}}(q)$ defined in eq. (H.9). Using this notation, the general relation between the Z_λ generating functions and the generating functions corresponding to irreducible

	$\lambda =$	[3]	[2,1]	[1,1,1]
$\mu =$	[3]	1	−1	1
	[2,1]	0	1	−2
	[1,1,1]	0	0	1

(a) $(K)^{-1}_{\mu\lambda}$ for $N = 3$

	$\lambda =$	[4]	[3,1]	[2,2]	[2,1,1]	[1,1,1,1]
$\mu =$	[4]	1	−1	0	1	−1
	[3,1]	0	1	−1	−1	2
	[2,2]	0	0	1	−1	1
	[2,1,1]	0	0	0	1	−3
	[1,1,1,1]	0	0	0	0	1

(b) $(K)^{-1}_{\mu\lambda}$ for $N = 4$

Table H.2: A list of inverse Kostka matrices for different Young tablaux sizes. Lists of the Kostka matrices $K_{\mu\lambda}$ up to $N = 8$ are given in ref. [186].

representations of the symmetric group, $\tilde{Z}_\lambda$, is

$$Z_\lambda = \sum_{\mu \trianglerighteq \lambda} K_{\mu\lambda} \tilde{Z}_\mu. \tag{H.11}$$

In this equation the coefficients $K_{\mu\lambda}$ are called Kostka numbers.[186] It is clear that eq. (H.11) is a matrix equation. Since the matrix of Kostka numbers is nonsingular, the relation can be inverted, which gives us our key result:

$$\tilde{Z}_\lambda = \sum_{\mu \trianglerighteq \lambda} (K)^{-1}_{\mu\lambda} Z_\mu. \tag{H.12}$$

A formal derivation of this result is given in appendix I.3. In table H.2 we have listed selected inverse matrices of Kostka numbers. Using these numbers, we can construct, for example,

$$\tilde{Z}^{\text{boson}}_{[2,1,1]} = Z^{\text{boson}}_{[2,1,1]} - Z^{\text{boson}}_{[3,1]} - Z^{\text{boson}}_{[2,2]} + Z^{\text{boson}}_{[2,1,1]}$$

Notice that if we restrict the allowed tableau shapes to have no more than two, rows then we recover the special case of the result given in eq. (H.6). An identical argument applies for the description of conjugate tableaux $Z^{\text{fermion}}_\lambda$.

We have used these results to calculate the lists of the dimensions of vector spaces associated with irreducible representations of the symmetric group listed in table 3.1 for the symmetry types not already included in the SU(2) case.

H.2.3 Calculation of Primitive Polynomials

We shall conclude our argument by describing the procedure by which we have calculated the primitive polynomials presented in Tables 3.2 and 3.3. We start with the most general fixed

degree translationally invariant polynomial as the spatial wave function:

$$\Phi_{\text{spatial}} = \sum_{i_1,\ldots,i_N} a_{i_1\ldots i_N} \tilde{z}_1^{i_1} \ldots \tilde{z}_N^{i_N} \quad \text{with} \quad \sum_{m=1}^{N} i_m = L.$$

We then apply the appropriately constructed symmetric group algebra projection operator: $\Phi\left(N,\lambda,1\right) = \hat{e}_{11}^{\lambda}\Phi_{\text{spatial}}$ (with $\lambda = [N_1, N_2, \ldots, N_n]$). This will leave a sum of terms that are of the correct permutation symmetry, and, hence, they can be written in terms of a basis of elementary symmetric polynomials (multiplied by an appropriate Jastrow factor, for the fermion case):

$$\Phi\left(N,\lambda,1\right) = \sum_{i_1,\ldots,i_N} b_{i_1\ldots i_N} e_{1,N_1}^{i_1}\left(\tilde{z}_1,\ldots,\tilde{z}_{N_1}\right)\ldots e_{N_1,N_1}^{i_{N_1}}\left(\tilde{z}_1,\ldots,\tilde{z}_{N_1}\right)\ldots e_{1,N_n}^{i_{N_{n-1}+1}}\left(\tilde{z}_{N_{n-1}+1},\ldots,\tilde{z}_{N_n}\right)$$
$$\ldots e_{N_n,N_n}^{i_{N_n}}\left(\tilde{z}_{N_{n-1}+1},\ldots,\tilde{z}_{N_n}\right) \qquad \text{with} \qquad \sum_{m=1}^{N_1} m\, i_m + \ldots + \sum_{m=N_n+1}^{N_n} \left(m - N_n\right) i_m = L.$$

This is equivalent to a basis involving primitive polynomials and fully symmetric polynomials only. We start with linearly independent coefficients $a_{i_1\ldots i_n}$, but once we apply the projection operator we have a smaller set of coefficients, $b_{i_1\ldots i_n}$. These coefficients are not linearly independent in general. We can express the b coefficients in terms of the a coefficients, and, in principle, it is possible to solve these systems of equations to determine all possible linear dependences between the b coefficients. Indeed, using this procedure, we have independently verified the number of linearly independent coefficients predicted by the generating function method up to polynomial degree ten.

If we perform this construction at a polynomial degree exactly corresponding to a primitive polynomial, then we can be sure that one of the basis polynomials (i.e., the terms multiplying one of the $b_{i_1\ldots i_n}$ coefficients) can be considered as the primitive polynomial. We can therefore extract the primitive polynomial by setting an appropriate number of the $b_{i_1\ldots i_n}$ coefficients to zero, such that the remaining expression contains the correct number of linearly independent coefficients required for the primitive polynomial. For $N \leq 5$, almost all of the primitive polynomials contain only one arbitrary coefficient and so this procedure can be reduced to setting all but one of the $b_{i_1\ldots i_n}$ coefficients to zero, such that different primitive polynomials are not related to each other by multiplication by any translationally invariant fully symmetric polynomial in N variables. The polynomials given in table 3.2 are all derived using this technique. We have elucidated the details of the technique here in order to point out that the primitive polynomials listed in table 3.2 are defined in a somewhat arbitrary way. Despite this, once we reconstruct the spatial wave functions from primitive polynomials multiplied by translationally

invariant symmetric polynomials with a fixed combined degree, then these functions will fully span the basis.

We began this construction procedure with the most general possible Φ_{spatial}. In practice, we are free to choose a less general starting spatial wave function if we know what properties to expect in the final spatial wave function after projection (in other words, we can effectively pre-empt the linear dependencies that will be introduced between the coefficients and this saves a great deal of computational time). The first part of the spatial wave function will be associated with the first standard tableau of the shape $\lambda = [N_1, N_2, \ldots, N_n]$. The corresponding polynomial will be translationally invariant and symmetric or antisymmetric in indices 1 to N_1, in indices $N_1 + 1$ to N_2, and so on. Using this information, we can choose the starting spatial wave function to be the most general translationally invariant analytic polynomial with these symmetries at a given degree, Φ_{reduced}. These symmetries are, in fact, uniquely associated with the $r = 1$ standard tableau and, as a result, it follows that

$$\Phi\left(N, \lambda, 1\right) = e_{11}^{\tilde{\lambda}} \Phi_{\text{reduced}}. \tag{H.13}$$

We shall now discuss a simple example illustrating the whole construction procedure in the case of a two-component system. For simplicity, there are no undetermined parameters in this example. Let us consider the three-particle $L = 1$, $S = 1/2$, $S_z = 1/2$ fermion wave function. We begin by constructing the spatial wave function associated with the first spin eigenfunction. To do this we, first, construct the $r = 1$ standard tableau associated with $N = 3$ and $S = 1/2$. We know that the spin eigenfunction $X(N = 3, S = 1/2, S_z = 1/2, r = 1)$ is constructed from

1	2
3	

The fermion spatial wave function associated with the spin eigenfunction $X(3, 1/2, 1/2, 1)$ is then constructed from the contragradient standard tableau, which is

1	3
2	

For bosons we instead construct the spatial wave function from the first tableau shown here.

We have already calculated $X(3, 1/2, 1/2, 1)$ in appendix G.1, and it is clearly symmetric under exchange of the first two spins but has no other symmetry. If we require that the overall wave function is antisymmetric (for fermions) then we know immediately that the spatial wave function $\Phi(N = 3, S = 1/2, r = 1)$ will at the very least be antisymmetric under exchange of the first two coordinates. Using this information we can choose the primitive spatial wave

function to be

$$\Phi_{\text{reduced}} = (\tilde{z}_1 - \tilde{z}_2)\,.$$

We then apply a projection operator to generate $\Phi(3, 1/2, 1)$ (see ref. [149] for tables listing the explicit forms of such projection operators)

$$\Phi(3, 1/2, 1) = \hat{e}^{\widetilde{[2,1]}}_{1,1}\Phi = \hat{e}^{\widetilde{[2,1]}}_{1,1}(\tilde{z}_1 - \tilde{z}_2) = (\tilde{z}_1 - \tilde{z}_2)\,.$$

As we have explained, this term is associated with the first primitive spin wave function and we know that all of the physics is contained in the construction

$$|\uparrow\uparrow\downarrow\rangle\,(\tilde{z}_1 - \tilde{z}_2)\,.$$

Given this information we can effectively determine the remainder of the wave function by antisymmetrizing in all the particle indices [see eq. (3.17)].

Although simply antisymmetrizing does indeed give the correct result, it may be necessary to write the result explicitly in terms of spin eigenfunctions. In this example we have $f^\lambda = 2$. We associate $\Phi(3, 1/2, 1)$ with the first spin eigenfunction:

$$X\,(3, 1/2, 1/2, 1) = \tfrac{1}{\sqrt{6}}\,(2\,|\uparrow\uparrow\downarrow\rangle - |\uparrow\downarrow\uparrow\rangle - |\downarrow\uparrow\uparrow\rangle)\,.$$

The second spin eigenfunction is

$$X\,(3, 1/2, 1/2, 2) = \tfrac{1}{\sqrt{2}}\,(|\uparrow\downarrow\uparrow\rangle - |\downarrow\uparrow\uparrow\rangle)\,.$$

The associated spatial wave function is given by

$$\Phi\,(3, 1/2, 2) = \hat{e}^{\widetilde{[2,1]}}_{21}\Phi(3, 1/2, 1) = \tfrac{1}{\sqrt{3}}\,(2\tilde{z}_3 - \tilde{z}_1 - \tilde{z}_2)\,.$$

The full wave function must be a the sum of these two terms: for $L = 1$ this is

$$|1, 1/2, 1/2, 1\rangle \propto (2\,|\uparrow\uparrow\downarrow\rangle - |\uparrow\downarrow\uparrow\rangle - |\downarrow\uparrow\uparrow\rangle)\,(\tilde{z}_1 - \tilde{z}_2) - (|\uparrow\downarrow\uparrow\rangle + |\downarrow\uparrow\uparrow\rangle)\,(2\tilde{z}_3 - \tilde{z}_1 - \tilde{z}_2)\,.$$

Comparing with eq. (3.17) we see that once the terms corresponding to each of the primitive spin wave functions are collected up then the results do indeed agree.

To obtain the equivalent boson wave function in this case we can simply interchange the associations between the spin and spatial parts. We can, of course, apply the same technique described in this example to construct the wave function at any degree, starting from the first part of the spatial wave function at that degree.

I Further Mathematical Details

I.1 Young Operators

The concept of Young operators may be familiar to many readers. The Young operators are idempotent projection operators that generate minimal left ideals in the regular representation of the symmetric group; in other words, the Young operators form a resolution of the identity that generates the irreducible representations of the symmetric group algebra.[152] By definition this means that they form a basis spanning the group algebra.

The Young operators are constructed as follows: with each standard tableau, T_r, we associate an operator

$$Y_r = Q_r P_r,$$

where P_r is product over all rows in the tableau of the sum of all permutations that permute the numbers in the same row and Q_r is product over all columns in the tableau of the sum of all permutations that permute the numbers in the same column multiplied by the sign of those permutations. Essentially, P_r symmetrizes in the row indices and Q_r antisymmetrizes in the column indices. The Young operator is the product of these two operators.

The set of Young operators can be used to generate all of the results derived in appendix F; however, the resulting projected functions do not form a fully orthogonal basis.[151] It is more convenient, therefore, to use a set of operators that automatically project out an orthogonal basis of generalized spin wave functions.

The advantage of the matric basis, defined in appendix E, is that it enables us to use the representation matrices of any irreducible representation to construct a corresponding basis of the group algebra, and, for convenience, we can choose the orthogonal representation to ensure orthogonal basis functions.

I.2 Generating Functions for Symmetric Polynomials

The generating function for a translationally invariant symmetric polynomial in N variables is given by[180]:

$$Z_N(q) = \prod_{m=2}^{N} \frac{1}{1-q^m}.$$

Consider a product of two generating functions for symmetric polynomials

$$Z_{N_1}(q) Z_{N_2}(q).$$

The dimension of the space of polynomials at degree L is given by

$$d(L, N_1, N_2) = \left[\frac{1}{L!}\left(\frac{d}{dq}\right)^L Z_{N_1}(q) Z_{N_2}(q)\right]_{q=0},$$

but we can expand this expression out using the Leibniz rule as follows:

$$\left(\frac{d}{dq}\right)^L Z_{N_1} Z_{N_2} = \sum_{k=0}^{L} {}^L C_k \left(\frac{d}{dq}\right)^{L-k} Z_{N_1} \left(\frac{d}{dq}\right)^k Z_{N_1}.$$

So the dimension of the space of the combined symmetry is given by the sum of the dimensions of the spaces of polynomials of the same symmetry but with all possible subdivisions of the angular momentum, L. This is precisely the result we require for the generating function of a polynomial with two combined symmetries. This result clearly generalizes to a product of arbitrarily many generating functions.

Now consider a modified generating function given by multiplying by a factor of q^J. The dimension of the space of polynomials arising from this modified generating function is effectively a special case of the above result:

$$\begin{aligned} d(L, N) &= \left[\frac{1}{L!}\left(\frac{d}{dq}\right)^L \left(q^J \prod_{m=2}^{N} \frac{1}{1-q^m}\right)\right]_{q=0} \\ &= \left[\frac{1}{(L-J)!}\left(\frac{d}{dq}\right)^{L-J} \left(\prod_{m=2}^{N} \frac{1}{1-q^m}\right)\right]_{q=0} = d_{\text{sym}}(L-J, N) \end{aligned}$$

In appendix H we made use of the following results for the two-component case:

$$\frac{Z_{N,S}(q)}{q^J \prod_{n=2}^{N} \frac{1}{1-q^n}} = \frac{\prod_{l=2}^{\frac{N}{2}+S} \frac{1}{1-q^l} \prod_{m=1}^{\frac{N}{2}-S} \frac{1}{1-q^m}}{\prod_{n=2}^{N} \frac{1}{1-q^n}} = \prod_{j=1}^{\frac{N}{2}-S} \frac{\left(1-q^{N+1-j}\right)}{\left(1-q^j\right)} = \left[\begin{matrix} N \\ \frac{N}{2}-S \end{matrix}\right]_q.$$

The final expression is a so-called q-binomial coefficient.[181] We can, thus, simplify the generating function to

$$Z_{N,S}(q) = q^J \prod_{n=2}^{N} \frac{1}{1-q^n} \sum_k b_k q^k,$$

where b_k are positive integer coefficients. Using the definition of q-binomials we can show

$$\sum_k b_k = {}^N C_{\frac{N}{2}-S}.$$

Using the result from eq. (H.6) we have

$$\frac{\tilde{Z}_{N,S}(q)}{\prod_{n=2}^{N}\frac{1}{1-q^n}} = q^J \begin{bmatrix} N \\ \frac{N}{2}-S \end{bmatrix}_q - q^{1+J+2S} \begin{bmatrix} N \\ \frac{N}{2}-S-1 \end{bmatrix}_q,$$

with J given in eq. (H.4). It follows that

$$\tilde{Z}_{N,S}(q) = q^J \prod_{n=2}^{N} \frac{1}{1-q^n} \sum_{k=1}^{k_{\max}} b'_k q^k,$$

where b'_k are positive integer coefficients, which can be derived from the previous formula above in terms of the q-binomial coefficients, and

$$k_{\max} = \left(\tfrac{N}{2}-S\right)\left(\tfrac{N}{2}+S\right).$$

A similar result also holds in the multicomponent case for $\tilde{Z}_\lambda$ defined in eq. (H.12).

I.3 Vector Spaces Associated with Representations of the Symmetric Group

In this final appendix we shall present an alternative derivation of the results presented in appendix H. Our aim is to construct a basis of polynomials that are in a one-to-one correspondence with irreducible representations of the symmetric group, and, hence, are labeled by Young tableau shapes $\lambda = [N_1, N_2, \ldots, N_n]$. The starting point of our derivation is the set of symmetric polynomials that have subsets of symmetries. Such polynomials can also be enumerated in terms of integer partitions and, hence, Young tableau shapes. The question is: how are these polynomial constructions related? In this appendix we shall explain how this question can be posed in a more precise mathematical sense, in terms of the representation theory of the symmetric group. Having demonstrated an equivalence to a problem in mathematics, we shall describe the solution and then finally explain how this solution can be applied in the context of our problem.

To begin with, recall the simple argument given in appendix H, which applied to the case of Young tableaux restricted to having no more than two rows. In that case we stated that the basis of polynomials of a given symmetry type actually contains polynomials of that particular symmetry type or of a greater symmetry type. We should make this statement more precise. Mathematically speaking the term "*greater symmetry*" is equivalent to whether one tableau shape dominates another.[185] When comparing two Young tableau shapes $\mu = [\mu_1, \mu_2, \ldots, \mu_n]$ and $\lambda = [\lambda_1, \lambda_2, \ldots, \lambda_l]$, we say that μ dominates (has "greater symmetry" than) λ, written

$\mu \trianglerighteq \lambda$ if

$$\mu_1 + \mu_2 + \ldots + \mu_i \geq \lambda_1 + \lambda_2 + \ldots + \lambda_i \quad \forall\ i \geq 1, \qquad \text{with} \qquad \mu_{i>l} = \lambda_{i>n} = 0.$$

In the special case where the Young tableau λ contains N boxes in two rows, with $N/2 + S_\lambda$ boxes in the first row, this definition reduces to just

$$\mu_1 \geq \lambda_1 \qquad \Rightarrow \qquad \frac{N}{2} + S_\mu \geq \frac{N}{2} + S_\lambda \quad , \quad \mu_1 + \mu_2 \geq \lambda_1 + \lambda_2 \qquad \Rightarrow \qquad N \geq N.$$

The second statement is clearly always satisfied, and the first statement is true for all spin eigenvalues $S_\lambda \leq S_\mu$, where S_λ is the spin eigenvalues associated with symmetry type λ. This is precisely the way in which we defined "greater symmetry" in appendix H. An important consequence of this result is that there are no possible cases of ambiguous dominance (that is, where two tableaux shapes do satisfy some but not all of the conditions for dominance, for example, [3,3] and [4,1,1]). We can represent the set of dominances diagrammatically in a Hasse diagram.[185] For the case of Young tableaux containing N boxes in only two rows the Hasse diagram is shown in fig. I.1 (a). The argument given in appendix H to derive eq. (H.6) follows directly form the ordered structure of this set of dominaces.

More generally, if we want to consider arbitrary shapes of Young tableaux, the set of dominances becomes more complicated. For example the Hasse diagram for all $N = 5$ Young tableaux is shown in fig. I.1 (b). In general we must be more careful take into account the exact structure of the inclusions each of these symmetry subsets, and in particular we cannot rule out that in general one subset may be included multiple times within a subset of greater symmetry. At this juncture we shall introduce an equivalent mathematical formulation of this problem.

In the mathematical theory of representations of the symmetric group the symbol M^λ denotes the polynomial space spanned by objects that correspond to the set of all Young tableaux of shape λ.[185] For example, $M^{[3,1]}$ has the basis

$$\begin{array}{|c|c|c|}\hline 2&3&4\\\hline 1\\\cline{1-1}\end{array} \qquad \begin{array}{|c|c|c|}\hline 1&3&4\\\hline 2\\\cline{1-1}\end{array} \qquad \begin{array}{|c|c|c|}\hline 1&2&4\\\hline 3\\\cline{1-1}\end{array} \qquad \begin{array}{|c|c|c|}\hline 1&2&3\\\hline 4\\\cline{1-1}\end{array}$$

We say that M^λ forms a representation of the symmetric group called a permutation module (a more strict definition is that a module over a ring is an algebraic structure generalizing the notion of a vector space over a field).[185] In the context of polynomials, the permutation module forms a "vector space" for the ring of polynomials associated with a particular symmetry type. This is because the symmetry type of a polynomial should correspond to a Young tableau

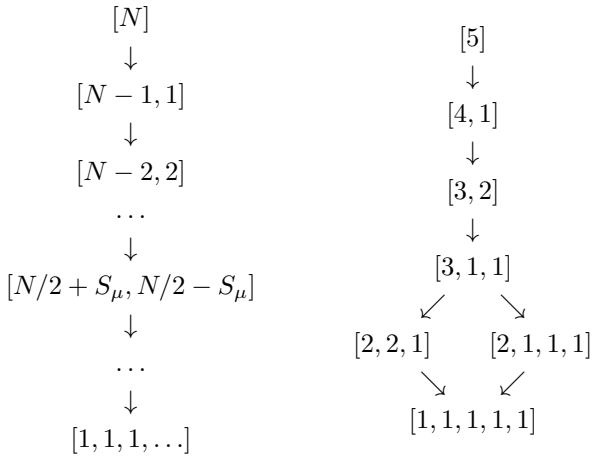

(a) Only two rows.

(b) All $N = 5$.

Figure I.1: Examples of Hasse diagrams representing Young tableau shapes of "greater symmetry".[185]

shape, as we have already explained, and because there should be no restriction on the order of the indices in a symmetric polynomial, so we must take into account all possible ways to place the numbers in a tableau of a given shape. The dimension of this polynomial vector space is, thus, given by the generating functions that we have denoted by Z_λ.

Our aim is to construct the space of polynomials corresponding to irreducible representations of the symmetric group. In the mathematical theory of representations of the symmetric group the symbol S^λ denotes the polynomial spaces that correspond to irreducible representations of the symmetric group (the notation is not to be confused with our S_λ, which is the spin eigenvalue associated with symmetry type λ). These vector spaces are spanned by objects that correspond to the standard Young tableaux of shape λ. For example, $S^{[3,1]}$ has the basis

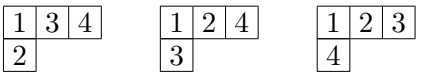

S^λ are called Specht modules.[185] In the context of polynomials, these Specht modules correspond exactly to the space of polynomials that becomes associated with irreducible representations of the symmetric group, in other words, precisely the space of polynomials that we require for our investigation. The dimensions of this space of polynomials are given by the generating functions that we have denoted by $\tilde{Z}_\lambda$.

A well-studied mathematical problem is to decompose the permutation module M^λ in terms of irreducible representations of the symmetric group or, equivalently, in terms of Specht modules. It turns out that it is possible to write M^λ as a direct sum of Specht modules, and

the result is[185]

$$M^{\lambda} \cong \bigoplus_{\lambda \trianglerighteq \mu} K_{\mu\lambda} S^{\mu}.$$

The coefficients appearing here are precisely the Kostka numbers that we discussed in appendix H.2.[186]

Finally, since this relation involves a direct sum of irreducible representations, it follows that the dimensions of these irreducible representations simply add together, and we find

$$d_{M^{\lambda}} = \sum_{\lambda \trianglerighteq \mu} K_{\mu\lambda} d_{S^{\mu}}.$$

It also follows that an equivalent relation must also be satisfied by the corresponding generating functions, and, hence, we find eq. (H.11).

Bibliography

[1] D. C. Tsui, H. L. Stormer, and A. C. Gossard, Phys. Rev. Lett. **48**, 1559 (1982). [pp. 1, 7]

[2] X. G. Wen and Q. Niu, Phys. Rev. B **41**, 9377 (1990). [p. 1]

[3] C. Nayak, S. H. Simon, A. Stern, M. Freedman, and S. D. Sarma, Rev. Mod. Phys. **80**, 1083 (2008). [pp. 1, 2, 26, 29, 80]

[4] B. I. Halperin, Phys. Rev. Lett. **52**, 1583 (1984). [pp. 12, 22, 23, 25]

[5] G. Moore and N. Read, Nucl. Phys. B **360**, 363 (1991). [pp. 1, 25, 79, 80, 85]

[6] N. Read and D. Green, Phys. Rev. B **61**, 10267 (2000). [pp. 1, 28, 30, 92]

[7] M. Levin and A. Stern, Phys. Rev. Lett. **103**, 196803 (2009). [p. 1]

[8] K. Sun, Z. Gu, H. Katsura, and S. Das Sarma, Phys. Rev. Lett. **106**, 236803 (2011). [p. 1]

[9] T. Neupert, L. Santos, C. Chamon, and C. Mudry, Phys. Rev. Lett. **106**, 236804 (2011).

[10] E. Tang, J.-W. Mei, and X.-G. Wen, Phys. Rev. Lett. **106**, 236802 (2011). [p. 1]

[11] N. R. Cooper, Advances in Physics **57**, 539 (2008). [pp. 1, 18, 19, 27]

[12] R. R. Du, A. S. Yeh, H. L. Stormer, D. C. Tsui, L. N. Pfeiffer, and K. W. West, Phys. Rev. Lett. **75**, 3926 (1995). [pp. 1, 26, 34, 37, 39, 47, 48, 50, 52, 53, 54]

[13] H. Cho *et al.*, Phys. Rev. Lett. **81**, 2522 (1998). [pp. 34, 49]

[14] I. V. Kukushkin, K. von Klitzing, and K. Eberl, Phys. Rev. Lett. **82**, 3665 (1999). [pp. 26, 34, 35, 37, 38, 39, 47, 48, 50, 52, 53, 54]

[15] B. I. Halperin, Helv. Phys. Acta **56**, 75 (1983). [pp. 13, 27, 79, 92]

[16] K. Park and J. K. Jain, Solid State Commun. **119**, 291 (2001). [pp. 1, 36, 37, 38, 39, 40, 44, 49, 56, 96]

[17] E. Ardonne and K. Schoutens, Phys. Rev. Lett. **82**, 5096 (1999). [pp. 1, 28, 30, 80, 85, 92]

[18] M. Barkeshli and X.-G. Wen, Phys. Rev. B **82**, 233301 (2010). [pp. 1, 28, 30]

[19] N. C. Bishop, M. Padmanabhan, K. Vakili, Y. P. Shkolnikov, E. P. De Poortere, and M. Shayegan, Phys. Rev. Lett. **98**, 266404 (2007). [pp. 1, 35]

[20] C. Zhang *et al.*, Phys. Rev. B **85**, 241302 (2012). [pp. 34, 45, 50, 57]

[21] W. Pan, K. W. Baldwin, K. W. West, L. N. Pfeiffer, and D. C. Tsui, Phys. Rev. Lett. **108**, 216804 (2012). [pp. 34, 45, 50, 57]

[22] B. E. Feldman *et al.*, Phys. Rev. Lett. **111**, 076802 (2013). [pp. 1, 14, 26, 36, 37, 47, 48, 50]

[23] R. E. Prange and S. M. Girvin, *The Quantum Hall Effect*, (Springer–Verlag, New York, 1990). [pp. 2, 3, 12, 13, 20]

[24] T. Chakraborty, and P. Pietiläinen, *The Fractional Quanutm Hall Effect*, (Springer–Verlag, Berlin, 1988). [p. 20]

[25] S. M. Girvin in *Topological Aspects of Low Dimensional Systems*, A. Comtet, T. Jolicoeur, S. Ouvry, and F. David, eds., (Springer, Berlin, 2000).

[26] D. Yoshioka, *The Quantum Hall Effect*, (Springer, Berlin, 2002). [pp. 12, 13, 20]

[27] J. K. Jain, *Composite Fermions*, (Cambridge University Press, Cambridge, 2007). [pp. 12, 13, 20, 22, 23, 24, 25, 26, 29, 36, 37, 38, 40, 41, 42, 43, 57, 97, 99]

[28] O. Heinonen, *Composite Fermions: A Unified View of the Quantum Hall Regime*, (World Scientific Publishing, 1998). [pp. 2, 23]

[29] B. Meyerson, Applied Physics Letters **48**, 797 (1986). [p. 3]

[30] A. Cho and J. Arthur, Prog. Solid State Ch. **10**, 157 (1975). [p. 3]

[31] L. Pfeiffer [http://www.princeton.edu/ee/people/display_person/?netid=loren] (2013). [p. 3]

[32] T. M. Lu, D. C. Tsui, C.-H. Lee, and C. W. Liu, Applied Physics Letters **94**, 182102 (2009). [p. 3]

[33] F. Stern and W. E. Howard, Phys. Rev. **163**, 816 (1967). [pp. 3, 15, 51]

[34] K. S. Novoselov *et al.*, Nature **438**, 197 (2005). [pp. 4, 9]

[35] E. Hall, American Journal of Mathematics **2**, 287 (1879). [p. 5]

[36] C. W. J. Beenakker and H. van Houten, Solid State Phys. **44**, 1 (1991). [pp. 7, 12]

[37] R. Willett, J. P. Eisenstein, H. L. Störmer, D. C. Tsui, A. C. Gossard, and J. H. English, Phys. Rev. Lett. **59**, 1776 (1987). [p. 7]

[38] V. Fock, Z. Phys. **47**, 446 (1928). [p. 8]

[39] L. Landau, Z. Phys. **64**, 623 (1930).

[40] C. G. Darwin, Proc. Cambridge Philos. Soc. **27**, 86 (1931). [p. 8]

[41] J. Singleton, *Band Theory and Electronic Properties of Solids*, (Oxford University Press, Oxford, 2001). [p. 11]

[42] D. J. Thouless, M. Kohmoto, M. P. Nightingale, and M. den Nijs, Phys. Rev. Lett. **49**, 405 (1982). [p. 13]

[43] R. L. Willett, H. L. Stormer, D. C. Tsui, A. C. Gossard, and J. H. English, Phys. Rev. B **37**, 8476 (1988). [p. 13]

[44] A. H. MacDonald and G. C. Aers, Phys. Rev. B **29**, 5976 (1984). [p. 15]

[45] M. R. Peterson, T. Jolicoeur, and S. D. Sarma, Phys. Rev. B **78**, 155308 (2008). [pp. 15, 40, 51]

[46] D. Yoshioka, Journal of the Physical Society of Japan **53**, 3740 (1984). [p. 15]

[47] D. Yoshioka, Surface Science **170**, 125 (1986).

[48] A. H. MacDonald, Phys. Rev. B **30**, 3550 (1984).

[49] I. Sodemann and A. H. MacDonald, Phys. Rev. B **87**, 245425 (2013). [pp. 25, 78]

[50] M. R. Peterson and C. Nayak, Phys. Rev. B **87**, 245129 (2013).

[51] S. H. Simon and E. H. Rezayi, Phys. Rev. B **87**, 155426 (2013). [pp. 15, 25, 78]

[52] F. D. M. Haldane, Phys. Rev. Lett. **51**, 605 (1983). [pp. 17, 23, 29, 40, 83, 95]

[53] D. Yoshioka, B. I. Halperin, and P. A. Lee, Phys. Rev. Lett. **50**, 1219 (1983). [pp. 18, 20]

[54] Nicolas Regnault *et al.* [http://www.nick-ux.org/diagham] (2013). [pp. 19, 86, 99]

[55] D. R. Hartree, Proc. Cambridge Philos. Soc. **24**, 89 (1928). [p. 20]

[56] V. Fock, Z. Phys. **61**, 126 (1930). [p. 20]

[57] H. Fukuyama, P. M. Platzman, and P. W. Anderson, Phys. Rev. B **19**, 5211 (1979). [p. 20]

[58] R. Moessner and J. T. Chalker, Phys. Rev. B **54**, 5006 (1996). [p. 20]

[59] R. Morf and B. I. Halperin, Phys. Rev. B **33**, 2221 (1986). [pp. 21, 28]

[60] R. Morf and B. I. Halperin, Z. Phys B **68**, 391 (1987). [p. 44]

[61] J. K. Jain and R. K. Kamilla, ArXiv: **cond-mat/9607147v2**, (1996).

[62] J. K. Jain and R. K. Kamilla, Phys. Rev. B **55**, R4895 (1997). [pp. 39, 42, 96]

[63] G. Möller and S. H. Simon, Phys. Rev. B **72**, 045344 (2005). [pp. 21, 39, 41, 42, 96, 97]

[64] R. B. Laughlin, Phys. Rev. Lett. **50**, 1395 (1983). [pp. 21, 22, 92]

[65] S. A. Trugman and S. Kivelson, Phys. Rev. B **31**, 5280 (1985). [pp. 21, 29]

[66] D. Arovas, J. R. Schrieffer, and F. Wilczek, Phys. Rev. Lett. **53**, 722 (1984). [pp. 22, 25]

[67] R. B. Laughlin, Surf. Sci. **142**, 163 (1984). [pp. 22, 23]

[68] S. M. Girvin, Phys. Rev. B **29**, 6012 (1984). [p. 22]

[69] N. Read, Phys. Rev. Lett. **65**, 1502 (1990). [p. 23]

[70] R. Morf and N. d'Ambrumenil, Phys. Rev. Lett. **74**, 5116 (1995). [pp. 24, 45]

[71] K. Park, V. Melik-Alaverdian, N. E. Bonesteel, and J. K. Jain, Phys. Rev. B **58**, R10167 (1998). [p. 24]

[72] V. W. Scarola, K. Park, and J. K. Jain, Nature **406**, 863 (2000). [p. 24]

[73] P. Di Francesco, P. Mathieu, D. Sénéchal, *Conformal field theory*, (Springer, New York, 1999). [pp. 24, 90]

[74] N. Read, Phys. Rev. Lett. **62**, 86 (1989). [p. 25]

[75] S. M. Girvin and A. H. MacDonald, Phys. Rev. Lett. **58**, 1252 (1987).

[76] S. C. Zhang, T. H. Hansson, and S. Kivelson, Phys. Rev. Lett. **62**, 82 (1989).

[77] S. C. Zhang, Int. Journal of Mod. Phys. B **6**, 25 (1992). [p. 25]

[78] M. Greiter, X.-G. Wen, and F. Wilczek, Phys. Rev. Lett. **66**, 3205 (1991). [pp. 25, 29]

[79] S.-S. Lee, S. Ryu, C. Nayak, and M. P. A. Fisher, Phys. Rev. Lett. **99**, 236807 (2007). [p. 25]

[80] M. Levin, B. I. Halperin, and B. Rosenow, Phys. Rev. Lett. **99**, 236806 (2007). [p. 25]

[81] E. H. Rezayi and F. D. M. Haldane, Phys. Rev. Lett. **84**, 4685 (2000). [pp. 25, 29]

[82] A. S. Goldhaber and J. K. Jain, Phys. Lett. A **199**, 267 (1995). [p. 25]

[83] C. A. Lütken and G. G. Ross, Phys. Rev. B **45**, 11837 (1992). [p. 26]

[84] D. R. Leadley *et al.*, Phys. Rev. Lett. **79**, 4246 (1997). [p. 26]

[85] M. Shayegan, E. P. De Poortere, O. Gunawan, Y. P. Shkolnikov, E. Tutic, and K. Vakili, Int. J. Mod. Phys. B **21**, 1388 (2007). [pp. 26, 35, 55]

[86] C. R. Dean *et al.*, Nature Physics **7**, 693 (2011). [pp. 26, 35]

[87] K. Bolotin, F. Ghahari, M. D. Shulman, H. L. Stormer, and P. Kim, Nature **462**, 196 (2009).

[88] X. Du, I. Skachko, F. Duerr, A. Luican, and E. Y. Andrei, Nature **462**, 192 (2009). [pp. 26, 35]

[89] D. P. Arovas, A. Karlhede, and D. Lilliehöök, Phys. Rev. B **59**, 13147 (1999). [pp. 27, 35]

[90] K. Lai, W. Pan, D. C. Tsui, S. Lyon, M. Mühlberger, and F. Schäffler, Phys. Rev. Lett. **93**, 156805 (2004).

[91] K. Eng, R. N. McFarland, and B. E. Kane, Phys. Rev. Lett. **99**, 016801 (2007).

[92] T. Kott, B. Hu, S. H. Brown, and B. E. Kane, ArXiv: **1210.2386**, (2012). [pp. 27, 35, 36]

[93] J. P. Eisenstein in *Perspectives in Quantum Hall Effect*, S. Das Sarma and A. Pinczuk, eds., (Wiley, New York 1997); also S. M. Girvin and A. H. MacDonald, *ibid.* [p. 27]

[94] J. Eisenstein, Science **305**, 950 (2004).

[95] J. P. Eisenstein and A. H. MacDonald, Nature **432**, 691 (2004). [p. 27]

[96] Z. Papić, G. Möller, M. V. Milovanović, N. Regnault, and M. O. Goerbig, Phys. Rev. B **79**, 245325 (2009). [p. 27]

[97] N. R. Cooper, Phys. Rev. Lett. **106**, 175301 (2011). [p. 27]

[98] R. N. Palmer and D. Jaksch, Phys. Rev. Lett. **96**, 180407 (2006). [p. 27]

[99] L. Hormozi, G. Möller, and S. H. Simon, Phys. Rev. Lett. **108**, 256809 (2012). [pp. 27, 80]

[100] E. H. Rezayi, Phys. Rev. B **39**, 13541 (1989). [p. 28]

[101] E. Ardonne, N. Read, E. Rezayi, and K. Schoutens, Nucl. Phys. B **607**, 549 (2001). [pp. 30, 80, 85, 92]

[102] E. Ardonne, F. J. M. van Lankvelt, A. W. W. Ludwig, and K. Schoutens, Phys. Rev. B **65**, 041305(R) (2002). [pp. 30, 92]

[103] J. W. Reijnders, F. J. M. van Lankvelt, K. Schoutens, and N. Read, Phys. Rev. Lett. **89**, 120401 (2002). [p. 30]

[104] J. W. Reijnders, F. J. M. van Lankvelt, K. Schoutens, and N. Read, Phys. Rev. A **69**, 023612 (2004). [pp. 28, 30, 80]

[105] T. Chakraborty and F. C. Zhang, Phys. Rev. B **29**, 7032 (1984). [p. 28]

[106] E. H. Rezayi, Phys. Rev. B **36**, 5454 (1987). [pp. 28, 30]

[107] S. L. Sondhi, A. Karlhede, S. A. Kivelson, and E. H. Rezayi, Phys. Rev. B **47**, 16419 (1993). [p. 28]

[108] S. E. Barrett, G. Dabbagh, L. N. Pfeiffer, K. W. West, and R. Tycko, Phys. Rev. Lett. **74**, 5112 (1995).

[109] A. Schmeller, J. P. Eisenstein, L. N. Pfeiffer, and K. W. West, Phys. Rev. Lett. **75**, 4290 (1995).

[110] A. H. MacDonald, H. A. Fertig, and L. Brey, Phys. Rev. Lett. **76**, 2153 (1996).

[111] N. R. Cooper, Phys. Rev. B **55**, R1934 (1997).

[112] A. Wójs, G. Möller, S. H. Simon, and N. R. Cooper, Phys. Rev. Lett. **104**, 086801 (2010).

[113] J. Romers, L. Huijse, and K. Schoutens, New Journal of Physics **13**, 045013 (2011). [p. 28]

[114] D. A. Abanin, S. A. Parameswaran, S. A. Kivelson, and S. L. Sondhi, Phys. Rev. B **82**, 035428 (2010). [p. 28]

[115] A. Kumar, S. A. Parameswaran, and S. L. Sondhi, Phys. Rev. B **88**, 045133 (2013). [p. 28]

[116] R. H. Morf, Phys. Rev. Lett. **80**, 1505 (1998). [pp. 29, 57]

[117] W. Bishara and C. Nayak, Phys. Rev. B **80**, 121302(R) (2009). [pp. 29, 31, 78]

[118] N. R. Cooper, Phys. Rev. Lett. **92**, 220405 (2004). [p. 29]

[119] N. Read and E. Rezayi, Phys. Rev. B **59**, 8084 (1999). [pp. 30, 61, 80, 92, 93]

[120] S. H. Simon, E. H. Rezayi, N. R. Cooper, and I. Berdnikov, Phys. Rev. B **75**, 075317 (2006). [pp. 30, 79, 87, 89, 92]

[121] D. Green, ArXiv: **cond-mat/0202455**, (2002). [pp. 30, 79, 80, 90, 92]

[122] S. H. Simon, E. H. Rezayi, and N. R. Cooper, Phys. Rev. B **75**, 195306 (2007). [pp. 30, 60, 61, 62, 63, 65, 78, 79, 83, 85, 86, 93]

[123] D. Yoshioka, A. H. MacDonald, and S. M. Girvin, Phys. Rev. B **39**, 1932 (1989). [p. 30]

[124] A. H. MacDonald, D. Yoshioka, and S. M. Girvin, Phys. Rev. B **39**, 8044 (1989).

[125] F. D. M. Haldane and E. H. Rezayi, Phys. Rev. Lett. **60**, 956 (1988). [pp. 80, 92]

[126] E. Rezayi and F. D. M. Haldane, Bull. Am. Phys. Soc **32**, 892 (1987). [p. 30]

[127] K. Yang and E. H. Rezayi, Phys. Rev. Lett. **101**, 216808 (2008). [pp. 31, 78]

[128] S. C. Davenport and S. H. Simon, Phys. Rev. B **85**, 245303 (2012). [pp. 33, 44, 46]

[129] M. J. Manfra, E. H. Aifer, B. B. Goldberg, D. A. Broido, L. Pfeiffer, and K. West, Phys. Rev. B **54**, 17327(R) (1996). [p. 34]

[130] P. Khandelwal, N. N. Kuzma, S. E. Barrett, L. N. Pfeiffer, and K. W. West, Phys. Rev. Lett. **81**, 673 (1998).

[131] J. G. Groshaus *et al.*, Phys. Rev. Lett. **98**, 156803 (2007). [p. 34]

[132] C. Hermann and C. Weisbuch, Phys. Rev. B **15**, 823 (1977). [p. 35]

[133] M. Padmanabhan, T. Gokmen, and M. Shayegan, Phys. Rev. B **80**, 035423 (2009). [pp. 35, 37, 47, 48]

[134] M. Padmanabhan, T. Gokmen, and M. Shayegan, Phys. Rev. B **81**, 113301 (2010). [pp. 35, 55]

[135] D. A. Abanin, B. E. Feldman, A. Yacoby, and B. I. Halperin, Phys. Rev. B **88**, 115407 (2013). [p. 36]

[136] C. Töke, M. R. Peterson, G. S. Jeon, and J. K. Jain, Phys. Rev. B **72**, 125315 (2005). [p. 45]

[137] C. Töke and J. K. Jain, Phys. Rev. Lett. **96**, 246805 (2006). [p. 46]

[138] Z. Papić, Phys. Rev. B **87**, 245315 (2013). [pp. 48, 56]

[139] D. R. Leadley *et al.*, Semicond. Sci. Technol. **13**, 671 (1998). [p. 49]

[140] E. Reyes-Gómez, N. Raigoza, and L. E. Oliveira, Phys. Rev. B **77**, 115308 (2008). [p. 49]

[141] G. A. Samara, Phys. Rev. B **27**, 3494 (1983). [p. 49]

[142] M. Polini, A. Tomadin, R. Asgari, and A. H. MacDonald, Phys. Rev. B **78**, 115426 (2008). [p. 50]

[143] J. S. Blakemore, J. Appl. Phys. **53**, R123 (1982). [p. 51]

[144] B. Yang, Z. Papić, E. H. Rezayi, R. N. Bhatt, and F. D. M. Haldane, Phys. Rev. B **85**, 165318 (2012). [p. 56]

[145] H. Wang, R. Narayanan, X. Wan, and F. Zhang, Phys. Rev. B **86**, 035122 (2012). [p. 56]

[146] M. Stern *et al.*, Phys. Rev. Lett. **108**, 066810 (2012). [p. 57]

[147] L. Tiemann, G. Gamez, N. Kumada, and K. Muraki, Science **335**, 828 (2012). [p. 57]

[148] E. H. Rezayi and S. H. Simon, Phys. Rev. Lett. **106**, 116801 (2011). [p. 57]

[149] S. C. Davenport and S. H. Simon, Phys. Rev. B **85**, 075430 (2012). [pp. 59, 78, 83, 106, 132]

[150] J. Liptrap, ArXiv: **1004.0364v1**, (2010). [pp. 62, 123]

[151] R. Pauncz, *Spin Eigenfunctions*, (Plenum Press, New York, 1979). [pp. 70, 73, 74, 105, 106, 114, 118, 133]

[152] M. Hamermesh, *Group Theory and its Application to Physical Problems*, (Addison-Wesley, Reading, MA, 1964). [pp. 72, 73, 74, 87, 104, 105, 106, 107, 108, 109, 110, 133]

[153] F. Hund, Z. Physik **43**, 788 (1927). [p. 72]

[154] F. Halzen, and A .D. Martin, *Quarks and Leptons: An Introductory Course in Modern Particle Physics*, (John Wiley & Sons, New York, 1984). [pp. 76, 107]

[155] C. Töke and J. K. Jain, Phys. Rev. B **75**, 245440 (2007). [p. 78]

[156] M. O. Goerbig and N. Regnault, Phys. Rev. B **75**, 241405(R) (2007).

[157] L.-K. Lim, M. O. Goerbig, and C. Bena, Phys. Rev. B **84**, 115404 (2011). [p. 78]

[158] S. C. Davenport. [http://www2.physics.ox.ac.uk/contacts/people/davenport] (2013). [p. 78]

[159] S. C. Davenport, E. Ardonne, N. Regnault, and S. H. Simon, Phys. Rev. B **87**, 045310 (2013). [pp. 78, 80, 83, 86, 87, 89]

[160] S. H. Simon, E. H. Rezayi, and N. R. Cooper, Phys. Rev. B **75**, 075318 (2007). [pp. 78, 79]

[161] E. R. Caianiello, Il Nuovo Cimento **10**, 1634 (1953). [p. 79]

[162] T. S. Jackson, N. Read, and S. H. Simon, Phys. Rev. B **88**, 075313 (2013). [pp. 79, 93]

[163] B. Estienne and B. A. Bernevig, Nucl. Phys. B **857**, 185 (2012). [pp. 80, 86, 87, 90, 93]

[164] M. Greiter, X.-G. Wen, and F. Wilczek, Nucl. Phys. B **374**, 567 (1992). [pp. 83, 85]

[165] N. Read, Phys. Rev. B **79**, 245304 (2009). [p. 87]

[166] B. A. Bernevig and F. D. M. Haldane, Phys. Rev. Lett. **100**, 246802 (2008). [pp. 89, 93]

[167] E. Ardonne and N. Regnault, Phys. Rev. B **84**, 205134 (2011). [p. 89]

[168] N. Regnault, B. A. Bernevig, and F. D. M. Haldane, Phys. Rev. Lett. **103**, 016801 (2009). [pp. 89, 92]

[169] M. Haque, O. Zozulya, and K. Schoutens, Phys. Rev. Lett. **98**, 060401 (2007). [p. 90]

[170] O. S. Zozulya, M. Haque, K. Schoutens, and E. H. Rezayi, Phys. Rev. B **76**, 125310 (2007).

[171] H. Li and F. D. M. Haldane, Phys. Rev. Lett. **101**, 010504 (2008).

[172] A. Sterdyniak, N. Regnault, and B. A. Bernevig, Phys. Rev. Lett. **106**, 100405 (2011). [p. 90]

[173] J. Fuchs, A. N. Schellekens, and C. Schweigert, Nucl. Phys. B **473**, 323 (1996). [p. 90]

[174] J. Fröhlich, J. Fuchs, I. Runkel, and C. Schweigert, Fortschr. Phys. **52**, 672 (2004). [p. 90]

[175] J. K. Jain, Phys. Rev. Lett. **63**, 199 (1989). [p. 92]

[176] N. Regnault, M. O. Goerbig, and T. Jolicoeur, Phys. Rev. Lett. **101**, 066803 (2008). [p. 92]

[177] S. H. Simon, E. H. Rezayi, and N. Regnault, Phys. Rev. B **81**, 121301 (2010). [p. 93]

[178] M. E. J. Newman, and G. T. Barkema, *Monte Carlo Methods in Statistical Physics*, (Clarendon Press, Oxford,1999). [p. 95]

[179] K. Park, *Composite Fermions*, Ph.D. thesis, (Stony Brook: State University of New York, 2000). [p. 97]

[180] I. G. Macdonald, *Symmetric Functions and Hall Polynomials*, (Oxford University Press, Oxford, 1979). [pp. 98, 133]

[181] G. E. Andrews, *The Theory of Partitions (Encyclopedia of Mathematics and its Applications)*, (Cambridge University Press, Cambridge , 1984). [pp. 102, 134]

[182] D. E. Rutherford, *Substitutional Analysis*, (Edinburgh University Press, Edinburgh, 1948). [pp. 105, 106, 113]

[183] W. Pfeifer, *The Lie Algebras of su(N)*, (Birkhäuser, Basal, 2003). [pp. 107, 108]

[184] R. Pauncz and J. Katriel, Chemical Physics Letters **46**, 319 (1977). [p. 120]

[185] B. E. Sagan, *The Symmetric Group: Representations, Combinatorical Algorithms, and Symmetric Functions*, (Springer, Berlin, 2001). [pp. 128, 135, 136, 137, 138]

[186] C. Kostka, Crelle's J. **93**, 89 (1882). [pp. 129, 138]